PRION: A NOVEL REGULATOR OF SPIRAL ARTERY REMODELING AT THE MATERNAL-FETAL INTERFACE

Thesis submitted for the degree of
Doctor of Philosophy (Science)
in
Life Science and Biotechnology

by

RUMELA BOSE

[22/19/Life Sc./26]
[Regn No. SLSBT1102219]

Department of Life Science and Biotechnology
Jadavpur University

CERTIFICATE FROM THE SUPERVISOR(S)

This is to certify that the thesis entitled ".....Prion: a novel regulator of spiral artery remodeling at the maternal-fetal interface" Submitted by ~~Sri~~ / Smt. .....RUMELA BOSE..... who got ~~his~~ / her name registered on.....14.08.2019..... for the award of Ph. D. (Science) Degree of Jadavpur University, is absolutely based upon her own work under the supervision of .....Dr. Rupasri Ain..... and that neither this thesis nor any part of it has been submitted for either any degree / diploma or any other academic award anywhere before.

Rupasri Ain 11/11/23

.....Dr. Rupasri Ain, FNASc.....

Chief Scientist, Cell Biology and Physiology Division
Professor, Academy of Sciemtific & Innovative Research (AcSIR)
CSIR-Indian Institute of Chemical Biology
(Ministry of Science and Technology, Govt. of India)
4, Raja S. C. Mullick Road, Jadavpur, Kolkata - 700 032, India

.....

(Signature of the Supervisor(s) date with official seal)

DEDICATED TO,

My Parents, My Grandparents, and my Husband

ACKNOWLEDGEMENTS

As the journey of my Doctoral research work has reached its completion, I would like to express my heartfelt gratitude to all the persons for their valuable guidance and support without which this research work could not take its present shape.

First and foremost, I would like to express my sincere respect and gratitude to my supervisor, Dr. Rupasri Ain, Chief Scientist, Cell Biology and Physiology Division, CSIR-Indian Institute of Chemical Biology, Kolkata, for giving me the opportunity to pursue my Ph.D research under her supervision. She has always been a source of inspiration for me. I first joined her lab as an MSc. Dissertation trainee, with lots of hope and ideas in my mind about the field of developmental biology; but with zero ideas about research. It was she, who slowly taught me to shape those ideas into concepts, concepts into thoughts and thoughts into actions; and finally made me an independent researcher that I am today. At times we had long fights, which I feel is a part and parcel of Ph.D life. But the very next day she would come up with new ideas and discuss with me, motivating me to complete my Ph.D with good track record. Her constructive criticism has helped me to improve each day and gradually reach perfection. Her wide knowledge, logical thinking and good leadership skills are the qualities I admire the most. She has always encouraged me to attend scientific seminars and conferences both in India and abroad which helped me to enrich my passion for science. I would have never got the flavour of doing research had she not given me the freedom to think and implement my own ideas in my project. I would like to thank her for believing in me at times, when I myself didn't, and encouraged me to learn from my mistakes.

I am extremely thankful to Dr. Samit Chattopadhyay, former Director, and, Dr. Arun Bandyopadhyay, present Director, CSIR-Indian Institute of Chemical Biology, Kolkata, for granting me the privilege and facilities to conduct my research work in this esteemed institute. I am also thankful to Dr. Partha Chakrabarti, Senior Principal Scientist, CSIR-Indian Institute of Chemical Biology, Kolkata, for his valuable suggestions regarding my project.

I am extremely grateful to Council of Scientific and Industrial Research (CSIR), Govt. of India, for finding me suitable for the prestigious Shyama Prasad Mukherjee Fellowship award. This was indeed a motivation for me at the beginning of my Ph.D course.

I would like to acknowledge my lab mates, Dr. Shreeta Chakraborty, Dr. Sarbani Saha, Dr. Madhurima Paul and Dr. Sarmita Jana, for sharing their knowledge and experience in my research; Dr. Trishita Basak, Miss Shreya Das and Mr. Safirul Islam, for extending their helping hands at every juncture of need. They had always helped me and trained me to handle difficult experiments, right from my first day in this lab. I also owe my thanks to Dr. Debdyuti Nandy, for teaching me how to handle laboratory animals; Mrs. Shipra Kanti Jana, Miss Swarnali Dey, Mr. Tamal Kanti Gope, Miss Madhubanti Ghosh, Miss Priyanka Das, Miss Poulomi Sarkar, Mr. Debankur Pal, Miss Shreya Deb, Mr. Sourav Ganguly, and Miss Baitali Guha for all the optimistic discussions and for offering a great work environment. I also want to thank Mr. Deepan Chatterjee, a former summer trainee under my supervision, for being the most composed, obedient, and diligent junior one can ask for.

I would be grateful to the Life Science & Biotechnology Department, Jadavpur University, Kolkata for allowing me to register and submit my thesis for the award of Ph.D degree.

I find myself really blessed to have such loving and supportive family. My parents, Mr. Rajat Bose and Mrs. Runa Bose, I cannot thank them enough for all their endless love and sacrifices. At times when I used to become morose and frustrated, they constantly motivated me with their patience, encouragement, care, and valuable advices, that had allowed me to start everything afresh. They have always believed in me and supported me to follow my dreams no matter what. Their simple and pious lifestyle has taught me to always stay grounded. They have taught me to become a human being with great values. I express my sincere respect towards my grandparents Mr. Ranajit Kumar Bose and Mrs. Anita Bose, who are the pillars of my strength. Without their blessings

and prayer, I would have not existed at all! My sincere thanks to all my relatives and friends who helped me and supported me several ways.

I would like to express my profound love and gratefulness towards my husband Dr. Aditya Banerjee, for his selfless love and moral support. Himself being in the same profession, he was always by my side whenever I needed him for any suggestion or scientific discussion. Many a times, his wisdom and decision-making ability have helped me to combat challenging situations both in lab and in life. His calm and composed nature have inspired me to solve critical problems at ease. In our brief conversations, we often shared each other's perception towards building a glorified scientific career. He has always appreciated my research work and achievements just like a true companion.

I owe my heartfelt acknowledgment to my parents-in-law for their constant support and motivation. In a society, where women are forced to abandon their dreams post marriage, they have always encouraged me to stay focused and excel in my Ph.D research work. My mother-in-law Mrs. Sharmistha Banerjee, a lady of wisdom herself, has constantly motivated me through her positive attitude and spirituality. Whenever I felt lonely, she has always given me a strong and compassionate shoulder to lean on. Her guidance, care and lessons have enlightened me not only from outside but mentally as well. I am also fortunate enough to get the blessings of my father-in-law, Dr. Dibyendu Banerjee; a dignified professor at the Department of Law, University of Calcutta, yet such a humble human being. He loves me as his own daughter and has mentored me several times through this topsy-turvy journey of Ph.D. He has always taken keen interest to listen to my research accomplishments and provided technical advices for writing my thesis.

Last, but not the least, I would like to thank God Almighty for showering his blessings on me, and bestowing upon me the self-confidence and perseverance that was required for the fulfilment of this work. Without His presence around me, I would have never shown the courage of walking this challenging path called, "Ph.D".

SYNOPSIS

SYNOPSIS

Development of the placenta is an elaborate process involving cellular differentiation and morphogenesis, which has made mammalian reproductive strategy the most complex and successful than other species. Based on the proximity of the chorion and the uterine wall, mammalian and rodent placentae are classified under Haemochorial placenta, where the trophoblast layers are in direct contact with the maternal blood circulation. It ensures the most intimate contact between the maternal and fetal compartments (Harland W. & Mossman., 1987), and more efficient transfer of nutrients and gaseous exchange. Along with the developing embryo, the mother's body also parallelly undergoes a series of adaptations to sustain a full-term pregnancy. The most remarkable among them is the establishment of an intricate arterial-venous circulation so as, to maximize the volume of blood flow into the utero-placental compartment.

The uterine spiral artery network arises from the radial arteries and supply to the endometrium (D'Errico & Stapleton, 2019). They develop during the secretory phase of the menstrual cycle under the influence of progesterone (Ferenczy et al., 1979), and are shed off along with the endometrium, when conception does not occur (Kliman, 2000). Notably, during pregnancy these highly convoluted vessels are able to calibrate themselves from high resistance vessel to flaccid low resistance vessels with 10-fold increase in vascular diameter (Kliman, 2000; Nandy et al., 2020), and 3-4 fold increase in blood volume (Thaler et al., 1990). All these changes, collectively are known as "Spiral Artery Remodelling" (SAR). Insufficient SAR leads to disastrous pregnancy outcome such as Intra-Uterine Growth restriction (IUGR), which takes a toll on the health and survival of both mother and fetus. The vascular smooth muscle cells (VSMCs) constitute the major cell types of tunica media and are known to maintain

the integrity and elasticity of the arterial wall (Hu et al., 2019). These cells undergo considerable phenotypic changes to remodel the spiral arteries.

The Cellular Prion protein (Prnp) is a GPI-anchored membrane bound glycoprotein (Steele et al., 2007), known to cause highly infectious neurodegenerative diseases, when mutated. During the last decade, cellular prion has gained prominence in guiding mammalian developmental events. For example, dysregulation of its expression can cause serious gestation-related morbidities (Sibai et al., 2005), it helps in chelation of Cu (II) ions (Alfaidy et al., 2013); lastly, Prnp knockout FVB/N embryos fail to form a functional ectoplacental cone as well all causes significant hemorrhage to the maternal uterine wall (Passet et al., 2012). But the underlying mechanism by which prion might be modulating these events, have remained elusive. ***Therefore, in this report we have aimed a) to understand the spatio-temporal regulation of cellular prion within maternal-fetal interface, b) to determine plausible functional role played by prion in the vascular smooth muscle cells, to accentuate the process of SAR, c) to designate global consequences occurring within vascular smooth muscle cells as a result of perturbed Prnp expression.***

Chapter 1, illustrates a detailed overview of the background of our study. This includes the origin and diversification of maternal spiral arteries within the hemochorial placenta, complex cellular and molecular factors that govern the preliminary events of spiral artery remodelling and development of the hemochorial placenta itself. This section also provides knowledge about structural features of Cellular Prion, its paralogs, alongside its function in various tissues and I early embryonic development.

Chapter 2 details all the materials and methods used to address every key question for this study; which includes animal tissue collection, molecular biology techniques, culturing mammalian cell lines, in-vitro assays, and bioinformatics.

In **Chapter 3,** we have discussed about the expression profile of cellular Prion protein in rat metrial gland tissue at different gestational time points, both at RNA and protein levels. With the help of immunohistochemical assay, we could decipher that PRNP is expressed by the vascular smooth muscle cells that are migrating outwards into the matrix, adjacent to the spiral arteries.

Chapter 4 details the functional importance of cellular prion protein in the VSMCs, in context of SAR. For our ex-vivo studies we have cultured rat aortic smooth muscle cell line A7r5, shown to express high levels of prion protein under ambient condition. We employed lenti-virus mediated delivery of shRNA oligos to functionally downregulate endogenous Prnp and various assays were performed. Results from wound healing and cell-invasion assays denote substantial hindrance in these processes when Prnp is decreased. Hence, Prnp is believed to potentiate migration and invasion in these cells. Focal Adhesion Kinase (FAK) stimulates PDGFBB mediated chemotaxis migration in VSMCs, by formation of an activating complex with PDGFRβ (Hauck et al., 2000). Co-immunoprecipitation assay revealed that PRNP interacts with this PDGFRβ-FAK complex in A7r5 cells, possibly acting as a co-receptor to facilitate smooth muscle cell motility. Similar results were observed when PRNP was pulled down from E16.5 rat metrial gland lysate, implying that PRNP might be responsible for the increased migratory potential observed in the VSMCs during spiral artery remodelling. Furthermore, increased apoptosis in cells lacking *Prnp,* led us to postulate its probable role in VSMC survival. Western blot was used to check for the relative levels of pro- and anti-apoptotic proteins. Relative abundance of the cleaved isoforms of caspase8 and caspase3 implied towards activation of the extrinsic pathway of apoptosis. Located in the outer leaflet of the plasma membrane, PRNP was found to interact with TRAIL receptor DR4, one of the mediators of the extrinsic

apoptosis pathway. Treatment of VSMCs with recombinant murine TRAIL, enhanced early apoptotic signals in *Prnp* knock down cells as compared to control group. These results highlight the role of prion protein in surveilling untimely apoptosis of VSMCs.

This report further identified Odd-skipped Related 1 or OSR1, a well characterized nephron precursor marker, as a potential regulator of expression of Prnp in VSMCs. Rat placentation is characterized by deep trophoblast invasion, as far as the metrial gland with concomitant de-differentiation of VSMCs (Nandy et al., 2020). Co-culture of VSMCs with primary rat trophoblast cells resulted in decrease in Prnp as well as Osr1 levels. It was therefore concluded that trophoblast derived factors suppress the action of Prnp in VSMCs through Osr1 axis.

In **Chapter 5,** we have identified different biochemical pathways or cellular processes that might be regulated by Prnp. Sequencing of total RNA from control and Prnp knock down cells revealed more than 250 differentially expressed genes. Out of these, using bioinformatics tool, 51 genes which showed significant fold change and high base counts, were shortlisted, and graphically represented in a volcano plot. This in-silico data were re-validated in our biological system by qPCR analysis, and the genes were grouped based on their respective function. These observations will provide further insights towards the broad range of biological aspects determined by prion in the VSMCs.

ABBREVIATIONS

µl	**Micro litre**
µm	**Micro metre**
3'UTR	**3' Untranslated region**
Ang	**Angiopoietin**
ATCC	**American Type Culture Collection**
BSA	**Bovine Serum Albumin**
BSE	**Bovine Spongioform Encephalopathy**
CCC	**cytotrophoblast cell column**
CD	**Cluster of differentiation**
CJD	**Creutzfeldt-Jakob disease**
CM	**Conditioned media**
CPA	**Chorionic plate artery**
CTB	**Cytotrophoblast cells**
CXCL10	**C-X-C motif Chemokine Ligand 10**
DD	**Death Domain**
DEPC	**Diethyl pyrocarbonate**
DMSO	**Dimethyl sulfoxide**
EC	**Endothelial cell**
ECL	**Enhanced chemiluminescence**
ECM	**Extracellular matrix**
EDTA	**Ethylenediamine tetraacetic acid**
eEVT	**endovascular extra-villous trophoblast cells**
EPC	**Ecto-placental cone**
EVT	**Extra-villous trophoblast cells**
FADD	**Fas activating death domain**

FAK	**Focal adhesion kinase**
FasL	**Fas ligand**
FBS	**Fetal bovine serum**
FFI	**Familial fatal insomnia**
FTIR	**Fourier-transform infrared**
GFP	**Green fluorescent protein**
GPI	**Glycosylphosphatidylinositol**
GSS	**Gerstmann-Straussler-Scheinker**
HIF-1	**Hypoxia-inducible factor-1**
HRP	**Horseradish peroxidase**
iEVT	**Interstitial extra-villous trophoblast cells**
IFN	**Interferon**
IL	**Interleukin**
IUGR	**Intrauterine growth restriction**
JNK	**C-Jun N-terminal kinase**
JZ	**Junctional Zone**
kb	**Kilobase**
kD	**Kilo Dalton**
LRS	**Lymphoreticular system**
LZ	**Labyrinth Zone**
MG	**Metrial gland**
MMP	**Matrix metalloprotease**
nm	**Nano metre**
ORF	**Open reading frame**
PBS	**Phosphate buffered saline**
PCR	**Polymerase chain reaction**
PDGF	**Platelet-derived growth factor**
PDGFR-β	**Platelet-derived growth factor receptor beta**

PI-PLC	**Phosphoinositide Phospholipase C**
PK	**Proteinase K**
PLP	**Prolactin (PRL)-like protein**
Prl7b1	**Prolactin family 7, subfamily b, member 1**
PVDF	**Polyvinylidene fluoride**
SDS	**Sodium Dodecyl Sulphate**
shRNA	**Short hairpin RNA**
SOD	**Superoxide dismutase**
SpA	**Spiral arteries**
STB	**Syncytiotrophoblast cells**
TGC	**Trophoblast Giant cells**
TGF-β	**Transforming growth factor beta**
TIMP	**Tissue inhibitor of metalloprotease**
TNF-R1	**TNF-Receptor 1**
TNF-R2	**TNF-Receptor 2**
TNF-α	**Tumour necrosis factor alpha**
TRADD	**TNF-receptor-associated death domain**
TRAF2	**TNF-receptor-associated factor 2**
TRAIL	**TNF-related apoptosis inducing ligand**
TRAIL-R1	**TRAIL-Receptor 1**
TRAIL-R1	**TRAIL-Receptor 1**
TRAIL-R2	**TRAIL-Receptor 2**
TRAIL-R3	**TRAIL-Receptor 3**
TRAIL-R4	**TRAIL-Receptor 4**
TSC	**Trophoblast Stem cells**
TSE	**Transmissible Spongioform Encephalopathy**
TUNEL	**Terminal deoxynucleotidyl transferase dUTP nick end labeling**
uNK cells	**Uterine Natural Killer cells**

uPA	**urokinase Plasminogen activator**
uPAR	**urokinase Plasminogen activator receptor**
vCTB	**Villous Cytotrophoblast cells**
VEGF	**Vascular endothelial growth factor**
VSMC	**Vascular smooth muscle cell**

CONTENTS

CHAPTER 1

BACKGROUND AND SIGNIFICANCE

1.1 Development of haemochorial placenta

The placenta is a temporary organ that connects the fetus with the mother and permits nutrient and gaseous exchange thus sustaining its growth throughout gestation. Haemochorial placentation is an evolutionary strategy adapted by humans, rodents, and non-human primates where the materal blood is in direct contact with the fetal trophoblasts optimized for maximum absorption of nutrients.

1.1.1 Development of haemochorial placenta in humans

In humans, implantation occurs 7-9 days post fertilization. The trophectoderm layer initially makes contact with the uterine lining, thereafter penetrates deep into the uterine decidua. Unlike in lower mammals, first signs of decidualization in humans is seen before conception, day 23 of menstrual cycle when the spiral arteries in the endometrium becomes prominent (Kliman, 2000). Immediately after implantation the trophectoderm layer of the blastocyst give rise to diverse trophoblast cells (Hamilton and Boyd, 1960) and (Cross et al., 1994). The trophoblast cells proliferate rapidly and cell fusion takes place to generate primitive syncytium representing the invasive trophoblast cells that invade the maternal endometrium and surrounds the inner layer of mononuclear cytotrophoblast cells (CTB) (Hemberger et al., 2020). As the primitive syncytium expands further into the decidual spaces, the CTB, migrates through these spaces to demark the formation of primary placental villi. Mesenchymal cells arising from the epiblast invaded the primary villi. These cells proliferate and differentiate to form a villous structure containing fetal blood vessels. These fetal blood vessels contain a mesenchymal core, surrounded by two layers of maternal trophoblasts, the inner villous CTB (vCTB) and outer syncytiotrophoblast (STB) (Fig 1.1)

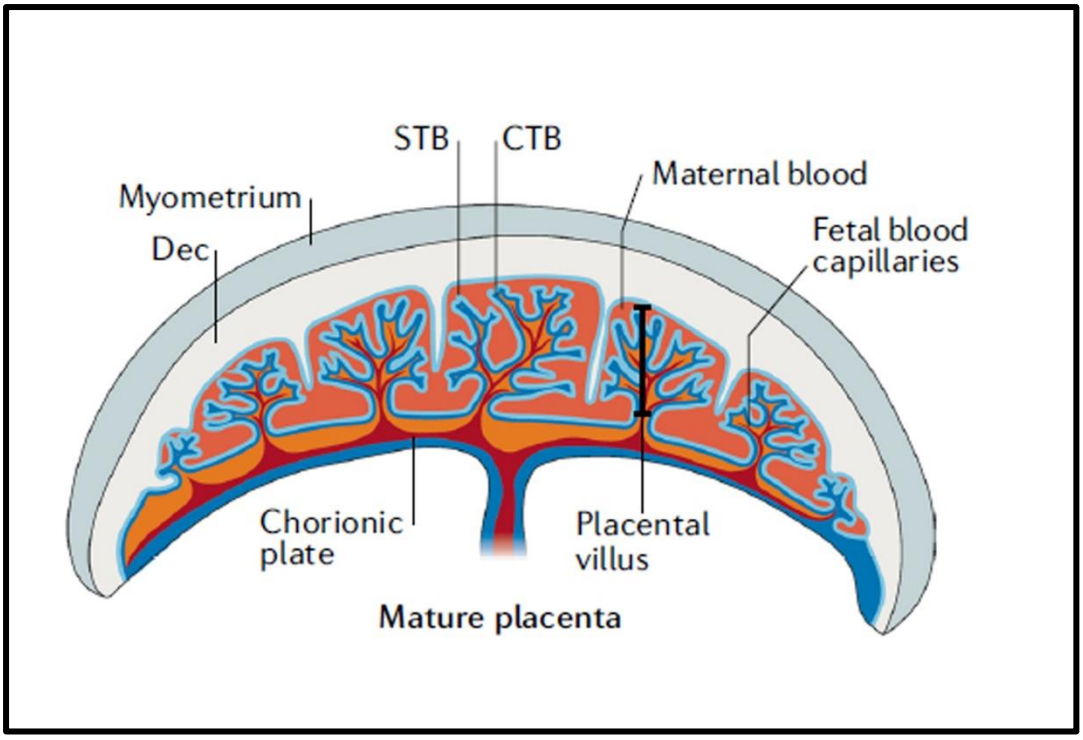

Figure 1.1. Structural features of mature human placenta (Hemberger et al., 2020)

Villi connected to the basal plate of human placenta give rise to proliferative cell columns from which extra-villous trophoblast (EVT) cells are generated. These trophoblast cells form multi-layered columns that invade the endometrium and its associated spiral arteries. At early stages of pregnancy, the invasive endovascular cytotrophoblasts plug the maternal arterioles to prevent the premature blood flow into the intervillous space to avoid generation of teratogenic reactive oxygen species (Burton et al., 1999). Although the basic structure of the definitive placenta is formed by the fourth week of gestation, the perfusion of maternal blood into the sinuses does not happen until tenth or twelfth week of pregnancy (Burton et al., 1999; Burton et al., 2002)

1.1.2 Development of haemochorial placenta in rats

Although the anatomical features of human and rodent placenta differ in their overall morphology, but the mechanisms underlying their development is quite

similar. At the time of implantation, the mural trophectoderm layer differentiates to form the primary trophoblast giant cells that encapsulate the embryo. The polar trophectoderm gives rise to two diploid cell lineages, the extra-embryonic ectoderm and the ectoplacental cone (EPC), the latter harbouring the trophoblast stem cell niche which contributes to the specialized trophoblast cells of the placenta (Rossant & Cross, 2001). The rat placenta, like in mice, is divided into the Junctional Zone (JZ) and the Labyrinth Zone (LZ). Trophoblast stem cells (TSC) within the ectoplacental cone differentiate into four distinct regions of the junctional zone—1) secondary trophoblast giant cells, 2) spongiotrophoblast cells, 3) glycogen cells, 4) invasive trophoblast cells (Ain et al., 2006.) TSCs located at the periphery of the ectoplacental cone differentiate into secondary TGCs that line the boundary of the decidua and placenta. The main constituent of the junctional zone is the spongiotrophoblast which also contribute to the endocrine function of the placenta. Glycogen cells first appear during midgestation, notably accumulate glycogen, and are probably progenitors for a subset of invasive trophoblast cells (Soares et al., 2012).

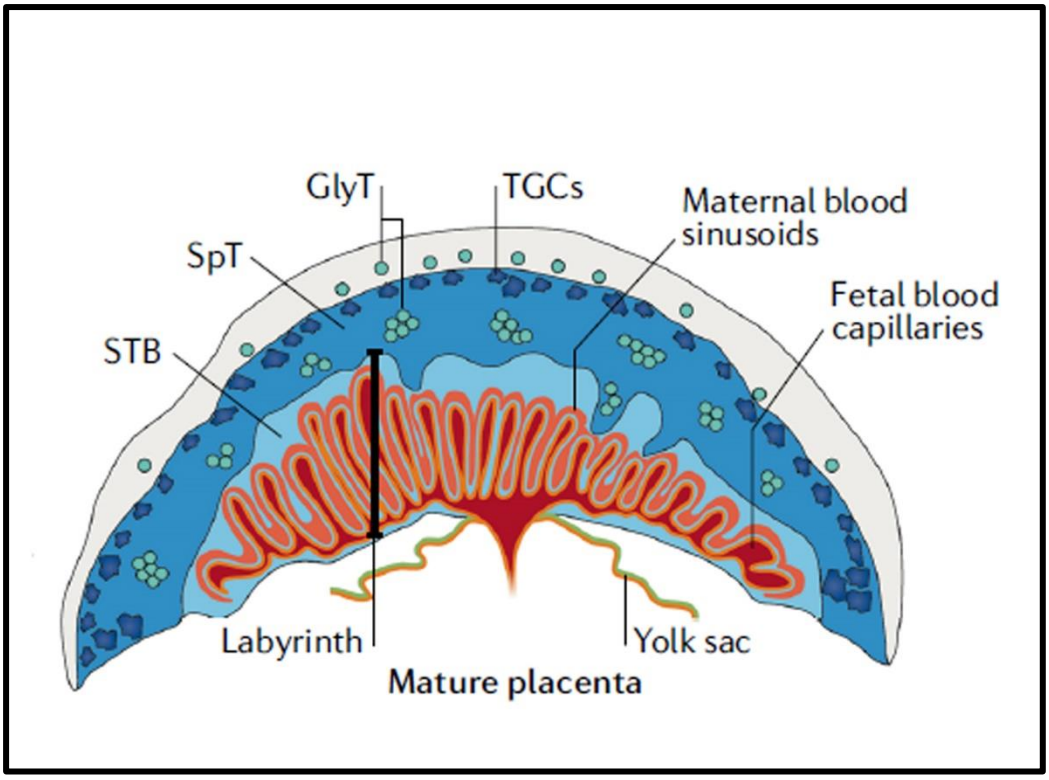

Figure 1.2. Structural features of mature rat placenta (Hemberger et al., 2020). The junctional zone is marked by the trophoblast giant cells (TGC), glycogen cells (GlyT) and Spongiotrophoblasts (SpT). The labyrinth zone is marked by the syncytiotrophoblasts (STB) and the complex network of maternal and fetal circulation

The labyrinth zone arises from the extra-embryonic ectoderm, yielding trophoblast cell syncytialization. Soon after chorio-allantoic fusion takes place at E8.5, the chorion fold into villi creating a space for the fetal blood vessels to form from the allantois. At this time, the chorionic trophoblast cells begin to differentiate into two labyrinth cell types. Multinucleated syncytiotrophoblast cells, formed by the fusion of trophoblast cells, surround the endothelium of the fetal capillaries. The maternal blood sinuses are lined by a layer of mononuclear trophoblast cells. Before the maternal-fetal circulation is established the fetus is supported by the secretions of the uterine glands. This mode of nutrition is called histiotrophic nutrition. The trophoblasts, together with the fetal vasculature generate extensively branched villi

of the labyrinth, which become more complex to allow the maternal and fetal blood to flow in a counter current manner to maximize nutrient transport.

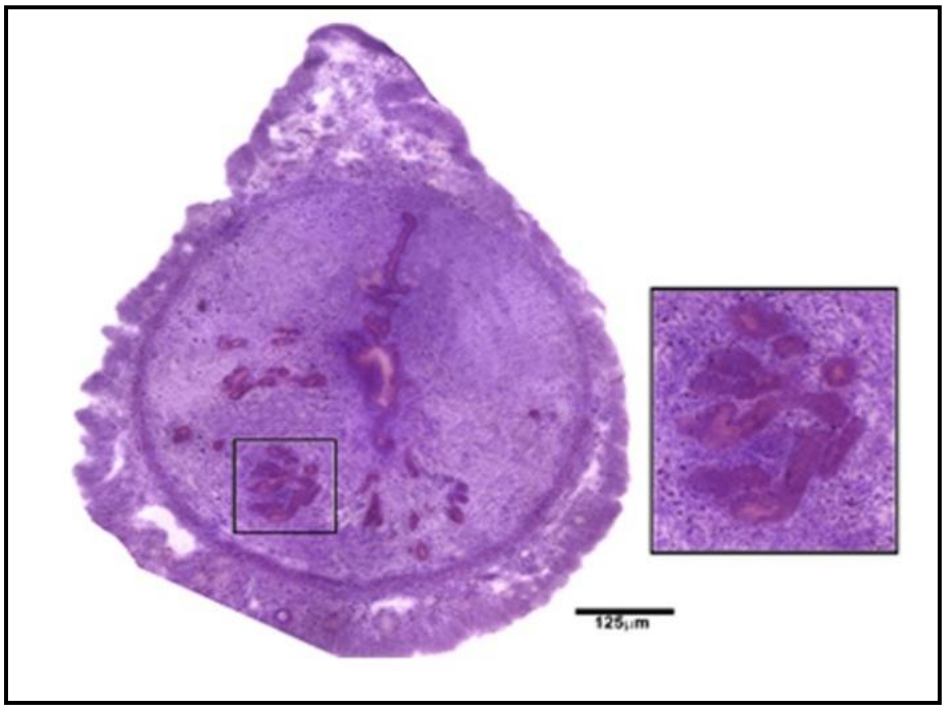

Figure 1.3. Histological section of mouse implantation site on embryonic day 5.5 (Bose & Ain, 2020) showing uterine lumen and uterine glands (inset). The light brown colour within the uterine glands and the lumen denotes presence of cellular Prion protein in those regions, after immunostaining with HRP conjugated antibody

1.2 Uterine Spiral Arteries

The uterine artery branches off to form arcuate network of vessels that supply blood to the uterine bed. The arcuate vessels branch out through the myometrium as radial arteries, which further subdivides into two channels; the basal artery—that drains the myometrium and the spiral arteries—that extends beyond the myometrium, into the endometrium and becomes the chief conduits of blood supply to the fetus (D'Errico & Stapleton, 2019).

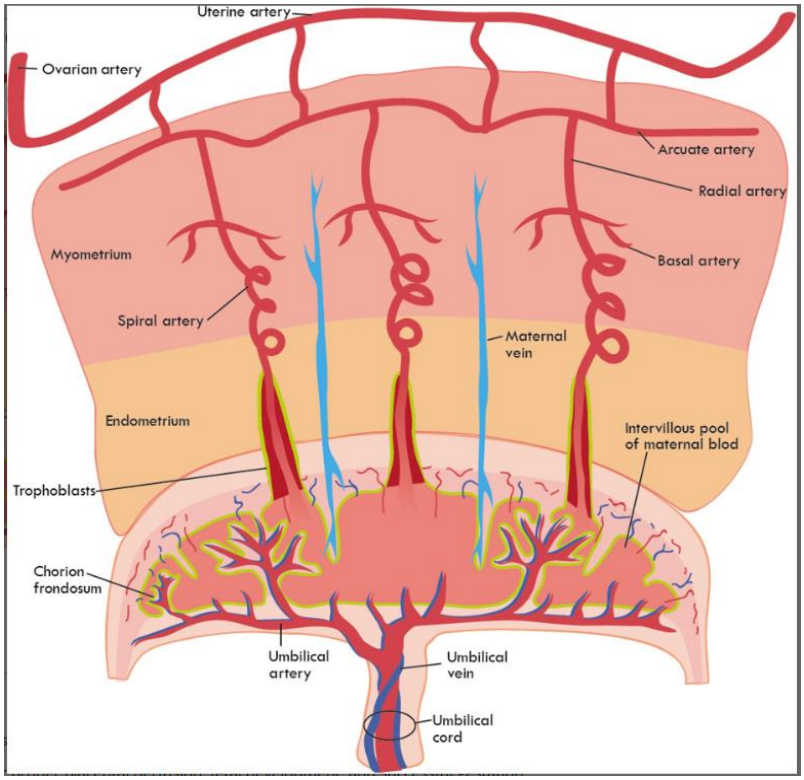

Figure 1.4. Arrangement and diversification of maternal arteries in a pregnant uterus (D'Errico & Stapleton, 2019)

The spiral arteries procure their terminology owing to their highly convoluted structure which allows them for maximal stretching to accommodate fetal growth. They develop during the secretory phase of the menstrual cycle under the influence of progesterone (Ferenczy et al., 1979). Over the next few days of menstrual cycle, the uterine stromal cells surrounding the spiral arteries become eosinophilic and start to differentiation into predecidual cells driven by progesterone. Following a cycle without conception, these vessels are shed off along with the endometrium in humans and other non-human primates in a process known as menstruation (Kliman, 2000). At term, these arteries support the growing placenta and the fetus by able to calibrate themselves from high resistance vessel to low resistance vessel with 10-fold increase in vascular diameter (Kliman, 2000; Nandy et al., 2020). The systolic to end-diastolic flow velocity ratio remarkably decrease from 5.3 in non-pregnant state to 2.3 near term. Moreover, the volume of blood flow increases about 3-4 folds; volume flow rate increases from 94.5ml/min to 342ml/min in the late gestation (Thaler et al., 1990).

1.3 Cellular and molecular factors involved during initial stages of pregnancy-associated Spiral Artery Remodeling

The molecular actuate for the remodeling process are still an oblivious subject, but it has been established that it undergoes by two major pathways; trophoblast-independent and trophoblast-dependent, the former being guided by the uterine Natural Killer (uNK) cells and macrophages.

1.3.1 Uterine Natural Killer (uNK) cells

The uterine natural killer cells form the major population of decidual leucocytes and surround the spiral arteries during first trimester of pregnancy (Smith et al., 2009). The peripheral NK cells are analyzed by their expression of surface antigen CD16, an immunoglobulin domain receptor, and dim expression of CD56, a cell adhesion molecule. About 1% of circulation NK cells are $CD16^{-}$ and $CD56^{bright}$ and co-express L-selectin (Campbell et al., 2001). On the contrary human uNK cells are $CD56^{bright}$ but lack both CD16 and L-selectin (Searle et al., 1999). They proliferate, produce cytokines (IFN-γ), interleukins (IL-18, IL-27), Perforin, and an array of angiogenic factors (Angiopoietin-1 and 2; Ang-1 and 2). VEGF-C, MMP-2, 9; all of which have implications in reprogramming vascular networks (B. Croy et al., 2003; Robson et al., 2012).

Their cytotoxic effects on trophoblasts hinder latter's precocial entry into the maternal arteries. uNK cell conditioned medium (uNK-CM), from 8-10 week of gestation, increased rounding of and separation of VSMC layer from the chorionic plate arteries (CPA). Interestingly, these CPA segments also showed reduced immunostaining for

ECM components like fibronectin and laminin in presence of uNK-CM (Robson et al., 2012).

In mice, uNK cells appear in the decidua basalis at day 6.5 of pregnancy and secrete IFN-γ, VEGF-A, placental growth factor (Chen et al., 2012). They play key roles in mice decidual spiral artery remodeling which occurs between E8.5 and E10.5, as NK cell deficient mouse have abnormal decidual arteries in mid gestation (Guimond et al., 1997). Administration of IFN-γ into these mice resulted in normal arterial remodeling (Ashkar et al., 2000).

Placentation sites from E13.5 NK cell depleted rats displayed spiral arteries lacking smooth muscle alpha actin and surrounded by endovascular trophoblast cells expressing the invasive marker Prl7b1 (Chakraborty et al., 2011). NK cell derived VEGF-A transcripts and protein are required for normal spiral artery development. uNK depleted arteries show increased hypoxic tension in the spiral arteries and activation of HIF1 signalling in the cells of ectoplacental cone; indicating its role in delivering oxygen to the developing placenta (Chakraborty et al., 2011)

1.3.2 Macrophages

The word macrophage is derived by combining two Greek words, ‘macros’ meaning large and ‘phagein’ meaning to eat. Therefore, in simple words, macrophages are large specialized cells of our immune system that recognize, destroy, and engulf target cells. During the remodeling process M2 macrophages infiltrate the decidua around the spiral arteries where they get activated by TGF-β, IL-6 and VEGFA produced by endometrial epithelial cells, uNK cells and trophoblasts in the decidua (Socha et al., 2021). Activated macrophages themselves secrete a wide range of cytokines, IL-1β, lL-4, IL-6, IL-8, IL-10, IL-13, and TNF-α, which further

extend the inflammatory response and angiogenic growth factors like Ang-1 and 2. The most important function of the uterine macrophages is the secretion of MMP-1, MMP-2, MMP-7, MMP-9, and MMP-10, disorganization of the extracellular matrix, and phagocytosis of apoptotic VSMCs and trophoblasts (Faas & de Vos, 2017; Lash et al., 2016). Conditioned medium of macrophages from 8-10 wk and not 12-14 wk gestation age facilitate breaking down of ECM proteins laminin and fibronectin around the vessel walls. These macrophages are also associated with VSMCs that migrate away as well as with VSMCs that are undergoing apoptosis (Lash et al., 2016). TNF-α and IFN-γ, secreted by uNK cells, are essential to stimulate uterine macrophages to produce CXCL10 (Qi et al., 2009), which is a potent chemoattractive molecule for trophoblasts. Therefore, during the placentation, macrophages not only facilitate but also stimulate spiral arteries invasion by trophoblasts.

1.4 Placental disorders due to improper Spiral Artery Remodeling

Once the hemotrophic nutrition is established the fetus depends completely upon the maternal supply of nutrients through the placenta. Glucose, amino acids, fatty acids, hormones, and other nutrients are transported via the placenta through different transporters. Fetal growth restriction is associated with reduced nutrition which can result from decreased utero-placental blood flow or reduced capacity of placental transporters (Cetin & Antonazzo, 2009). Impaired endovascular invasion of trophoblast cells into maternal decidua leads to insufficient transformation of spiral arteries to vessels of low resistance (Pijnenborg et al., 1983).

Preeclampsia is another common cause of maternal and neonatal morbidity and mortality worldwide. Accounting for 5 to 7% of pregnancy cases, preeclampsia is

associated with cardiovascular pathology, hypertension, and proteinuria. In preeclamptic placentas, the cytotrophoblasts fail to develop into on-time invasive subtype, ensuing improper spiral artery remodeling (Zhou et al., 1997). Inadequate remodeling of the spiral arteries results in narrow maternal vessels with atherosclerotic lesions, leading to placental ischemia (De Wolf et al., 1975).

1.5 Cellular prion protein and its isoforms

The Prion protein (Prp^c or simply Prnp) is a conserved glycoprotein tethered to the cell membrane by a glycosylphosphatidylinositol (GPI) anchor (Steele et al., 2007). Prion diseases are a group of transmissible, chronic, progressive infections of the nervous system which show common pathological effects and are invariably fatal (S. B. Prusiner, 1998). The prion diseases are collectively called as Transmissible Spongioform Encephalopathy (TSE) which includes Bovine Spongiform Encephalopathy (BSE), commonly known as mad cow disease, scrapie in sheep and Creutzfeldt-Jakob disease (CJD), Familial fatal insomnia (FFI), Gerstmann-Straussler-Scheinker disease (GSS), Kuru in humans. The name 'spongiform encephalopathies' has been coined due to the characteristic myriad of tiny holes in the cortex of affected brain tissue viewed under the microscope. Prion was initially recognized as the causative agent of scrapie in sheep. Transmissibility of scrapie was first demonstrated in 1939 (Cuille, 1939) and that the scrapie agent could multiply without a nucleic acid template was first suggested by Tikvah Alper in 1966. In 1982, Stanley Prusiner coined the term prion (proteinaceous-infectious particle) (S. B. Prusiner, 1982). Prp^c denotes “cellular” or normal Prp to distinguish it from Prp^{Sc} for “scrapie” or its disease-causing isoform. Immunohistochemical studies localized Prnp to neurons and surrounding

neuropil in hippocampus; septal, caudate, and thalamic nuclei; dorsal root ganglia cells; and large-diameter dorsal root axons. In non-neuronal hamster tissues, Prnp was detected in circulating leukocytes, heart, skeletal muscle, lung, intestinal tract, spleen, testis, ovary, and some other organs (Bendheim et al., 1992). The presence of Prnp in extracerebral tissues indicates that it's a ubiquitously expressed protein, whose physiological role is not clearly understood.

1.5.1 Structure of prion

Cellular Prion protein is encoded by the Prnp gene located on chromosome 20p13 (Sparkes et al., 1986). This gene is composed of three exons, the terminal exon containing the open reading frame (ORF) encodes a 254 amino acid containing prion protein (Das & Zou, 2016). It is synthesized in the rough ER and undergoes several posttranslational modifications: cleavage of N and C-terminal signal peptides, N-linked glycosylation at residues 181 and 197, formation of a disulphide bond between C-179 and C-214. A GPI anchor is added at residue 231 following cleavage of the C-terminal hydrophobic peptide (Stahl, 1987, (Haraguchi et al., 1989; Harris, 2003; Turk et al., 1988). Mature PRNP consisting of 209 residues is transported to the cell membrane via the Golgi complex where it is tethered by the C-terminal GPI anchor. However, brain mitochondria from 6-12 weeks wild type and transgenic (overexpressing Prnp) mice show fully processed Prion protein without the GPI anchor (Faris et al., 2017). Protease treatment of purified mitochondria suggested that mitochondrial Prp^{c} exists as a transmembrane isoform with the C-terminus facing the mitochondrial matrix and the N-terminus facing the intermembrane space. The N-terminus has five or six repeats of eight glycine rich residues (PHGGGWGQ), known as the octapeptide repeat region which can bind to Cu (II) and other divalent cations.

Prion protein from mouse brain and cultured cells bound to three and between one to four Cu atoms respectively. These results suggest that Prion can bind to variable amounts of Cu and thus exhibit antioxidant activity (Brown et al., 2001).

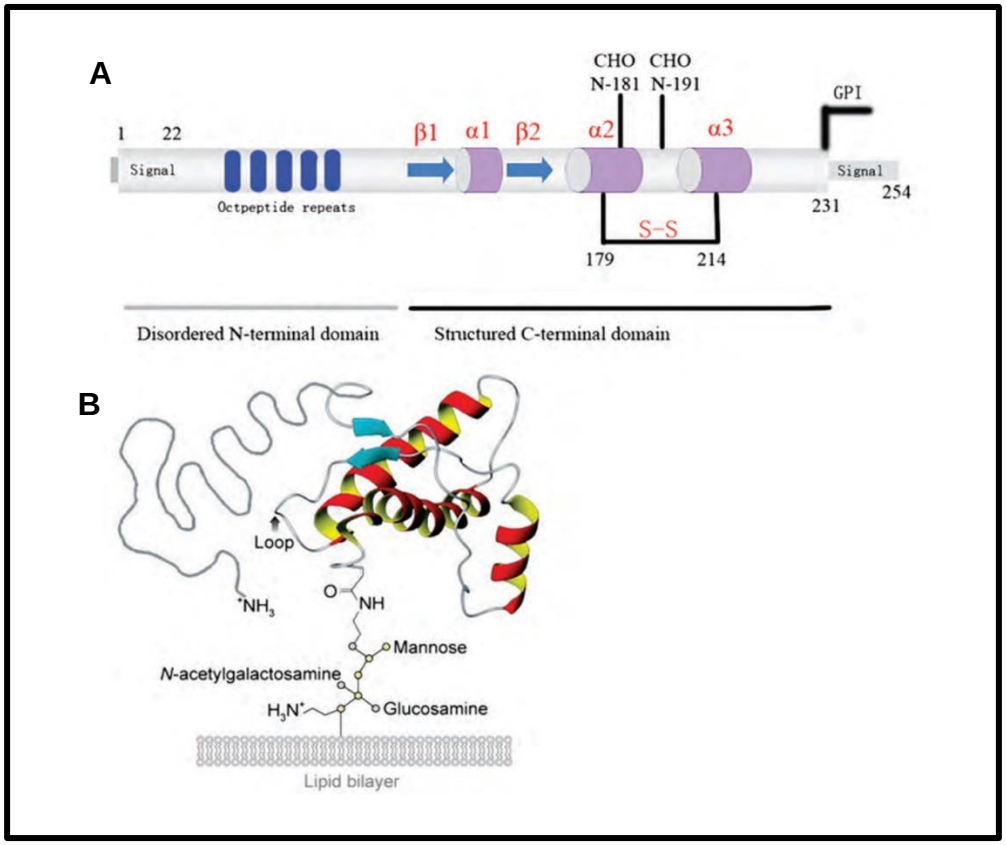

Figure 1.5. Structural features of cellular Prion protein (Huang et al., 2013). A) Primary structure of Prion showing N-terminal signal peptide (residues 1-22), Octapeptide repeats, α-helices and β-sheets, disulphide bonds (S-S), N-linked Glycosylation (CHO) and GPI tagging signal at residue 231. **B)** Tertiary structure and membrane localization of Prion

Fourier-transform infrared (FTIR) spectroscopy demonstrated that Prp^{c} has a high alpha-helix content (42%) and no beta-sheet (3%). These findings were confirmed by circular dichroism measurements. In contrast, the beta-sheet content of PrP^{Sc} was 43% and the alpha-helix 30% as measured by FTIR. N-terminally truncated Prp^{Sc} derived by limited proteolysis, designated as Prp 27-30, has an even higher beta-sheet content (54%) and a lower alpha-helix content (21%)(K. M. Pan et al., 1993).

Prp^{Sc} in purified fraction from scrapie-infected hamster brain was resistant to Proteinase K hydrolysis for 2hours at 37degrees under nondenaturing condition(McKinley et al., 1983). Prolonging the digestion resulted in concomitant decrease in both Prp^{c} and Prp^{Sc}. In 1992 Richard Bessen and Richard Marsh first identified two different Proteinase K resistant Prp^{Sc} fragments, Hyper and Drowsy, in Syrian hamsters with transmissible mink encephalopathy (Bessen & Marsh, 1994). They have different migration rates on the gel; Hyper migrates at ~21kD and Drowsy at ~19kD, presumably because they have different PK cleavage site exposed due to their different conformation, generating unique sized fragments. However, the existence of a PK sensitive Prp^{Sc} strain was by Safar et al. by conformation-dependent assay (Safar et al., 1998).

1.5.2 Conversion of Prp^{c} to Prp^{Sc}

In prion diseases the cellular Prp is converted to its β-rich scrapie counterpart but how this conversion takes place is not clearly understood and a highly debated topic. After its synthesis in the ER, the Prp^{c} is translocated to the cell membrane via the Golgi vesicles. The Prp^{c} that is misfolded during maturation in the ER, enters the cytosol of mammalian cells through retrograde transport in order to be degraded by the proteasomal complex (Ma & Lindquist, 2001). When the proteasomal action is blocked the Prp molecules aggregate in the cytosol and when the number exceeds the quality control capacity of the cytosol, some Prp^{c} is converted to Prp^{Sc} (Ma & Lindquist, 2002).

The glycosylation increases the stability of the Prp^{c}molecule as an increased amount of glycosylation provides a high energy barrier, thereby preventing the pathological conversion to Prp^{Sc} (Rudd et al., 2001). Among the di, mono and un-glycosylated

isoforms of Prp^{Sc} in sCJD, the band intensity for the diglycosylated isoform on the gel was the smallest, suggesting that most of the diglycosylated form did not convert to Prp^{Sc}. Treatment with tunicamycin to inhibit N-linked glycosylation facilitated formation of Prp^{Sc} in scrapie infected cells (Taraboulos et al., 1990).

Expression of a C-terminally truncated Prp lacking the GPI anchor, in mouse neuroblastoma cells (ScN2a), did not inhibit Prp^{Sc} formation but the Prp^{Sc} also lacked the GPI anchor (Rogers et al., 1993). It was reported by McNally and coworkers that cells expressing anchor-less Prp^{c} did not support persistent infection in scrapie-infected cells (McNally et al., 2009). Moreover, PI-PLC treatment in ScN2a cells reduced the Prp^{Sc} formation (Caughey & Raymond, 1991; Enari et al., 2001). Treatment with glimepiride that was showed to upregulate endogenous PI-PLC, significantly decreased the level of Prp^{Sc} in three infected neuronal cell lines (SMB, ScGTI and SCN2a) (Bate et al., 2009). Some Prp^{c} are internalized into endosomes from the cell membranes and again recycled back. It is in these endosomes that the Prp^{c} to Prp^{Sc} conversion takes place.

1.5.3 Transmission of Prion diseases

According to the 'protein only' hypothesis, the causative agent of transmissible spongioform encephalopathies commonly known as prion diseases is a conformational isomer of cellular Prp, a host protein predominantly expressed in brain. This protease-resistant pathological counterpart is called the Prp^{Sc} and it requires pre-existing Prp^{c} s for its autocatalytic conversion (Laurent, 1996), as Prp knockout mice are resistant to prion diseases. The BSE epidemic was fueled by BSE-prion contaminated cattle feed (Kimberlin & Wilesmith, 1994) The kuru epidemic in Papua New Guinea was caused due to ritualistic cannibalism and believed to have originated

from a case of sporadic CJD (S. Prusiner & Hadlow, 1979) Variant CJD is thought to come about by ingestion of BSE-prion contaminated food stuff. Experimental animals, non-human primates can be infected with the BSE agent through oral route. Although the source for the sheep scrapie epidemic has not been established but natural transmission through infected placenta has been suggested(Race et al., 1998). The relative resistance of prions to protease digestion probably allows a significant proportion of them to survive passage through the digestive tract (Maignien et al., 1999). M cells which transport antigens and pathogens can mediate transport of prions. Thus, after oral uptake, these infectious agents penetrate the intestinal mucosa through the M cells and reach the Payer's patches(Maignien et al., 1999) as well as the enteric nervous system (Beekes & McBride, 2000). Recent reports suggest that the myeloid dendritic cells mediate transport thorough the lymphoreticular system (LRS) (Aucouturier et al., 2001; Huang et al., 2013). Mature B cells are required for the maturation of follicular dendritic cells, the cells where prion formation and accumulation occur, and in a way, they are also contributing to amplification of prions in spleen(Mabbott et al., 2000; Montrasio et al., 2000). From the LRS and from other sites, prions move along the peripheral nervous system to reach the brain, either via the vagus nerve(Baldauf et al., 1998) or spinal cord(Bencsik et al., 2001). The prion transmission may also be modulated by polymorphic variations of the Prnp gene. For example, humans with homozygous Prnp met129 variant are more likely to contract sporadic CJD than the met129/val129 heterozygotes(Collinge et al., 1996).

1.5.4 The prion family of proteins

The prion gene family consists of the Prnp and its two mammalian paralogs Sprn (encodes Shadoo) and Prnd (encodes Doppel) which share some of the structural features with Prnp, the founder of the prion family of proteins. These three genes are supposedly evolutionarily derived by retro-transposition event of ancestral zinc transporter encoding ZIP LIV-1 genes (Ehsani et al., 2011; Schmitt-Ulms et al., 2009).

The Sprn gene is located on chromosome 10 and about 3,952 bp in size. Among the two exons, exon 1 is noncoding and the entire 444 bpSho protein coding sequence is located on exon 2. To generate $Sprn^{0/0}$ mice, this region has been targeted. The 3' UTR of Sprn gene overlaps with the transcriptionally opposite Mtg1 gene making the latter an off-target for shRNA mediated knockdown of Shadoo. Prnd, on the other hand is located on chromosome 20, approximately 20kb downstream of the cellular Prnp gene. It is predominantly expressed in testis. Unlike Shadoo and Prp^{c}, Doppel (Dpl) has a neurotoxic role as its ectopic expression can cause neurodegradation (Passet et al., 2012). Both sho and dpl are glycosylated membrane-bound proteins having molecular weight around 14.522kD and 20.293kD respectively. Increased Prnp gene expression in extra-embryonic membranes is detected as early as 6.5days post coitum, D6.5, when there is transition to oxidative metabolism (MIELE et al., 2003). Mouse embryonic stem cells are reported to express all three genes (Miranda et al., 2011) and Sprn is suspected to occur in mouse trophectoderm (Passet et al., 2012). Sprn and Prnd expression is detected in mouse embryos at days 10.5 and 13.5(Young et al., 2011).

1.6 Role of Prion in embryonic development

Expression of cellular prion protein and its paralogs have been reported in placenta and early embryos. Potential role of Prp^c in placental physiology is suggested by the observation that deregulation of its expression (knockout or overexpression) leads to pathological condition. One of the most studied, yet mysterious human gestational disease is preeclampsia. Preeclampsia is characterized by gestational hypertension and proteinuria and is the source of neonatal mortality (Sibai et al., 2005). It is often associated with oxidative stress and abnormal placental levels of copper and zinc with pre-term gestation and IUGR. Preeclamptic placentas were found to overexpress Prnp mRNA as well as Prnp protein (Nishizawa et al., 2007). However, this overexpression is restricted to the syncytiotrophoblast and cytotrophoblast layers of the placenta (Makzhami et al., 2014). It is hypothesized that this rise in Prnp level can be a compensatory mechanism induced by preeclamptic state. The Prp^c N-terminal flexible domain can bind to divalent cations like Cu (II) and Zn (II) (having greater affinity for copper) and thus plays a role in internalization of ions, signal transduction and, oxidative stress due to its putative Cu^{2+}/Zn^{2+}superoxide dismutase (SOD) like activity. It is reported by Alfaidy et al. in 2013 that siRNA mediated knock down of Prp^c increased ROS production in HTR cells upon Cu treatment. Overexpression of Cu high-affinity-binding Prp^c leads to overchelation of Cu that affects the activity of other Cu/Zn SOD enzymes. As a consequence, ROS production and cell death increased (Alfaidy et al., 2013).

Passet et al. performed comparative histological analysis of E7.5 mouse embryos having FVB/N genetic background. Comparison was done between FVB/N $Prnp^{KO}$ and FVB/N $Prnp^{KO}$ embryos that were injected at the zygotic stage with either—FG12 (used as control as it encodes only GFP) or LS2 (shRNA targeting Sprn) lentiviral

solutions. All the in vitro manipulated embryos showed delayed development. Although the FG12 injected embryos did not show any other defect except minor haemorrhage, the LS2 injected embryos were characterized by highly reduced and disorganized ectoplacental cone and also fragmented invasive chorionic trophoblast cell layer(Passet et al., 2012). The embryonic lethality for FVB/N $Prnp^{KO}Sprn^{KD}$ embryos is reported to occur at a stage at which the cells of trophoblastic lineage proliferate and differentiate to provide adequate nutrients and metabolic exchanges to the fetus via maturing and developing the placenta. Surprisingly, double knockout mice ($Prnp^{0/0}$ $Sprn^{0/0}$) lacking both Prp^{c} and Sho are fertile and viable upto 690days of age (Daude et al., 2012). This difference in the two results might occur due to i) using mice with similar but not identical genetic background (FVB/N and FVB/NCr x 129Pas used for knockdown and knockout studies respectively), ii) in theoretical point of view, constitutive absence of Sho protein in early embryogenesis might induce the expression of a protein with Sho-like activity, iii) knockdown strategy targeting the 3'UTR of Sprn mRNA could well perturb the expression of the transcriptionally opposed Mtg1 gene (Passet et al., 2012). However, the latter can be dismissed as shRNA targeting sequences outside the Mtg1 overlapping region also gave the same result (Young et al., 2009). Comparative transcriptomic analysis of E6.5 and E7.5 shadoo-knockdown embryos with their wild-type counterparts suggested that shadoo has functions complementary but not necessarily overlapping to that of Prp^{c}, associated with cell movement, haematopoeisis etc. (Passet et al., 2012).

All these observations gave rise to several unanswered questions which set up the bedrock for our own research. The questions are as follows: -

- What are the expression dynamics of Prion at the maternal-fetal interface?
- By what mechanism does it affect development?

- Whether or not there is some cell or tissue specific function of Prion?
- What are the upstream and downstream effectors of Prion?

We laid down specific objectives, that aim to answer each question

1. To elucidate the dynamics of cellular Prion in the uteroplacental compartment at different stages of rat gestation.
2. To assess the phenotypic change in VSMC by gain or loss of function of Prnp.
3. To identify the signalling pathways regulated by Prion to confer the proposed phenotype.
4. To assess the regulation of Prnp expression in VSMC by trophoblast derived factors.

CHAPTER 2

MATERIALS AND METHODS

2.1 Animal handling and tissue collection:

To obtain timed pregnant rats, 8 weeks old sexually mature Sprague Dawley female rats were caged overnight with 10 weeks old fertile males. For every one male, two female rats were caged. Next day morning, vaginal smears were collected from each female, in clean slide on sterile saline and observed under microscope. Successful copulation was assured by presence of sperm in the vaginal smear and it was assigned as day 0.5 of pregnancy. Animals were euthanized on days 11.5, 13.5, 16.5 and 19.5 of pregnancy and metrial gland and whole conceptuses were collected separately. Metrial glands were snap-frozen in liquid nitrogen for RNA and protein isolation and whole conceptuses were chilled in dry ice-cooled hexane for cryo-sectioning. All the tissues were stored in -80ºC freezer until used. All procedures for handling and experimentation with rodents were done with prior approval of the IICB Animal Care and Use Committee and in accordance with the regulations set forward by the Committee for the Purpose of Control and Supervision of Experiments on Animals, Govt. of India (http://cpcsea.nic.in).

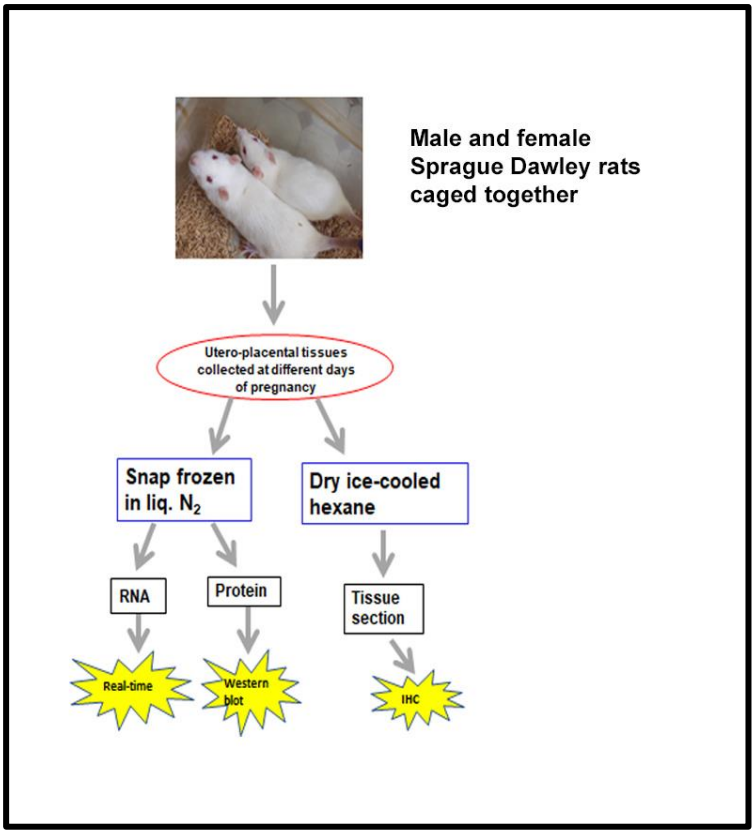

Figure 2.1. Flow chart showing strategy for mating rats and collection of utero-placental tissues

2.2 Immuno-histochemistry

Immuno-histochemical analyses were performed directly on 10-micron tissue sections prepared with the aid of a cryostat (Leica, USA). Tissue sections were fixed in ice-cold acetone for 5 minutes, and incubated with 0.3% ice-chilled H_2O_2 in phosphate buffered saline (PBS) for 5 minutes to block the endogenous peroxidase reaction. Excess H_2O_2 was removed by gentle wash with PBS. Non-specific binding was blocked by incubation with 1.5% normal goat serum in PBS for 1hr. Excess blocking agent was gently soaked from the sections, with a paper towel and then exposed for 1 hr to anti-PrnP antibodies in 1:600 dilution in PBS. Unbound antibodies were washed with 3 changes of PBS, each for 5 minutes followed by incubation with biotinylated anti-rabbit secondary antibodies for 30 minutes (Vector laboratories, USA) diluted in PBS (0.5µl in 100 µl). Samples were then washed three times with PBS for 5 minutes each and were incubated with ABC reagents (Vector laboratories, USA) for

30 minutes. Sections were washed again three times with PBS for 5 minutes each and were developed with AEC reagents (Vector laboratories, USA) in dark and were monitored continuously under microscope until specific reddish-brown colour developed. Samples were dipped in tap water and then counterstained with haematoxylin (SIGMA, USA). Stained tissue sections were mounted on coverslips and images captured with a Leica microscope equipped with a CCD camera and Leica Application Suite X (LAS X).

2.3 Immuno-fluorescence staining

Tissue sections were fixed in ice-cold acetone for 5-10 min, washed with PBS. Background signal was blocked with blocking buffer containing 5% goat serum and 0.3% Triton-X-100 in PBS for 1hr. Sections were then incubated with either H-caldesmon (1:200), or Prnp (1:200) for 2hrs at room temperature, and overnight at 4 degrees, respectively. Samples were then washed three times with PBS, 5min each, to remove unbound antibodies, followed by incubation with FITC conjugated anti-rabbit IgG (1:200 dilution) (SIGMA, USA) or TRITC conjugated anti-rabbit IgG (1:1000 dilution) (SIGMA, USA) for 1.5hrs at room temperature. Sections were again washed in three changes of PBS, followed by nuclear staining with Hoechst at a concentration of 2µg/ml. Sections were again washed 5 times with PBS before mounting with Fluoroshield solution (SIGMA, USA). Images were captured with a Leica microscope equipped with a CCD camera and Leica Application Suite X (LAS X).

2.4 RNA preparation, reverse transcription PCR and Real Time PCR analysis

2.4.1 Total RNA isolation from tissues and cells

Total RNA from tissues or cells were isolated using TRIzol reagent (Invitrogen, USA), as per the manufacture's protocol. Tissue samples were homogenized and cultured cells were scraped in ice-cold trizol. Phase separation was done by adding chloroform and centrifuged at 12000 rcf for 15min at 4ºC. The upper aqueous phase was collected in a separate DEPC-treated tube and to it 100% isopropanol was added, inverted slowly for few times for uniform mixing, and allowed to stand at room temperature for 10min. RNA was precipitated from the aqueous phase using isopropanol by centrifugation at 12000 rcf for 10min at 4ºC, followed by washing the pellet with 75% ethanol. The RNA pellet was dissolved in nuclease-free DEPC treated water.

2.4.2 Preparation of first-strand cDNA from total RNA

First-strand cDNA was synthesized with 2.5µg of total RNA using M-MLV Reverse Transcription enzyme (Invitrogen, USA), oligo dT primer and 10mM dNTP mix (Invitrogen, USA). Reaction steps include denaturation at 65ºC for 5 min, then quick chill in ice for 2 min, followed by oligo dT primer annealing and eradication of RNase contamination at 37ºC for 2 min and extension with M-MLV RT enzyme at 37ºC for 53 min. Reaction is stopped by heating at 70ºC for 15 min. After completion of the reaction, residual RNAs were removed using RNase H enzyme (Ambion, USA). The cDNAs were stored in -20ºC for further use.

2.4.3 Quantitative real-time PCR analysis

Ten-fold dilution of cDNAs and Power SYBR GREEN PCR Master Mix (Applied Biosystems, USA) was used in the real-time PCR reaction. Reactions were run using a 7500 Real-Time PCR System (Applied Biosystems, USA). Conditions included initial

holding stage (95°C for 10 min) and 40 cycles (95°C for 15 s and 60°C for 1 min) followed by a dissociation stage (95°C for 15 s, 60°C for 1 min, and then 95°C for 30 s). Primers used in this study are listed in Table 1. Expression of rpL7 RNA was used as an endogenous control. At least three different biological replicates were used. Samples were normalized to the control sample for each gene. The amount of a specific mRNA was normalized relative to the amount of rpL7 ($\Delta Ct = Ct_{gene} - Ct_{rpL7}$). Fold change of gene expression was measured by using $2^{-\Delta\Delta Ct}$, where $\Delta\Delta Ct$ denoted the change in ΔCt values between samples and reference sample. Error bars represents standard error of mean from three different biological replicates

Table 1: Sequence of primers used for real time PCR reactions

Template	Primer Sequence (5' to 3')		Gene bank accession no.
rPrnp	Forward	AGTGTACTACAGGCCGGTGGAT	NM_012631.3
	Reverse	ACCACACGCTCCATCATCTTC	
rOsr1	Forward	TGCGGTGTCCAGCCTAATG	NM_001106716.3
	Reverse	AAGGCCAGGTTAGCGAAATCA	
rrpL7	Forward	GCCCTCAAGACACTGCGAAA	NM_001100534.1
	Reverse	TGGTTCTGCGGGCACATAG	

2.5 Protein isolation, estimation, and Western Blot analysis

2.5.1 Total protein isolation from tissues and cells

Total protein from tissues and cells were isolated with in ice-cold 1X RIPA buffer (20 mM TrisHCl, pH 7.5, 150 mM NaCl, 1mM EDTA, 1mM EGTA, 1% NP40, 1% sodium deoxycholate, 2.5 mM sodium pyrophosphate, 1mM β-glycerophosphate, 0.2

mM PMSF, and 1mM sodium orthovanadate) supplemented with protease inhibitor cocktail (Cell Signalling Technology, USA) and 0.2% PMSF. The homogenate was then centrifuged at 14000 rcf for 10min at 4°C and the supernatants were collected, aliquoted and stored at -80°C until further use.

2.5.2 Protein estimation using Bradford assay

Protein samples were quantitated by Bradford protein assay kit (Bio-Rad, USA) as per manufacturer's instructions using micro-assay procedure in microtiter plates. Standard curve was prepared with six known concentrations of BSA ranging from 8 µg/ml to 80µg/ml. In each separate tube, 140 µl of dye was mixed with 560 µl of either standard or sample, mixed well and dispensed 200 µl in the microtiter plate. Each standard and samples were used in triplicate. The plate was incubated at room temperature for ~5 minutes. At the end of incubation period absorbance was measured at 595 nm using a multi-mode plate reader (PerkinElmer, USA). Protein concentrations were determined from the standard curve

2.5.3 Western Blot analysis

Protein samples at required amount were denatured by boiling in a water bath for 5 minutes with SDS sample buffer (62.5 mM Tris-HCl, pH6.8, 2.5% SDS, 0.002% Bromophenol blue, 5% β-Mercaptoethanol, 10% glycerol) and then centrifuged briefly. 20 to 70 µg of protein extracts were loaded on SDS-polyacrylamide gel under denaturing condition and transferred onto PVDF membranes (Millipore, USA) under 4-degree temperature and at 100 volts. List of antibodies used in this study are given in table 2. Membranes were blocked with either 2% or 5% skimmed milk for 1hour, then incubated overnight at 4°C with primary antibodies (diluted to required concentration) on an orbital shaker. Primary antibodies were diluted in either BSA or

skimmed milk as per mentioned in the datasheet. Membranes were rinsed and incubated with HRP-conjugated secondary antibodies for 1.5 hours at room temperature on an orbital shaker. An ECL kit, Clarity Max^{TM} Western ECL Substrate (Biorad, USA) was used to develop chemiluminescence signals associated with protein bands. Images were acquired with the Chemidoc Imaging System (UVP, USA).

Table 2: List of antibodies used in Western blot analysis

Name of the antibody	**Catalogue No.**	**Dilution used**
Prnp	14025 (CST)	1:1000 (3% BSA)
FAK	3285 (CST)	1:1000 (5% BSA)
PDGFR-β	3169 (CST)	1:1000 (5% BSA)
Caspase-3	9665 (CST)	1:1000 (5% BSA)
Cleaved Caspase-3	9664 (CST)	1:1000 (0.5% milk)
Caspase-8	4790 (CST)	1:1000 (5% BSA)
Cleaved Caspase-8	AHP967	1:1000 (0.5% milk)
Bax	2772 (CST)	1:1000 (5% BSA)
Bcl-xL	2764 (CST)	1:1000 (0.5% milk)
GAPDH	5174 (CST)	1:4000 (5% BSA)
OSR1	Sc-376545 (Santa cruz)	1:200 (0.8% milk)
DR4	BML-SA225-0100 (Enzo Life sciences)	1:1000 (5% BSA)
Anti-Rabbit Secondary antibody HRP- conjugated	A120-101P (Bethyl laboratories)	1:10,000 (TBS-T)

Anti-mouse Secondary antibody HRP- conjugated	A90-134P (Bethyl laboratories)	1:10,000 (TBS-T)

2.5.4 Co-immunoprecipitation

Immuno-precipitation of proteins was done using Pure Proteome protein A/G magnetic beads (Millipore, USA). 250 µg of cell or tissue lysate was incubated with Prnp antibody at 1:50 dilution overnight at 4ºC with continuous mixing. 25 µl of uniformly suspended Pure Proteome protein A/G magnetic beads was washed with 500 µl of binding buffer (PBS, pH7.4 supplemented with 0.05% Tween20) with the aid of a magnetic stand (Millipore, USA). The magnetic beads were then incubated with the protein-antibody solution for 2 hours at room temperature with continuous mixing to capture the immune complex. The unbound fraction was gently removed with the help of a pipette and tip. The beads bound with the anti-antibody complex were then washed three times for 30 seconds each with 500 µl of binding buffer with the aid of the magnetic stand. After the last wash 40 µl of 1x SDS sample buffer was used to resuspend the beads and was heated at 70ºC for 8 min. The beads were then captured with the magnetic stand and the supernatant was used for western blotting.

2.6 Cell culture

2.6.1 Culture of rat aortic smooth muscle cell line (A7r5)

A7r5 (rat thoracic aortic smooth muscle cell) cell lines were obtained from ATCC (USA). A7r5 cells were cultured in complete growth medium consisting of, DMEM high glucose basal media (D7777, SIGMA, USA) supplemented with 10% FBS and 1% Penicillin-Streptomycin (Invitrogen, USA). Cells were passaged at regular intervals in 1:2 ratio. For sub-cultivation, used media was discarded and cell monolayer was briefly

rinsed with sterile DPBS to remove traces of serum. The cells were incubated with 0.25% Trypsin-EDTA (Invitrogen, USA) for 2min, then gently tapped to dislodge any clumps of cells, followed by neutralization with 5ml of complete growth medium. Cells were cryopreserved in complete growth medium supplemented with 5% DMSO and stored in liquid nitrogen vapour phase.

2.6.2 Culture of HEK293T cell line

HEK293T (Human Embryonic Kidney 293 cells containing SV40 large T antigen) were obtained from ATCC (USA). HEK293T cells were cultured in complete growth medium consisting of DMEM (D7777, SIGMA, USA) supplemented with 10% FBS, 2 mM L-glutamine and 1% Penicillin-Streptomycin (Invitrogen, USA). Cells were passaged at regular intervals in 1:5 ratio. For sub-cultivation, used media was discarded and cell monolayer was briefly rinsed with sterile DPBS to remove traces of serum. The cells were incubated 0.25% Trypsin-EDTA (Invitrogen, USA) for 3min, then gently tapped to dislodge any clumps of cells, followed by neutralization with 5ml of complete growth medium. Cells were cryopreserved in complete growth medium supplemented with 5% DMSO and stored in liquid nitrogen vapour phase.

All the cells were maintained in presence of 5% CO_2 at 37°C in a humidified incubator.

2.6.3 Isolation of rat primary trophoblast cells and co-culture with VSMC

Junctional zones, isolated from rat placentas on E16.5, were thoroughly washed with sterile DPBS and minced into fine pieces. They were further minced in presence of 0.05% Trypsin-EDTA (0.5ml) for 2 minutes. Then 5 ml 0.05% Trypsin-EDTA was added and the suspension was incubated in presence of 5% CO_2 at 37ºC for 15 min. Following incubation, the cell suspension was pipetted vigorously until a slurry-like

appearance was obtained. Trypsin neutralization was then performed using 5 ml trophoblast media [RPMI-1640 (Sigma-Aldrich) supplemented with 20% FBS [Invitrogen] 1% Penicillin-Streptomycin [Invitrogen], 1% Glutamax [Invitrogen], 1mM sodium pyruvate [Sigma-Aldrich] and 100µM β-mercaptoethanol [Sigma-Aldrich]. Cells were then washed three times with DPBS and the pellet was resuspended in 5 ml RBC lysis buffer (1.5 M NH_4Cl, 140 mM $NaHCO_3$, 10mM EDTA, pH 7.3), incubated for 5 minutes at room temperature. 10 ml DPBS was added to the cell suspension and centrifuged at 1000rpm for 5min. The cell pellet was resuspended in fresh TS media and strained using 70 µm cell strainer to obtain single cell suspension. $2x10^5$ cells were plated on each culture insert (BD Falcon, USA) which were placed on companion plates (BD Falcon, USA) containing 24 hrs culture of A7r5 cells. After 48hrs of co-culture RNA and protein was isolated from the A7r5 cells.

2.7 Knockdown experiment

2.7.1 Designing and cloning of shRNA oligos in pLKO.1 vector

shRNA oligos targeting exons of coding region of the transcripts were designed using the Broad institute portal https://portals.broadinstitute.org/gpp/public/seq/search. The oligos having high intrinsic scores were selected and purchased from IDT (USA). The sequence of the oligos is given in Table 3.

Individual shRNAs were cloned in separate pLKO.1 vector (Addgene, USA). Forward and reverse oligos were annealed using 20 µM of each of the oligos in 50 µl of NEB buffer2, by boiling for 4 minutes followed by slow cooling at room temperature. The vector was digested with EcoR1 and Age1 enzymes and ligated with shRNA oligos

having compatible sticky ends in a 1:10 molar ratio with NEB T4 Ligase enzyme (NEB, USA) following the standard ligation protocol for 16ºC for 16hrs. One Shot® Mach1t1™ chemically competent E. coli (Invitrogen, USA) cells were transformed with the ligated mix following standard protocol. The transformants were then plated on LB agar plates containing ampicillin as a selection marker. The plates were incubated at 37ºC in BOD incubator for 16hrs. Next day, 2 single isolated colonies from each plate were selected to inoculate 5 ml LB+Ampicilin broth which was incubated at 37ºC in an incubator shaker for 16hrs. From the suspension culture, glycerol stock was made and stored at -80°C for future use and plasmid DNA was isolated using plasmid miniprep kit (Qiagen, USA). The DNAs from each clone were quantified and restriction digestion was performed using EcoR1 and Age1 to verify the presence of shRNA insert.

Table 3: Sequence of PrnP and Osr1 shRNA oligos

	Sequence (5' to 3')	
Prnp-shRNA1 (targets exon 3)	Forward oligo	CCGGTCGTGCACGACTGTGTCAATACTCGAGTATTGACACAGTCGTGCACGATTTTTG
	Reverse oligo	AATTCAAAAATCGTGCACGACTGTGTCAATACTCGAGTATTGACACAGTCGTGCACGA
Prnp-shRNA2 (targets exon 2)	Forward oligo	CCGGGTGGCAGGACTCCTGAATATACTCGAGTATATTCAGGAGTCCTGCCACTTTTTG
	Reverse oligo	AATTCAAAAAGTGGCAGGACTCCTGAATATACTCGAGTATATTCAGGAGTCCTGCCAC
Prnp-shRNA3 (targets between exon1 and 2)	Forward oligo	CCGGTTTCAACCCAACTGAAGTATTCTCGAGAATACTTCAGTTGGGTTGAAATTTTTG
	Reverse oligo	AATTCAAAAATTTCAACCCAACTGAAGTATTCTCGAGAATACTTCAGTTGGGTTGAAA
Osr1-shRNA	Forward oligo	CCGGCTACGGGACCACAGATATATTCTCGAGAATATATCTGTGGTCCCGTAGTTTTT

(targets between exon1 and 2)	Reverse oligo	AATTCAAAAACTACGGGACCACAGATATATTCTCGAGAATATATC TGTGGTCCCGTAG

2.7.2 Preparation of lentiviral particles carrying shRNA

For producing lentiviral particles, HEK293T cells ($7x10^5$ cells) were plated on 6 cm tissue culture plates and incubated at 37°C, 5% CO_2 overnight. Next day, prior to transfection, transfection cocktail was prepared using 1µg pLKO.1 shRNA plasmid, 750 ng psPAX2 packaging plasmid, 250 ng pMD2.G envelope plasmid (Addgene, USA) to a final volume of 100µl serum free OPTI-MEM. In a separate tube 100µl Master Mix was prepared with 6µl Fugene and 94µl OPTI-MEM and incubated for 5min. The master mix was added to transfection cocktail to make a final volume of 200µl and allowed to stand for 20-30min. Following the incubation period DNA:Fugene mix was added drop wise on cells and spread by gentle swirling. Next day, the transfection reagents were removed and replaced with fresh serum containing media. Media containing viral particles were harvested after every 48h in two rounds. Two batches of media containing viral particles were pooled, mixed uniformly and stored in small aliquots at -80°C.

2.7.3 Transduction of lentiviral particles in A7r5 cell line

Cells were plated on 35mm dishes and allowed to reach ~ 70% confluency overnight ($1x10^5$ cells per dish). Next day morning, the media was removed and fresh media supplemented with lentiviral particles containing empty vector or shRNAs were added in separate dishes. After 24hrs the lentiviral containing media was discarded

and replenished with fresh medium. After 48hrs, cells were harvested for RNA and protein isolation and real-time PCR and Western blot was done to confirm down regulation of Prnp and Osr1.

2.8 Cloning and characterization of rat Osr1 cDNA

Rat Osr1 full length cDNA was cloned in pCAG-DsRed vector (Addgene, USA) using directional cloning strategy. RNA isolated from heart ventricle was reverse-transcribed using MMLV-RT (Invitrogen, USA). Full length rat Osr1 (NM_001106716.3) cDNA was amplified from the ventricular cDNA pool using LA-Taq DNA polymerase (TaKaRa, Japan). Primers used were Forward primer: 5'-TATA**GGTACC**AATGGGCAGCAAAACCT-3' and Reverse primer: 5'-TATA**GCGGCCGC**TTAGCATTTGATCTTG-3' having KpnI and Not1 Restriction sites respectively (marked in bold). Following PCR reaction, the product was purified through DNA binding columns (Qiagen, USA) and was digested using KpnI and NotI (Thermo Scientific, USA) for 20min at 37˚C followed by purification using DNA binding column. The vector was digested with the same restriction enzymes, followed by dephosphorylation using Antarctic phosphatase (New England Biolab, USA) treatment for 30min at 37ºC. The vector was then gel purified. The vector and the insert were then ligated using T4 DNA ligase (NEB, USA) taking vector to insert in molar ratio of 1:10 at 16ºC for 16hrs. One Shot® Mach1t1™ chemically competent E. coli (Invitrogen, USA) cells were transformed with the ligated mix following standard protocol. A brief heat-shock was given to the cells at 42ºC for 30seconds, then allowed to recover for 1hr in SOC media. The transformants were then plated on LB agar plates containing ampicillin as a selection marker. After confirming the correct clone, the DNA

was sequenced for further confirmation of cloned DNA sequence. 1µg of the purified DNA was used to transfect rat aortic smooth muscle cell line A7r5. Transfection was performed using lipofectamine 2000 reagent (Invitrogen, USA) as per manufacturer's instruction. Transfected cells were incubated for 48 h and were subjected to RNA and protein isolation as described before. Over expression of Osr1 was assessed using real time PCR and immunoblotting.

2.9 Functional assays

2.9.1 Scratch wound assay

A7r5 cells were seeded at a density of $1x10^5$ cells per ml in 35mm dish such that after 24hrs they form a confluent monolayer. Cells were treated with either control vector, or a cocktail of shRNA containing lentiparticles to downregulate *Prnp.* Next day, the virus containing media was replenished with fresh media and a scratch was made using sterile cell combs (cell comb scratch assay kit, Merck Millipore) to form a cell free area of approximately 700µm of width. Images of different fields along the scratch were taken at two time points, immediately after scratch (t=0 hr) and 24 hours after scratch (t=24 hr). The length of the wound was measured at these time points, which corresponds to the migration ability of the cells under the two different conditions.

2.9.2 Invasion assay

A7r5 cells were seeded at a density of $1x10^5$ cells per ml in 35mm dishes. Next day they were treated with control and shRNA cocktail as described under 'scratch wound assay' and were cultured for 24 hrs after transduction. Cells were trypsinized and seeded on ECMatrix™ inserts (Cell Invasion Assay kit, ECM550, Merk Millipore)

at a density of $1x10^5$ cells per insert in 300 µl of serum-free media. Media with 10% FBS was added to the lower chamber. After 24 hours of migration, the residual media as well as non-invaded cells were removed from the inner surface of the inserts using cotton swabs. The inserts were dipped in staining solution for 25 min and the background was destained with several changes of distilled water. Images of invaded cells were taken and counted under a Leica Microscope. The cells were quantified by dissolving the stain at the lower surface in 10% acetic acid and measuring the absorbance at 560nm using a multi-mode plate reader (PerkinElmer, USA).

2.10 Flow cytometric analysis to detect early apoptosis using AnnexinV-PI staining

A7r5 cells were seeded at a density of $0.5x10^3$ cells per ml so that they reach nearly 70% confluency after 24hrs, when they were transduced with either control or shRNA cocktail lentivirus. 48 hrs following transduction, cells were trypsinized and harvested at a concentration of $3x10^5$/ml. Cell suspension was again centrifuged to remove the residual media and the pellet was dissolved in 96µl of Annexin V binding buffer followed by Annexin V staining for 15 min at 4ºC. Propidium iodide was added as per the manufacturer's instruction and incubated for 5min (Annexin V FITC Early Apoptosis Detection assay kit, 6592, Cell Signaling Technology, USA). Percentage of cells undergoing early apoptosis were analyzed using a Flow cytometer (LSR, Fortessa, BD, USA).

To detect TRAIL-induced apoptosis, A7r5 cells transduced with either control or sh-Prnp lenti-particles, were treated with recombinant murine TRAIL (Preprotech, USA) at a concentration of 10ng, 50ng and 100ng per ml for 24 hrs at 37ºC followed by

Annexin V and PI staining as described above. Percentage of cells undergoing early apoptosis were analyzed using a Flow cytometer (LSR, Fortessa, BD, USA).

2.11 Total RNA sequencing and in-silico pathway analysis

Total RNA from control and Prnp knockdown A7r5 cells were isolated using TRIzol reagent (Invitrogen, USA) as per the manufacturer's protocol. The total RNA was column purified using RNeasy MinElute cleanup kit (Qiagen, USA). 2-3µg of purified RNA from both the samples, with $A_{260}/_{280}$ ratio >= 1.95 were then subjected to Total RNA sequencing, and a bulk data in the form of fastq files was generated. The generated fastq files were initially quality controlled by using TrimGalore. Quality-controlled fastq files were mapped to *Rattus norvegicus* mRatBN7.2 (Ensembl 104) genome by using the STAR aligner. Generated BAM files were processed by using SAMtools and featureCounts to generate a count table. The generated count table was processed by using the DESeq2 package in R. Genes with greater than 0.5 or less than -0.5 log2foldchnage and Pvalue <0.05 were considered significant. Further, clusterProfiler package was used to carry out GO enrichment analysis on all significant genes. The genes of interest were were VST transformed and plotted using pheatmap package, and EnhancedVolcano package was used to generate the volcano plot.

Table 4: Sequence of primers used for validation of RNA-Seq result

Template	Primer Sequence (5' to 3')		Gene bank accession no.
rKi67	Forward	GAAGAGCCCATACCACAAAGA	NM_001271366.1
	Reverse	CTGTGCCGAAGACTCCTTAAA	
rAtf4	Forward	GCCATCTCCCAGAAAGTGTAATA	NM_024403.2
	Reverse	GGAATGATCTGGAGTGGAAGAC	

rIl6st	Forward	ATGGACACCGCCATCTAAAC	NM_001008725.3
	Reverse	CTCTCCAGTAGGCTTCCTCTTA	
rCcnd2	Forward	TCAAGTGCGTGCAGAAGGAC	NM_022267.2
	Reverse	CTCCAGCCAAGAAACGGTCC	
rCcdc47	Forward	ATGGAGGCTTTGCTACCCCT	NM_001013974.1
	Reverse	AAGTTCTCTTCCACGCGT	
rJdp2	Forward	GCCAGATGCCGGAACAAGAA	NM_053894.3
	Reverse	GCTGCTGCCTCTCAAGCT	
rSlc7a1	Forward	TGCTGTGATGGCCTTCCTCT	NM_001399982.1
	Reverse	GGTTGTTCTGGCTGGTACCG	
rDnmt3a	Forward	CTCGCTGGGTCATGTGGTTC	NM_001003958.1
	Reverse	ATGGCTTTGCGGTACATGGG	
rCdca4	Forward	GGAAGCCTTCAGAAGTCCCT	NM_001037214.1
	Reverse	TCCTGTTAGCACTGTGTCCA	
rLonp1	Forward	TATCATCGCCCTGAACCCTC	NM_133404.1
	Reverse	CATCTTGCAGCTCATGGGAC	
rAngel1	Forward	CAGTACAATGGGATGCCAGC	NM_001108717.1
	Reverse	TTGGGATGACAGGAGGTGAC	
rNrap	Forward	CTCAGTACCACGTCTCCCTC	NM_001113743.1
	Reverse	CCCACTCCACCTTCATGTCT	
rAgap1	Forward	CGCTCCTACTCAGTCTCCAG	NM_001401593.1
	Reverse	CTGCTGGAGATACTTGGGCT	
rPvr	Forward	CGCTCCTACTCAGTCTCCAG	NM_017076.2
	Reverse	CTGCTGGAGATACTTGGGCT	
rRhobtb1	Forward	AGTTGGCGCAGTTTCACAAT	NM_001107622.2
	Reverse	GGTGGCGTTCAAAGTACTCC	

rFrem1	Forward	TTGATCCAAGGGTCCATGCT	NM_001411535.1
	Reverse	TGAAGGAAGCCAGAGACAGG	
rLimk1	Forward	GGGCATCATCAAGAGCATGG	NM_031727.2
	Reverse	AGTTGAGGTCTCGGTGGATG	
rZfp3651	Forward	TCTCATCGAGCAGGAAGTCC	NM_001025145.1
	Reverse	CTCGCTCATCCTTGGCTTTC	
rDdx5	Forward	AGTCAGAGGTCACAACTGTCCAAA	NM_001007613.1
	Reverse	TCCAATCCACTGAGAGCAACTG	
rActr3	Forward	GACTGTGGCACGGGATATACAA	NM_031068.1
	Reverse	TCATCCACGCCTTTCATCAC	
rLaptm4a	Forward	ACAAAGATGACCTCCTGGCATT	NM_199384.3
	Reverse	CAATCTCTGGCACATTTCTATTGTTG	
rTacc1	Forward	GCTTTTGCTCTGCCACTGGTA	NM_001004107.4
	Reverse	CGGCTCCTTCATCCTGAGAA	
rRnf145	Forward	TTTCCTGACAAGCATCGCCG	NM_001105778.3
	Reverse	AGGCTCGATATCCCTGCA	
rNptn	Forward	ACGCTGGGTTTGTCAAGTCG	NM_001413347.1
	Reverse	CCGGTTGACTTCTGCGTACC	
rCapza2	Forward	GGGTCTGCACTGTGTATGGC	NM_001009180.3
	Reverse	CTGGGTGGTGGAAGGAGTGA	
rCox6c	Forward	GTTGTGGCCCTAGGAGTTGC	NM_019360.2
	Reverse	GAAAGACACCAGCCTGCCTC	
rBcl2l13	Forward	AACGTCTTGGCAGTCAGAGA	NM_001398849.1
	Reverse	CCGCTGCTATCTAGGCTCTT	
rTmem18	Forward	ACCTGCTGTGCCTACTTCTC	NM_001007748.1
	Reverse	CCAGTTCATTGCAGCCACTT	

rPak4	Forward	TGAGGTGGTGATCATGAGGG	NM_001106238.1
	Reverse	TCATTCATCCTGGTGTGGGT	
rAktip	Forward	GCAAACGAGCTGAAGGTGAA	NM_001011926.1
	Reverse	AGGCTTCGATATGGGCAGAG	
rSpsb1	Forward	GTGTCCTACGATGTCCAGCT	NM_001107994.2
	Reverse	ACGTGTGTACCCAACTTTGC	
rUblcp1	Forward	CCCAGAGCGCCAGAAATTAC	NM_001014117.2
	Reverse	CTTCCAAGCTCTCCTCACGA	
rCggbp1	Forward	CCGCCTGCTAGAAATCGTTC	NM_001105900.1
	Reverse	GCGAACATGATTCAGCACCA	
rSpcs3	Forward	TGCTCTGAACCAAGTTGTCC	NM_001191073.1
	Reverse	CCCTTGAGGCCATTTCCATC	
rMtfr1l	Forward	AAACTACCTGCAGCTCGTCT	NM_001013935.1
	Reverse	GTAAACTCCGGCTCAGGTCT	
rOlfml3	Forward	TTCAGGAAGAGTGGACCGTC	NM_001107708.1
	Reverse	TTCTCATTTCTCCGGCCCTT	
rKpna6	Forward	TTGCCTCTGGAACCTCTCAG	NM_001015029.2
	Reverse	TGTTTCCAAGAGCCCAGACT	
rTmem87b	Forward	TCGCCTGCTTGTGATCATTG	NM_001191854.1
	Reverse	GACACCTTCAATGGCTGCAA	
rScarb2	Forward	GCTGGCTTCTGTATACCCGA	NM_054001.2
	Reverse	ACTTCTCGTCGGCTTGGTAA	
rSsr2	Forward	TAGCCGTCAGTCAAGCAGAA	NM_001106442.1
	Reverse	AATTCCACGTCTAATGCCGC	
rSfxn1	Forward	CTTCAATGCCGTGGTCAACT	NM_001012213.1
	Reverse	CGACACATGCTTGGTTAGGG	
	Forward	CGCTCCCTAACCTCCAGAAT	NM_019302.1

rCrk	Reverse	CTTCCCACTGACCACTCACA	
rDdhd2	Forward	GCTTGCGGTAACTCTGGATG	NM_001318416.1
	Reverse	ACCCCATTCATCAGACCCTG	
rSkap2	Forward	CAGAGGAGGAAGAGGACACC	NM_130413.1
	Reverse	AAGAGATCCAGTGCAGTCCC	
rHat1	Forward	GCAATCGAGCTGAAACTGGT	NM_001009657.1
	Reverse	AGGCCCTTGTAACCAAAAGC	
rDram2	Forward	GCATTGCCTTACATCAGCGA	NM_001025018.1
	Reverse	TCTCTTCAGGGTTCAGTGCA	
rAmz2	Forward	ACGGCAAGGACTTCTACACC	NM_001014121.1
	Reverse	AGTCTTACAGGATCGCAGCA	
rPpp2cb	Forward	GGCCCAATGTGTGATCTCTT	NM_017040.3
	Reverse	GCCGTTGGCATGGTTAAATG	
rPtma	Forward	GGTGAGGAAGAAGATGGAGATG	NM_021740.2
	Reverse	TCTGCTTCTTGGTCTCAACAT	
rEts1	Forward	CGACTCTCACCATCATCAAGAC	NM_012555.2
	Reverse	CAGTGCCTGGGACATCATT	
rCops2	Forward	TGAGCCCAACGTGGATTT	NM_153297.2
	Reverse	CCATTCTCCCTTCTCACCTTC	

2.12 BrdU incorporation assay

BrdU cell proliferation assay was done using BrdU cell proliferation assay kit (Cell Signalling Technology, USA). Control and Prnp knock down cells were seeded in a 96 well plate (10 x 10^3 cells/well) and cultured for 24hrs in complete growth medium

supplemented with 1X BrdU solution. Next day, the BrdU treated cells were incubated with 100µl fixation/denaturing solution at room temperature for 30min. The fixation solution was removed and cells were incubated with detection antibody at 1:100 dilution for 1hr, followed by three washes with wash buffer. The cells were then incubated with HRP-linked secondary antibody (1:100) for 30min and again washed with wash buffer. 100 µl of TMB substrate solution was added to each well and allowed to stand for ~7min till the blue colour developed. The reaction was stopped using stop solution, and absorbance was taken at 450nm in a multimode plate reader 9Perkin Elmer, USA).

2.13 Ki67 staining assay

A7r5 cells were plated on 35mm dish ($1x10^5$ cells per dish) to downregulate Prnp by transduction with lentiviral particles. 24 hours following viral transduction, cells were trypsinized, counted and seeded at a density of $20x10^3$ cells per well of an 8 well glass chamber slide (Nunc, Thermo Fisher, USA) in 100µl of CGM. The chamber slide was incubated overnight in the CO_2 incubator at 37ºC, under sterile condition. Next day, immune-fluorescence staining was performed with Ki67 antibody. First, the cells were fixed in 4% PFA, then blocked using 5% goat serum and 0.3% Triton-X-100 in PBS for 1hr. Ki67 primary antibody (Cell Signalling Technology, USA) was diluted in a ratio 1:100 in antibody dilution buffer (1%BSA, 0.3% Triton-X-100 in PBS) and directly added to each well of the chamber slide, and incubated for 2hrs. Cells were washed in PBS for three times and incubated with TRITC-conjugated anti-rabbit secondary antibodies (1:1000) for 1.5hrs at room temperature. Cells were again washed with PBS, followed by counterstaining of nucleus with Hoechst. Before mounting, the slide was detached from the wells, At least five different fields were captured for each biological replicate, using Leica microscope equipped with a CCD

camera and Leica Application Suite X (LAS X). For each field, the ratio of Ki67-positive nuclei versus total nuclei was calculated and represented in a bar graph.

2.14 Statistical analysis

All experiments were performed at least three times to get three biological replicates. Standard deviation and standard error of mean were calculated using Graph Pad Prism software. Statistical significance among experiment groups were calculated by unpaired student's t-test and Mann-Whitney U test for non-parametric variables.

CHAPTER 3

EXPRESSION DYNAMICS OF CELLULAR PRION WITHIN RAT UTERO-PLACENTAL COMPARTMENT

3.1 Background

The metrial gland develops from the mesometrial uterus in rodents during normal pregnancy. It is a maternally derived tissue that marks the entry point of maternal blood vessels and composed of primarily large granular metrial gland (GMG) cells, endothelial cells, smooth muscle cells, stromal cells, and fibroblasts(Picut et al., 2009). The granulated cells, the hallmark of the metrial gland, are bone-marrow derived, perforin-containing, precursors of uNK cells (Croy & Kiso, 1993). Trophoblast cells that leave the chorioallantoic placenta and invade into the metrial gland, assume endocrine-like functions. They secrete PRL family of hormones/cytokines (PLP-A, PLP-L, PLP-M, PLP-N), the targets of which are found on a population of cells within the metrial gland (Ain & Soares, 2004). The uNK cells surrounding the spiral arteries in the metrial gland, secrete several cytokines, growth factors and MMPs that disrupt VSMC integrity and degradation of ECM. uNK cells can regulate trophoblast entry by releasing IL-8 and interferon-inducible protein-10, and general mechanisms like cytotoxicity, local cytokine production and apoptosis (Wei XW, 2022).

Thus, it is evident the metrial gland is the major site for maximum spiral artery remodelling. We therefore, carefully isolated rat metrial glands at embryonic days 11.5, 13.5, 16.5 and 19.5 without contaminating with the surrounding smooth muscle layer, and whole implantation sites.

3.2 Results

To evaluate the temporal expression pattern of *Prnp* transcripts, quantitative real-time PCR was performed. With increase in gestation days, *Prnp* mRNA levels showed a gradual upregulation with maximum expression on E16.5 (Fig 3.1A), followed by a sharp decrease on E19.5. Our real time data was further affirmed by analyzing the PRNP protein levels in these tissue lysates using western blotting. The most abundant

isoform of PRNP protein in MG was detected between 26-32kDa, which followed a similar expression dynamic with the respective mRNAs (Fig 3.1B). NIH ImageJ software was used to quantify the protein bands after normalizing with the loading control GAPDH (Fig 3.1C).

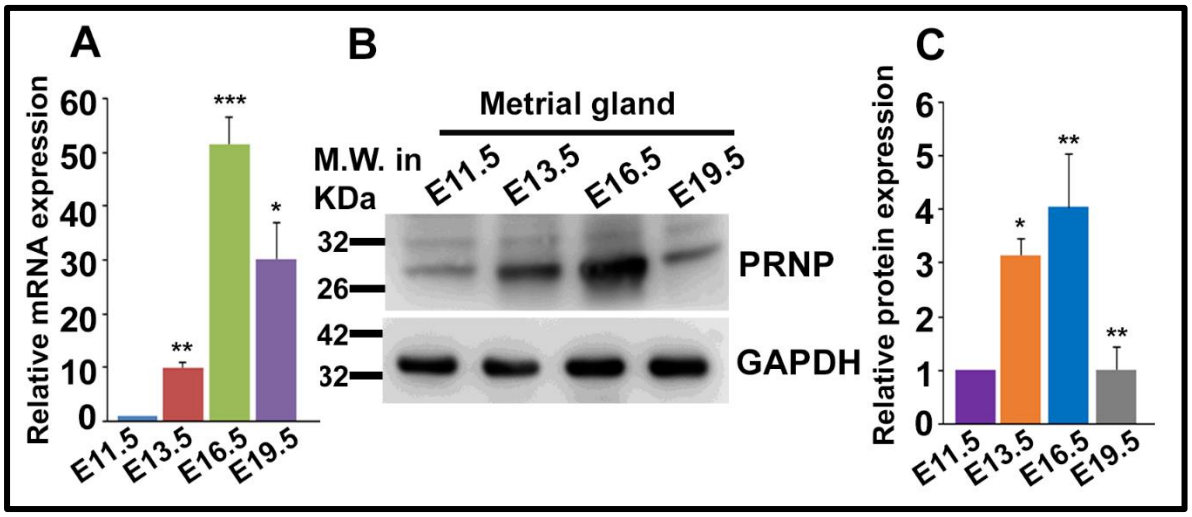

Figure 3.1. Prnp expression dynamics in the metrial gland of different gestational days of rat. A) Real time PCR analysis of *Prnp* transcript and **B)**, Western blot analysis of PRNP protein in the metrial gland lysates of E11.5,13.5,16.5,19.5 **C)** Quantification of the protein bands has been done by NIH ImageJ software, after normalizing with the loading control GAPDH.Error bars indicate SEM *p<0.05, **p<0.005, ***p<0.0005.

Owing to the heterogenous nature of the metrial gland, we sought to decipher the specific cellular source of prion within this tissue by immuno-histological methods. Immuno-staining of PRNP protein on 10micron cryosections revealed that the primary site of PRNP synthesis is the smooth muscle cells in the metrial gland (MG) on E11.5 (Fig 3.2B) and very less in the vascular smooth muscle cells (Fig 3.2C, D, see inset). On gestation day 13.5, specific signals were found in the smooth muscles of the metrial gland (Fig 3.2F) as well as in the vascular smooth muscle cells that seem to migrate away from the arterial wall (Fig 3.2G and H inset). By E16.5, maximum population of

the VSMCs express prion and more migration is observed as the cells have moved farther away from the arterial lining (Fig 3.2J and K, L see inset). Staining E13.5 metrial gland with a smooth muscle marker, caldesmon (green, Fig 3.2N) or Prnp (red, Fig 3.2O), revealed that VSMCs surrounding almost all the arteries, express caldesmon (Fig 3.2N). Upon merging two fluorescent images of the boxed region shown in Fig 1M, few cells were also found to express Prnp as denoted by yellow colour (Fig 3.2P), thus verifying these cells to be indeed VSMCs. On closer examination of individual arteries, it could be noticed that, only the cells which are still strongly attached to the tunica of the arteries, happen to express both caldesmon and Prnp, as the colour of the cells are yellow denoting colocalization of both markers (Fig 3.2 Q, R, S white asterisk). On the other hand, the VSMCs which are actively migrating and invading through the ECM, around their respective arteries, exclusively express prion and not caldesmon (Fig 3.2 Q, R, S white arrowheads).

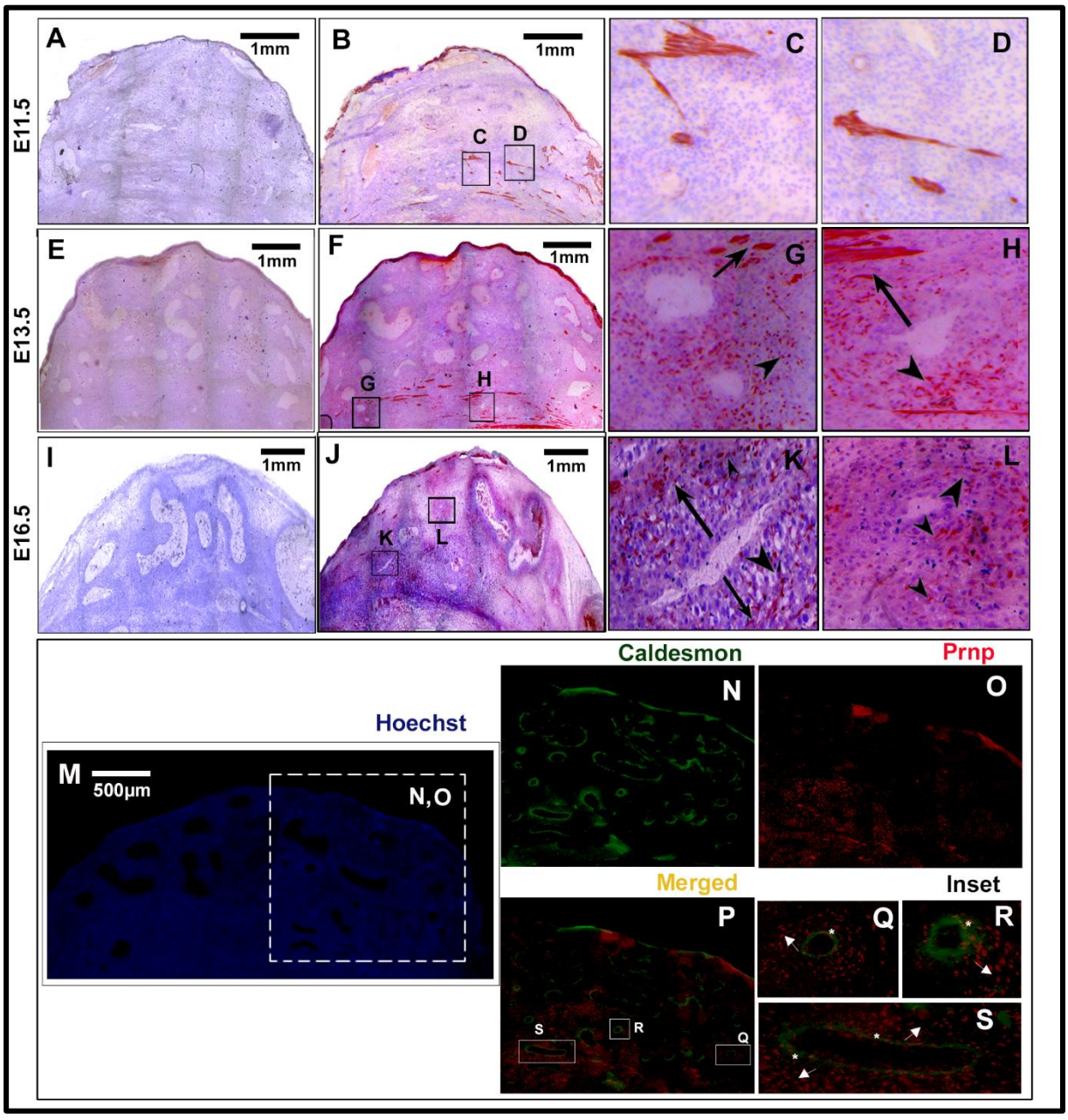
E11.5
E13.5
E16.5
A
B
C
D
E
F
G
H
I
J
K
L
1mm
M
500µm
N,O
Hoechst
Caldesmon
Prnp
N
O
Merged
Inset
P
Q
R
S

Figure 3.2. Cellular localization of PRNP on rat metrial gland. Immunohistochemical identification of prion protein on E11.5 **(A-D)**, E13.5 **(E-H),** and E16.5 **(I-L)**. (**A, E, I)** Negative control showing specificity of PRNP immuno-staining. **C,D,G,H,K,L)** Magnified images of the boxed areas of the middle panel. Black arrows and arrow heads showing cells away from the arteries. **(M)** Hoechst staining on E13.5 cryo-section to show the morphology of metrial gland. Immunofluorescence staining of consecutive sections with caldesmon (green) **(N)** and Prnp (red) **(O)**. **(P)** Merged image of N and O**. Q,R,S)** showing cells surrounding some arteries, which express both caldesmon and Prnp (see inset, white asterisk) , or only Prnp (see inset, white arrowheads). The latter are the ones which are actively undergoing migration.

3.3 Discussion

We have demonstrated that cellular prion is expressed in the VSMCs surrounding the maternal arteries in metrial gland of rats. As stated, the metrial gland is a complex modification of the myometrium of the pregnant uterus known to perform endocrinological and immunological function during pregnancy (Ain & Soares, 2004) and the primary site for spiral artery remodelling (Rosario et al., 2008) owing to the extended trophoblast invasion. In E11.5 Prnp is scarcely detected both at the RNA and protein levels, in the metrial glands. Gradually, through E13.5 expression increases till E16.5 followed by a trip at E19.5. This gestation time dependent expression of Prnp is what led us to seek its precise role in the molecular events occurring in the metrial gland at these time points.

Although Passet et al.'s laboratory had demonstrated the immediate developmental catastrophe by functionally abolishing *Prnp* gene, they did not, however, pin-point the spatio-temporal site of Prnp expression. With the help of immuno-histochemical tool, we have been able to locate the source of Prnp in the metrial gland, i.e., the VSMCs, which also seem to migrate away from the arterial wall. It is indeed noteworthy that only those VSMCs, which are yet to be detached from the tunica media of the spiral arteries, express both caldesmon and Prnp. The fact that only migrating VSMCs express prion and not the smooth muscle gene caldesmon, indicate towards a plausible phenomenon where VSMCs achieve migratory potential by switching on endogenous Prion expression.

CHAPTER 4

FUNCTIONAL IMPLICATIONS OF PRION IN VASCULAR SMOOTH MUSCLE CELLS IN CONTEXT OF SPIRAL ARTERY REMODELLING

4.1 Background

4.1.1 VSMCs undergo proliferation and migration during spiral artery remodeling

VSMCs, present in the tunica media layer of the blood vessels, maintain the vessel elasticity and are responsible for regulating the volume of blood supplied. They can assume two different phenotypic states i) contractile or differentiated state or ii) synthetic or de0differentiated state, both states marked by their respective markers. In the contractile state they express proteins like α-smooth muscle actin (α-SMA), calponin1 (CNN1), SM-myosin etc. and in the synthetic state they express proteins like non-muscle isoforms of myosin (myosin IIB), vimentin, embryonic form of smooth muscle myosin heavy chain (SMemb) (Rensen et al., 2007).

Earlier it has been demonstrated from our lab that on gestation day 13.5, when very less trophoblasts are found in the metrial gland, spiral arteries are surrounded by α-SMA-positive VSMCs. Whereas on day 16.5, cytokeratin positive trophoblasts were dispersed all over the metrial gland, and there was robust rise in Smemb positive cells surrounding spiral arteries. On day 19.5 VSMCs expressing Smemb was abundant while α-SMA-positive VSMCs were barely detected (Nandy et al., 2020). Co-culturing rat VSMCs with murine trophoblast cell line, led to increase in the synthetic markers in VSMCs. Signalling pathways that are activated when exposed to growth factors, mitogens, or peptides, involve both proliferation and migration, however, independent to each other. It is commonly known that Platelet-derived growth factors (PDGF) and its receptor (PDGFR) regulates many physiological and pathological processes in VSMCs such as, wound healing, proliferation, survival, migration, and differentiation. Mouse trophoblast cell lines on 3 of differentiation, secrete PDGF-BB, which binds and

activate PDGFR-β expressed on the VSMCs, leading to activation of the Akt and Erk pathway, which accounts for the phenotypic switch to the de-differentiation state (Nandy et al., 2020).

The transition of VSMCs from contractile to synthetic phenotype affects both proliferation and migration. Activation of the PDGFR-β is coupled via phosphatidylinositol 3-kinase (PI3K) and phospholipase Cγ to changes in myoplasmic calcium, hydrolysis of PIP_2, and activation of mitogen-activated protein kinases (MAPK) (Bornfeldt et al., 1995). Complete loss of PDGF signaling in mice leads to mal-formed blood vessels.

Decidual Spiral arteries (SpA) from human placental bed biopsies with associated EVTs show H-caldesmon positive migrating VSMCs (Bulmer et al., 2012). Interestingly higher number of VSMCs show migration from SpA in the placental bed which have associated EVTs than those without EVTs and those in the decidua parietalis. Proteolytic digestion of the ECM components is required for cellular migration within tissue. Two key protease families involved in vascular remodeling are Matrix metalloprotease (MMPs) and urokinase Plasminogen activator (uPA) system, which are regulated by their inhibitors (TIMPs) and uPA receptors (uPAR). VSMCs lying outside the endothelial layer in SpA undergoing remodeling, highly express MMP-2, uPA and uPAR indicating their high migratory potential (Bulmer et al., 2012).

Lamellipodia extension of any migrating cell requires breakage of focal points at the trailing edge and formation of new focal contacts between the cell membrane and extra cellular matrix. Focal Adhesion Kinases (FAK), a renowned non-receptor tyrosine kinase, is one of the predominant regulators of cell migration and is upregulated during intimal hyperplasia. Endogenous FAK recruitment to the activated PDGFRβ enhances PDGF-BB induced VSMC migration.

4.1.2 Role of trophoblast cells in spiral artery remodeling

One of the earliest cell lineages to have differentiated from the blastocyst are the trophoblast cells, which constitute the main structural and functional components of a haemochorial placenta. Just after attachment to the uterine epithelium, the trophectoderm layer of human blastocyst, fuses to form a primary syncytium. Following implantation, the primary syncytium further spreads deep into the uterine endometrium (now, the decidua) and give rise to the syncytiotrophoblast (SCT) layer. The SCT being the outer lining of the placental villi, is in direct contact with the maternal blood flow and the main site for nutrients and gaseous exchange.

The trophoblast cells lying beneath syncytium, proliferate and branch off to form primary villous trees, as they penetrate through the primary syncytium and surround the conceptus like a shell. These cells are known as cytotrophoblast cells(Turco & Moffett, 2019). With increase in the size of the placenta the cytotrophoblast shell becomes discontinuous and cytotrophoblast cell column (CCC) arises from the free ends of the anchoring villi attached to the decidua. At around day 17-18 dpf the extraembryonic mesenchymal cells penetrate through the villous core to form the secondary villi. Individual cytotrophoblast cells from the cytotrophoblast shell undergo EMT to invade into the decidua as extra villous trophoblast (EVT). The interstitial EVTs (iEVTs) migrate through the decidual stroma towards the maternal spiral arteries, while the endovascular EVTs (eEVTs) migrate through inside of the spiral arteries (Pijnenborg et al., 1980) (Fig 5.1). As the iEVTs surround the arteries, there is loss of alpha actin form the smooth muscles in the arterial wall, which is replaced by an amorphous eosinophilic material (Pijnenborg et al., 2006). At this stage the arteries lose their vasoactivity and are transformed into flaccid vessels capable of carrying nutrients at a relatively low pressure(Brosens et al., 1967). The iEVTs move as far as

till the myometrium where they fuse to form placental bed giant cells. On the other hand, the eEVTs migrate in a retrograde fashion to form a plug in the arteries to prevent untimely pouring of blood into the intravillous spaces(Burton et al., 1999).

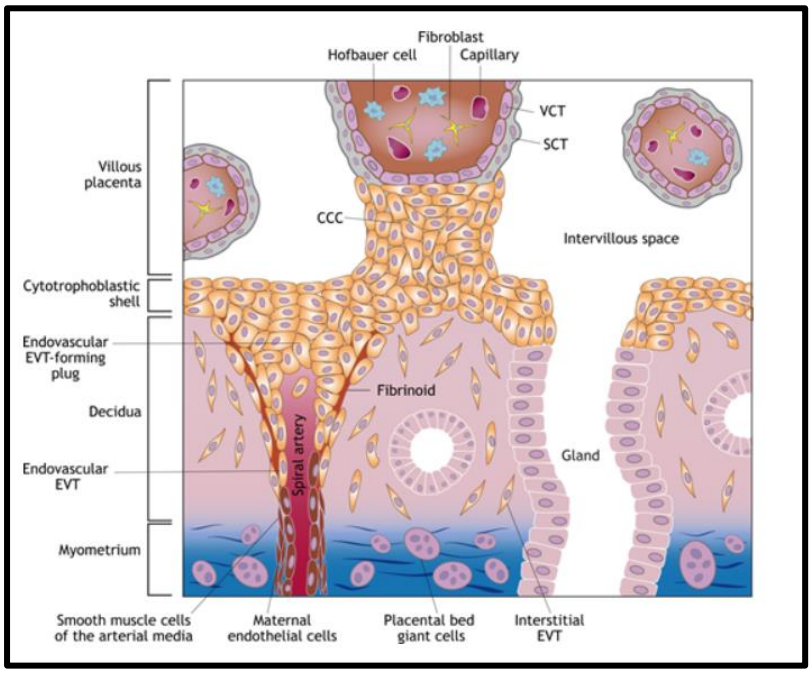

Figure 4.1. Trophoblast sub types at the maternal fetal interface (Turco and Moffet, 2019). The SCT is in direct contact with the intervillous space which is drained by maternal blood. The CCC emerges from the distal ends of the cytotrophoblastic shell. The interstitial EVTs migrate through the decidual stroma and surround the arteries, whereas the endovascular EVTs migrate within the spiral arteries and form Endovascular plug.

Based on the direction from where blood enters the placenta, the rat uteroplacental compartment, like mice, is divided into two regions. The site from where blood vessel enters is termed mesometrial compartment and the opposite side where the embryo gets implanted is termed as the antimesometrial compartment. Following implantation, the uterine NK cells increase in number and infiltrate the mesometrial decidua. As gestation progresses, the placenta enlarges and the natural killer cells start to disappear from the regressing decidua. The departing uNK cells marks the precise time point for invasive trophoblasts to leave the chorioallantoic placenta and enter through the uterine decidua (Ain et al., 2003). The reciprocal relationship of uNK cells and trophoblasts were further confirmed when cyto-keratin positive trophoblasts showed accelerated migration into the maternal decidua on day 13 of gestation in NK cell deficient Tgε26 transgenic mice(Ain et al., 2003). The invasive trophoblast

population emerges from the junctional zone and enter the decidual region between embryonic days 14 and 15 in rats and day 14 in mouse. While in mice the invasion is limited till the decidua, in rats they infiltrate the mesometrial triangle and surround the uterine vasculature(Ain et al., 2006). Depending upon their extent of invasion, the invasive trophoblast cells are classified under three categories, i) the Endovascular trophoblast cells that replace the endothelium, ii) the intramural trophoblast cells that ae embedded within the vascular wall, iii) the interstitial trophoblast cells that remain in between the vasculature (Fig 5.2). Metrial glands isolated on day 18 of gestation expressed a subset of Prolactin-like-proteins PLP-A, PLP-M, PLP-L; of which PLP-A and PLP-M are also expressed in the junctional zone of placenta from day 14 to day 20. PLP-A and PLP-M mRNA levels gradually increased as gestation advanced, whereas PLP-L mRNA levels were constant from day 16 to day 20 of gestation (Ain et al., 2003). Thus, the rodent invasive trophoblasts possess endocrine phenotype which invariably affect the remodeling of the spiral arteries at the maternal fetal interface.

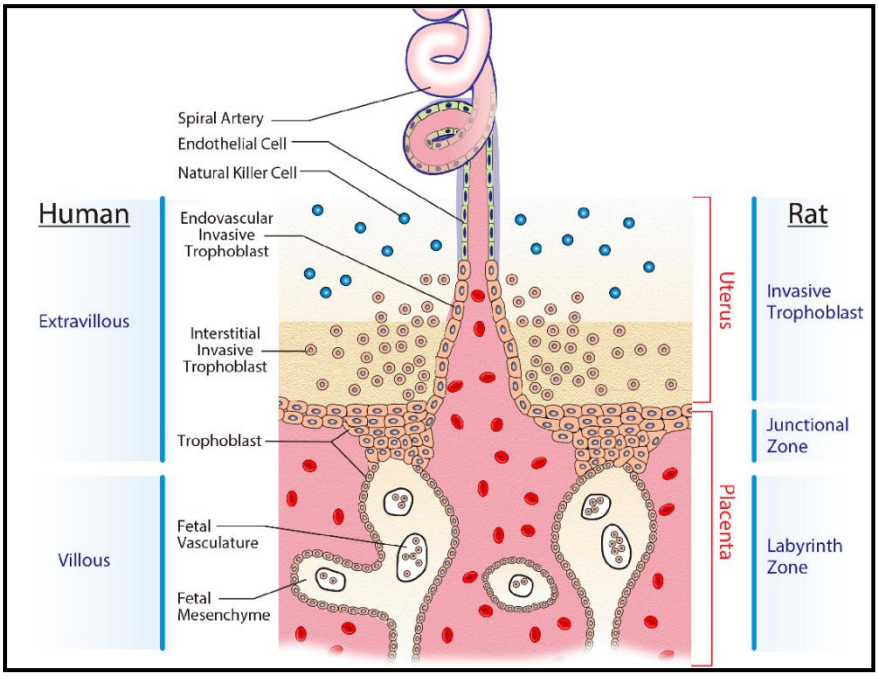

Figure 4.2. Schematic representation of hemochorial placentation in human and rats, showing the different homologous layers of placenta, the spiral arteries, and the spatial orientation of the uNK cells and invasive trophoblast cells around the spiral arteries. (Soares et al., 2014)

4.1.3 Apoptosis of VSMCs during spiral artery remodeling

Apoptosis of vascular smooth muscle cells is a critical phenomenon during cardiovascular development, normal vessel regression ad pathophysiological conditions alike atherosclerosis and thrombosis (Korshunov & Berk, 2008). The fate of individual VSMCs within the lumen of the vessels depends on the cross-talk between the pro and anti-apoptotic signals. Excess cell death can lead to vascular wall instability like in the pathological conditions of aortic aneurism. However, during spiral artery remodeling, apoptosis does not happen at the expense of vascular stability implying a tighter regulatory mechanism during this process.

Mostly the invading trophoblast cells shift the balance in the vessels towards cell death, by either directly secreting apoptotic ligands or indirectly by loss of cellular adhesion with the endothelium. Three members of the tumour necrosis factor (TNF) family of cytokines, which have been implicated in the regulation of vascular cell apoptosis: tumour necrosis factor-α (TNFα), TNF-related apoptosis inducing ligand (TRAIL) and Fas ligand (FasL) are all expressed/produced by trophoblasts (Hammer et al., 1999; R. J. Keogh et al., 2007; King et al., 1995; Pijnenborg et al., 1998)

TNFα binds to and activates two distinct receptors TNF-receptor 1 (TNF-R1) and TNF-R2; both are expressed on endothelial cell (EC) and VSMC. Activation of TNF-R1 leads to recruitment of the intracellular adapter molecule TNF-receptor-associated death domain (TRADD) together with a number of proteins including TRAF2 (TNF-receptor-associated factor 2). This transiently activates the JNK pathway and promotes cell survival. However, if TRAF2 recruits the Fas activating death domain (FADD), pro-caspase 8 undergoes cleavage and apoptosis is induced (Whitley & Cartwright, 2010).

TRAIL signalling is made more complex by the existence of five different receptors: TRAIL-receptor 1 (TRAIL-R1) and TRAIL-receptor 2 (TRAIL-R2) contain intracellular DDs and can signal to cause apoptosis; TRAIL-receptor 3 (TRAIL-R3) lacks a DD, and TRAIL-receptor 4 (TRAIL-R4) has a truncated DD, neither of which can signal and are thought to act as decoy receptors; and finally a fifth, soluble receptor, osteoprotegerin, can bind and sequester TRAIL, although its importance in regulating TRAIL signalling is yet to be clearly defined. TRAIL-receptor 1 (TRAIL-R1; death receptor 4 (DR4)) and TRAIL-R2 (DR5) initiate apoptosis and are expressed on EC and VSMC in a membrane bound form, the carboxy-terminus of which can be cleaved by cysteine proteases generating a soluble form (Mariani & Krammer, 1998). There are also two decoy receptors (DcR1 and DcR2) which are expressed by EC. Binding of TRAIL to the decoy receptors does not induce apoptosis but may compete for TRAIL binding with TRAIL-R1 and -R2. TRAIL is synthesised by first trimester cytotrophoblasts and extravillous-like trophoblast cell lines, and both TRAIL-R1 and R2 are expressed on VSMC and to a lesser extent on EC of first trimester spiral arteries (R. J. Keogh et al., 2007). TRAIL transduces its apoptotic signal via receptor trimerization and activation of the extrinsic pathway of apoptosis. The adaptor molecule Fas-associated death domain (FADD) binds to the intracellular death domain (DD) of the clustered receptors and recruits and activates caspase-8 followed by caspase-3, thus initiating activation of the caspase cascade leading to apoptosis (R. J. Keogh et al., 2007).

FasL binds to and activates the cell surface receptor Fas (CD95). FasL has been detected at the maternal–fetal interface(Runic et al., 1996) where it is expressed by villous, extravillous and syncytiotrophoblast, and was proposed to contribute to the immune privilege observed in this utero–placental environment by inducing apoptosis of activated Fas-expressing maternal lymphocytes. Fas expression has been shown

in both EC and VSMC of term spiral arteries. Treatment of cultured human aortic smooth muscle cells with Fas-activating antibody induced apoptosis in these cells (L. K. Harris et al., 2006). On the other hand, dissected spiral arteries when perfused with cytotrophoblast (CTB)-conditioned medium, in absence or presence of FasL neutralizing antibody showed higher and lower frequency of TUNEL positive VSMCs respectively (L. K. Harris et al., 2006).

The overall balance between pro- and anti-apoptotic factors present in the local environment determines which pathway is activated.

4.1.4 Odd-Skipped Related Transcription factor 1

The Odd skipped Related Transcription factor-1 (Osr1), ortholog of the Drosophila odd-skipped gene (*Odd*) is a C2H2-containing zinc finger transcription factor that binds around consensus sequence 5' GCTNCTG 3' (O'Brien et al., 2018) and participate in the development of heart, limb and urinogenital compartments in mammals.

Figure 4.3. OSR1 consensus binding motif (Lori L. O'Brien et al., 2018)

It was initially identified as a class of pair-rule genes in *Drosophila,* mutation of which causes loss of the odd-number segments in *Drosophila* embryos (Coulter & Wieschaus, 1988; Nüsslein-Volhard & Wieschaus, 1980). In mice embryos, Osr1 transcripts start to express in the intermediate mesoderm at embryonic day 8.5 (E 8.5) and further expands in the brachial arches and limb buds(So & Danielian, 1999). Mice embryos with homozygous null $Osr1^{-/-}$ mutants die between E11.5 and E12.5. Embryos at E12 showed blood aggregated into the liver and veins, whereas their yolk sac lacked blood

circulation (Wang et al., 2005). In addition to that, embryos examined at E11.5 showed dilated atria, enlarged venous valves, and lacked a complete atrio-ventricular septum. During limb development, the myogenic precursors migrate from the somites to the nascent limb buds, where they subdivide to form individual muscle fibres from premascular mass (Duprez, 2002). Interstitial Muscle connective tissue (MCT) that arises from the lateral plate mesoderm, support proper muscle patterning in embryos. In adults, Fibro-adipogenic progenitors (FAP) are involved in parallel pathways for muscle regeneration following injury (Joe et al., 2010). In mice Osr1 expression was found in embryonic limb mesenchyme fated for myogenic differentiation between E11.5 and E13.5, and interstitial to the myofibers at E14.5 Osr1 (Vallecillo-García et al., 2017). $Osr1^{+}$ cells are identified as a subpopulation of embryonic MCT fated towards fibrogenic and adipogenic lineages, resembling adult FAPs by creating a pro-myogenic niche(Vallecillo-García et al., 2017). In these cells Osr1 drives the expression of not only the Collagens, but also other ECM components essential for matrix assembly such as Lumican, Matrillin, Decorin and Fibromodulin (Kadler et al., 2008).

Osr1 expression in the kidney precursor cell mass, marks it as one of the earliest known markers for metanephric kidney differentiation. In $Osr1^{-/-}$ mutant mice embryos condensation of ureteric bud and metanephric mesenchyme is completely arrested at E11.5 (James et al., 2006). Alongside, these embryos lack expression of Pax2, Eya1, Six2, Gdnf,(Moore et al., 1996; Torres et al., 1995; Xu et al., 1999) which are known to be required for proper differentiation of metanephric kidney, thus establishing Osr1 as the earliest factor that drives the expression of the other markers (James et al., 2006).

4.2 Results

4.2.1 RNA interference strategy substantially downregulated endogenous Prnp in rat aortic smooth muscle cell line

Cellular Prion protein is extensively expressed in E16.5 metrial gland as well as in VSMCs, as assessed by western blot and imuno-cytochemical analysis (Fig 4.4A and B).

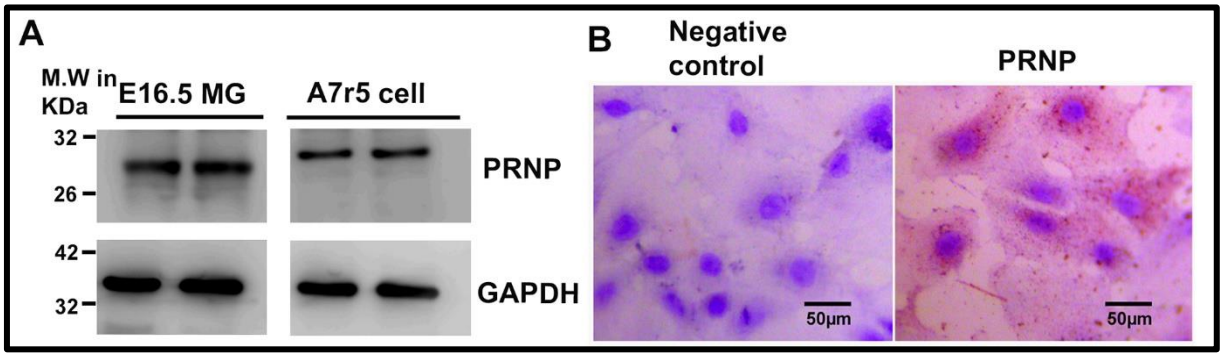

Figure 4.4. Expression of Prnp in rat metrial gland tissue and vascular smooth muscle cells (A7r5 cell line). A) Western blot images depicting levels of PRNP protein expressed in the metrial gland at embryonic day 16.5 and in vascular smooth muscle cells (A7r5 cells) **B)** Immunocytochemical localization of cellular Prion protein in vascular smooth muscle cells. Negative staining (left panel) without primary antibody to eliminate any background signal, showing specificity of PRNP immuno-staining. Nuclei are counterstained with haematoxylin

shRNA oligos targeting different exons of PrnP, were cloned individually in pLKO.1 vector and A7r5 cells were transduced with lenti particles as described in Materials and Methods. Real-time PCR analysis revealed that each shRNA oligo differentially regulated the *Prnp* transcript. While shRNA1 had the least effect on *Prnp* transcript, shRNA3 had the most, when given individually (Fig 4.5A and B). With this observation, we fed the cells with optimal lentiviral titre containing a cocktail of shRNA 1,2,3, and found effective downregulation (about 80%) both at the RNA and protein level (Fig 4.5C-E).

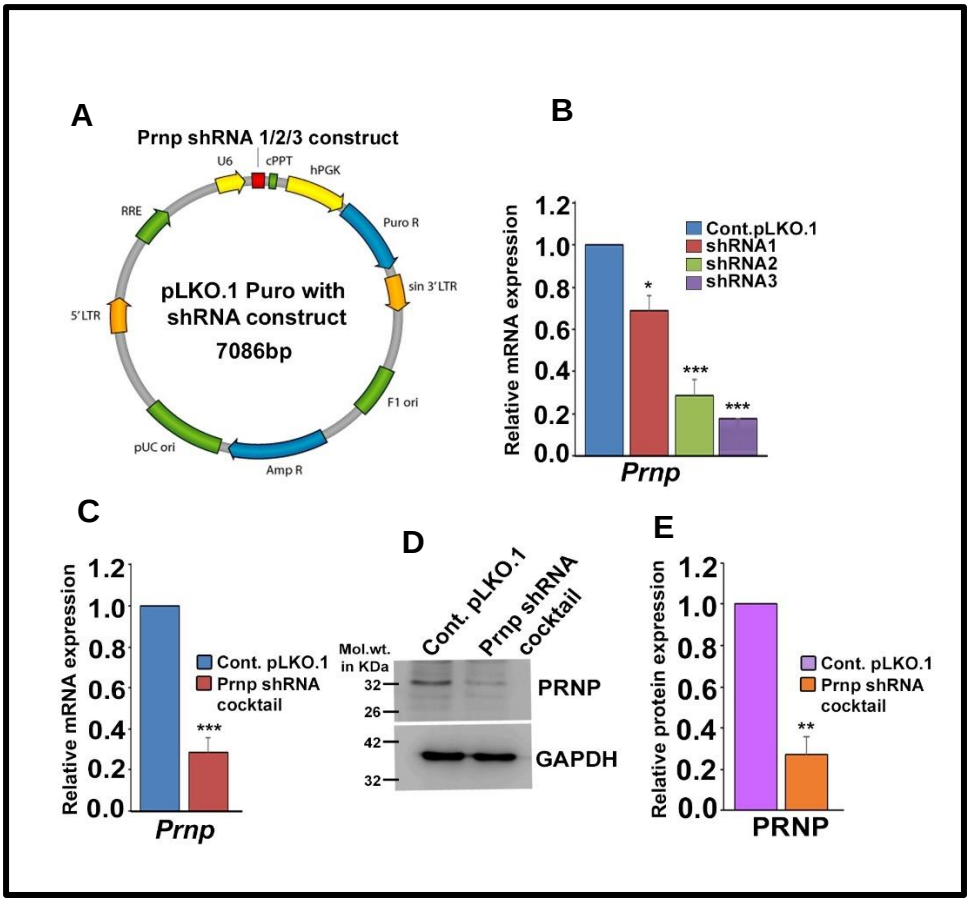

Figure 4.5. Downregulation of Prnp by short hairpin oligos in vascular smooth muscle cells. A) schematic diagram showing three shRNA oligos cloned in the pLKO.1 vector, driven by the u6 promoter. **B)** Real time PCR analysis showing extent of *Prnp* downregulation with individual shRNA oligos and with cocktail **C)**, Western blot analysis showing significant downregulation of PRNP protein using cocktail of shRNA oligos in VSMCs. Quantification of the protein bands has been done by NIH ImageJ software, after normalizing with the loading control GAPDH. Error bars indicate SEM *p<0.05, **p<0.005, ***p<0.0005

4.2.2 Prnp promotes migration and invasion in A7r5 cells.

To address the functional significance of Prnp in cell motility and migration we did scratch wound assay. Micrographic images depicting the width of the wound at the beginning of the experiment and after 24 hrs is shown in Fig 4.6A. Cells transduced with empty vector showed around 62.2% of wound healing capacity as compared to the cells where endogenous Prnp is downregulated, which showed only 23.3% of

wound closure after 24 hours (Fig 4.6B). Prion's role in regulating cellular invasion towards chemoattractant was demonstrated using a trans-well invasion assay. The invading cells were visualized by staining the lower surface of the inserts and followed by capturing microscopic images (Fig 4.6C). At least five different fields per well were captured from three biological replicates and the cells in each field were counted. We observed a significant decrease in the number of invaded cells where Prnp is downregulated. Relative percentage of cell count between two groups is shown in Fig 4.6D, which indicates nearly 30-35% less cells have invaded when Prnp is knocked down. Quantitative analysis was done by dissolving the stain in 10% acetic acid and measuring the OD at 560nm, which revealed a 40% decrease in absorbance indicating reduced invasion (Fig 4.6E).

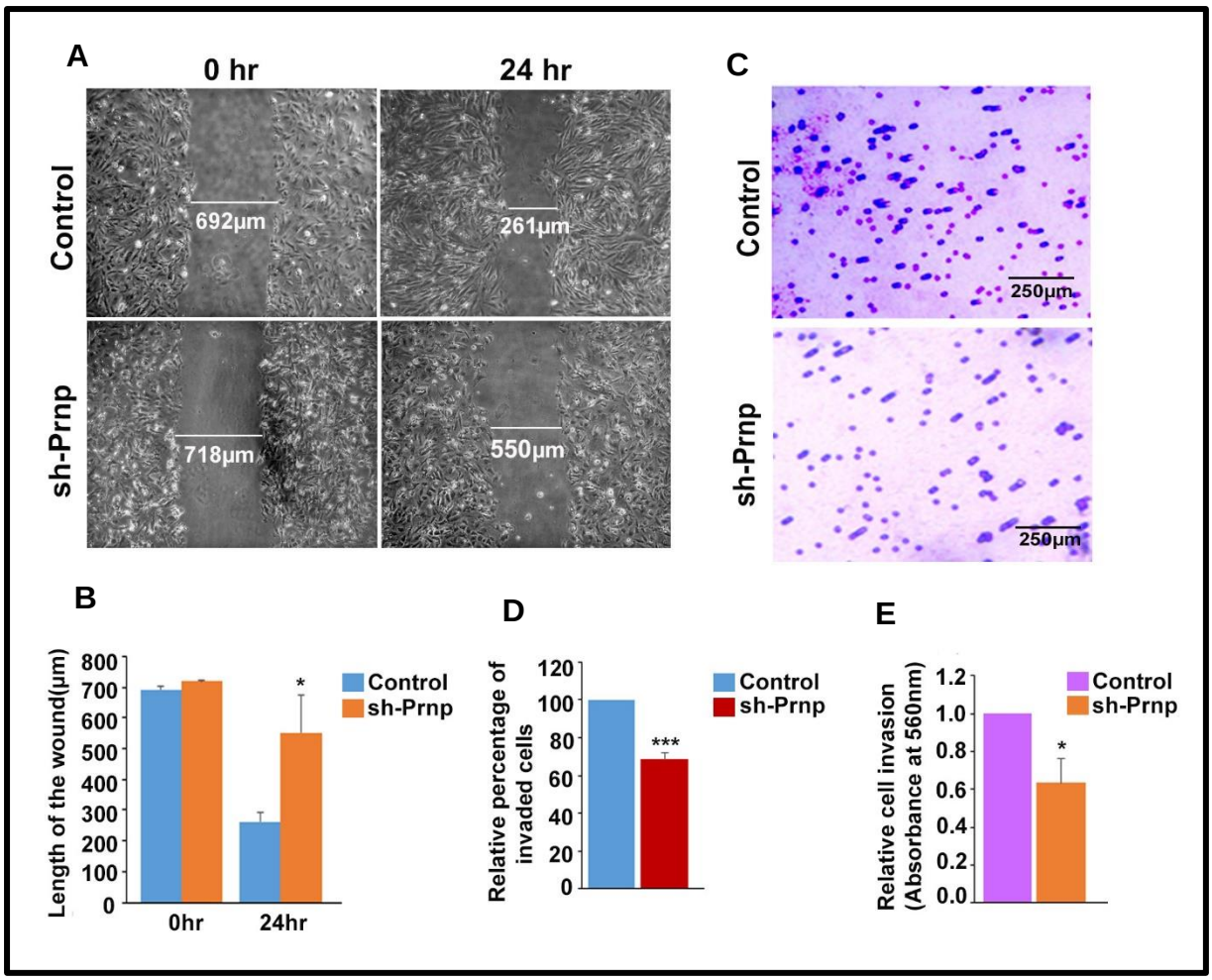

Figure 4.6. Downregulation of *Prnp* impairs migration and invasion in vascular smooth muscle cells **A)** Photomicrographic images of scratch wound assay showing length of wound after 24 hours of scratch in control and Prnp downregulated cells. **B)** Quantification and comparison of the percentage of wound closure from at least 6 measurements taken from each of the three biological replicates. **C)** Photomicrographic images of invaded VSMCs from Matrigel invasion assay, **D)** Bar graphs showing relative percentage of invaded cells between scramble and Prnp knocked down cells. **E)** Colorimetric quantification of the stained, invaded cells at the lower surface of the membrane, from the two treatment groups. Error bars indicate SEM *p<0.05, *p<0.0005

4.2.3 PRNP forms a ter-molecular immune complex with PDGFRβ and FAK

While investigating a plausible mechanistic justification for our above observation, we sought to examine the impact of Prnp, if any, on extracellular

signalling molecules involved in VSMC migration. As stated earlier, activation of FAK through PDGF-PDGFRβ pathway, is one of the crucial signalling pathways that play key role in VSMC migration during de-differentiation. The membrane localization and abundance of PrnP in the VSMCs of metrial gland, led us to assume that it might act as a co-receptor to the PDGFRβ-FAK axis. In line with our assumption, both FAK and PDGFRβ co-immunoprecipitated with PrnP from E16.5 metrial gland lysate (Fig 4.7A). Interestingly, we were able to recapitulate the same result when we performed the co-immunoprecipitation assay with A7r5 protein (Fig 4.7B). This finding led us to anticipate that Prnp might be involved in direct or indirect contact with PDGFRβ, thus acting as a co-receptor, which in turn activates several FAK molecules thereby amplifying the downstream migratory signals.

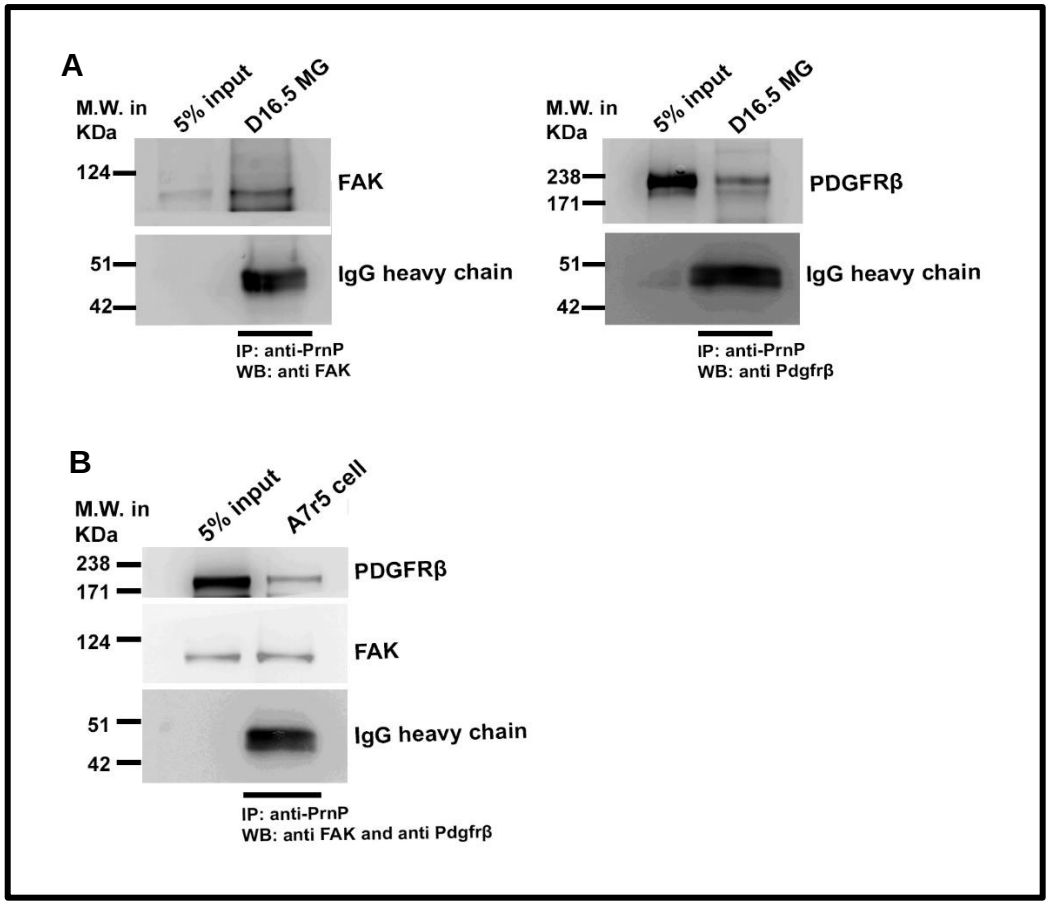

Figure 4.7: PRNP interacts and forms a ter-molecular complex with PDGFRβ and FAK A) Immunoprecipitation with anti-Prnp antibody followed by immunoblotting with anti-FAK and anti-PDGFRβ antibodies in rat metrial gland **(A)**and VSMCs **(B).**

4.2.4 RNA interference of Prnp promotes apoptosis in VSMC

Leading on from PRNP's ability to promote migratory and invasive properties of A7r5 cells, we postulated that PRNP facilitates the VSMCs to migrate away from the arterial wall thus averting them from undergoing apoptosis. To test this hypothesis, PRNP was down regulated in A7r5 cells using RNA interference. Microscopic images show morphologically many dead cells in the culture plate as compared to control (Fig. 4.8A). Furthermore, flow cytometric analysis was used to test early stages of apoptosis by Annexin-V-PI staining in PRNP-knocked down A7r5 cells. Knock down of PRNP substantially increased the percentage of Annexin-V positive and PI negative cells

(9.2%) as compared to control (2.3%) cells (Fig 4.8B and 4.8C). These are the population of cells showing early signs of apoptosis. Analysis of apoptotic markers was done to further validate this observation. Substantial elevation of the cleaved form of caspase-3 and caspase-8 was observed in PRNP-downregulated cells (Fig. 4.8D - G). In line with this, pro-apoptotic marker Bax increased and anti-apoptotic marker Bcl-XL decreased in PRNP-knocked down VSMCs (Fig. 4.8D and E).

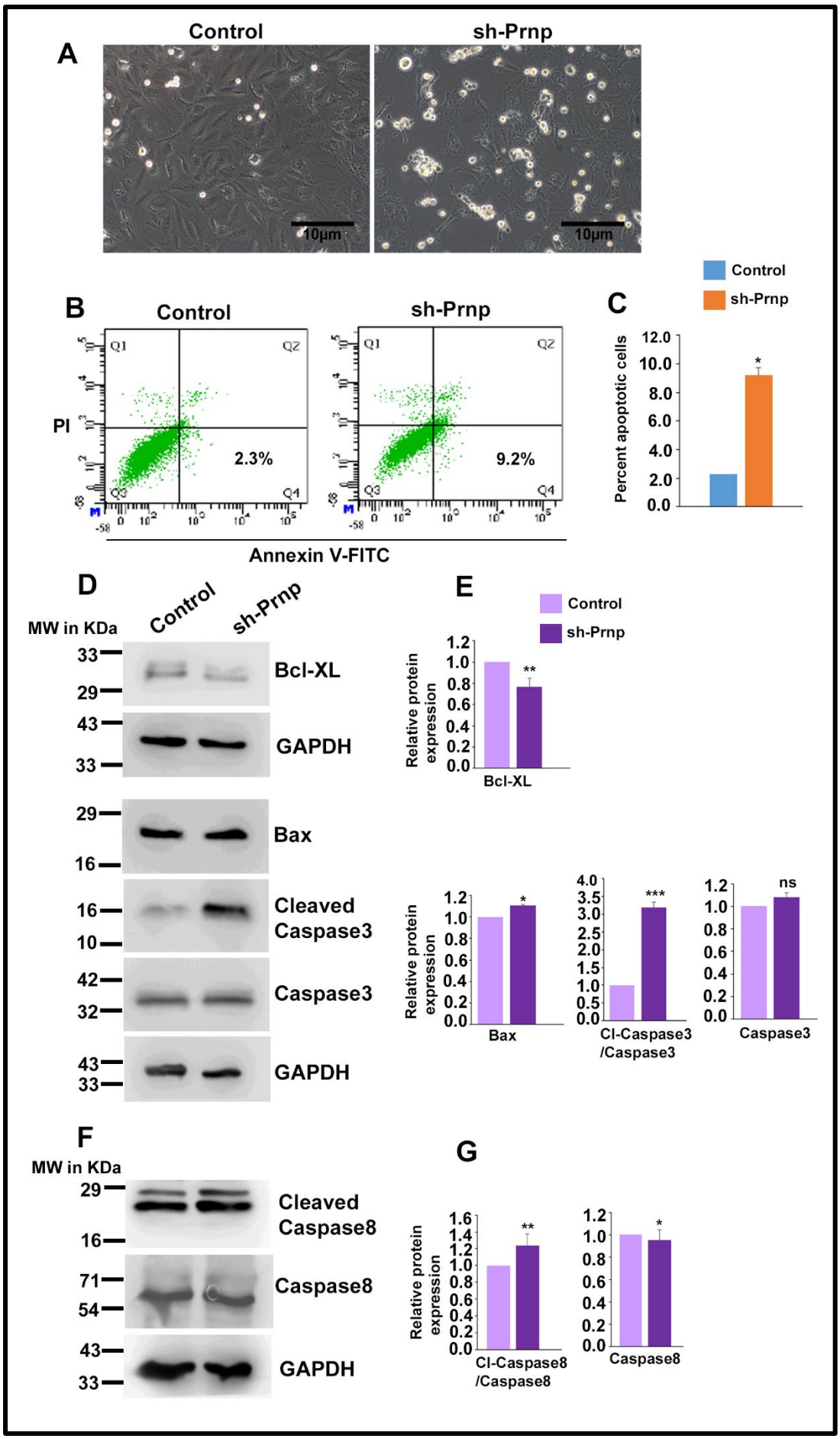
A
Control
sh-Prnp
10μm
10μm
B
Control
sh-Prnp
PI
Q1
Q2
Q3
Q4
2.3%
9.2%
Annexin V-FITC
C
Control
sh-Prnp
Percent apoptotic cells
12.0
10.0
8.0
6.0
4.0
2.0
0.0
*
D
MW in KDa
Control
sh-Prnp
33
29
Bcl-XL
43
33
GAPDH
29
16
Bax
16
10
Cleaved Caspase3
42
32
Caspase3
43
33
GAPDH
E
Control
sh-Prnp
Relative protein expression
1.2
1.0
0.8
0.6
0.4
0.2
0.0
**
Bcl-XL
*
Bax
4.0
3.5
3.0
2.5
2.0
1.5
1.0
0.5
0.0
***
Cl-Caspase3 /Caspase3
ns
Caspase3
F
MW in KDa
29
16
Cleaved Caspase8
71
54
Caspase8
43
33
GAPDH
G
Relative protein expression
1.6
1.4
1.2
1.0
0.8
0.6
0.4
0.2
0.0
**
Cl-Caspase8 /Caspase8
*
Caspase8

Figure 4.8: PrnP knockdown induces apoptosis in VSMCs. A) Photomicrographs showing VSMCs transduced with lentivirus harbouring either scrambled or *Prnp* shRNAs following 48h of transduction. **(B)** Flow cytometric analysis to detect early apoptosis in control and *Prnp* down regulated VSMCs. Apoptotic cells are marked with Annexin V-FITC and are shown in Quadrant 4(Q4). **(C)** Quantification of apoptotic VSMCs (PI negative and Annexin V-FITC positive) in presence of scrambled and *Prnp* shRNAs from B. **(D,F)** Western blot analysis ant-apoptotic (Bax and Bcl-XL) and pro-apoptotic (cleaved Caspase-8 and cleaved Caspase-3) markers using lysates from VSMCs transduced with lentivirus harbouring either scrambled or *Prnp* shRNAs following 48h of transduction. **(E,G)** Quantification of protein bands from D using NIH Image J software. GAPDH was used as an endogenous control. Error bars indicate SEM. *p<0.05, **p<0.005, ***p<0.0005.

4.2.5 Prnp inhibits VSMC apoptosis by blocking TRAIL-DR4 ligand-receptor complex formation

Previous studies from our laboratory demonstrated that trophendothelial cells secrete TRAIL, which causes selective demise of endothelial cells but not trophoblast cells (Paul et al., 2022). We, therefore, tested whether PRNP has any role TRAIL-induced apoptosis. PRNP being located in the outer leaflet of the plasma membrane, we first tested whether it interacts TRAIL receptor DR-4. Interestingly, DR4 co-immunoprecipitated with PRNP in A7r5 cells (Fig. 4.9)

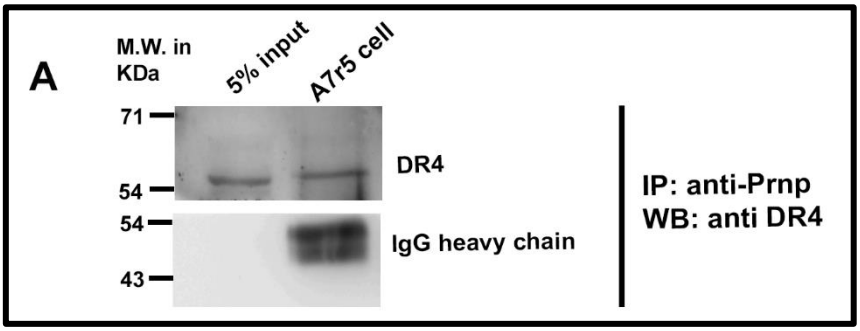

Figure 4.9: PRNP interacts with DR4 A) Immunoprecipitation with anti-Prnp antibody followed by immunoblotting with anti-DR4 in wild type A7r5 cells

This led us hypothesize that PRNP protects VSMCs from TRAIL-mediated apoptosis. Treatment of A7r5 cells with increasing doses of TRAIL (10, 50, 100 ng/ml) induced more apoptotic death in PRNP down regulated cells as compared to control (Fig. 4.10A-F). This data indicates that PRNP might prohibit TRAIL binding to its receptor on VSMCs leading to their protection from TRAIL-induced apoptosis.

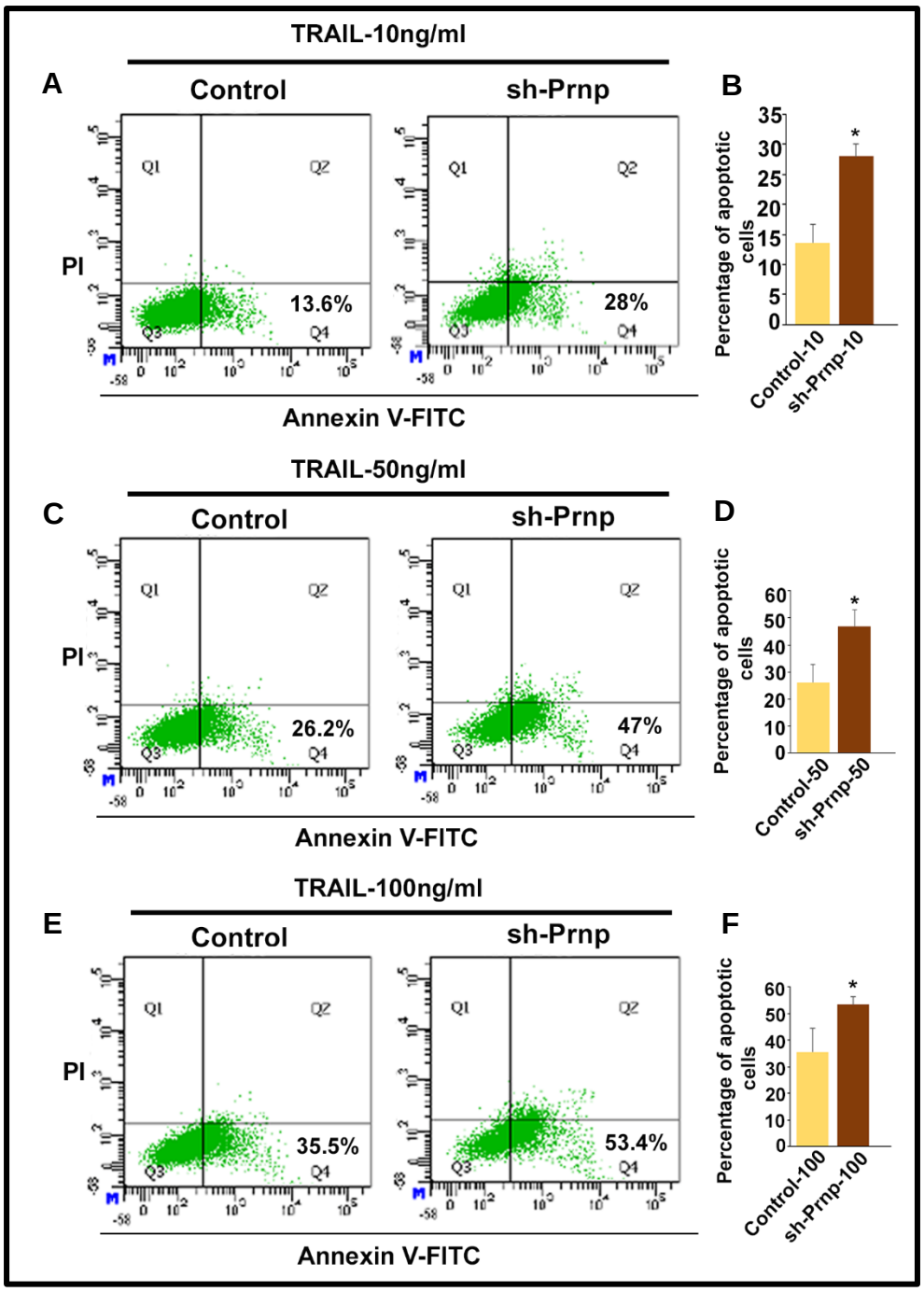

Figure 4.10: Prion inhibits TRAIL-mediated apoptosis in VSMCs A,C,E) Flow cytometric analysis to detect early apoptosis between control and PRNP downregulated A7r5 cells stained with Annexin V-FITC and PI treated with 10ng/ml (B), 50ng/ml (C), 100ng/ml (F) of murine recombinant TRAIL. **B,D,F)** bar graphs representing percentage of cells undergoing apoptosis between these two groups

4.2.6 Odd-skipped Related Transcription Factor 1 (OSR1) transactivates *Prnp* in rat VSMC cell line A7r5.

In silico promoter analysis of the rat *Prnp* gene (ENSRNOG00000021259) revealed 2 putative OSR1 binding motifs GCT/CNCTG(O'Brien et al., 2018) at 732bp and 3.2kb upstream of the transcription start site (Fig 4.11A). Full length *Osr1* cDNA (NM_001106716.3) was cloned and expressed in A7r5 cells (Fig 4.11B).

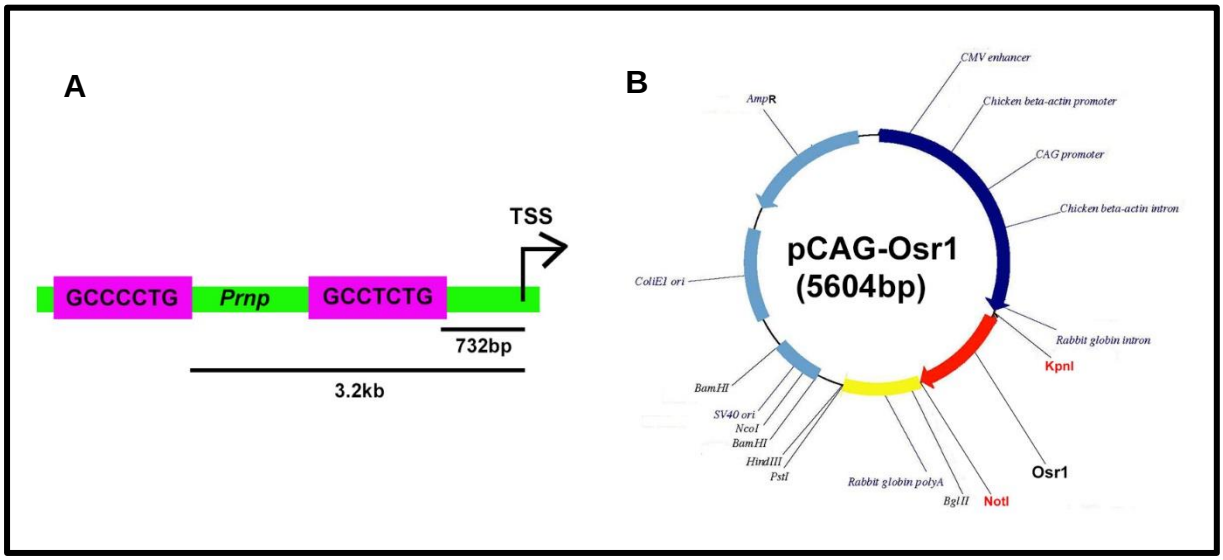

Figure 4.11. Promoter analysis of Prnp gene and cloning of full length Osr1 cDNA. A) Schematic diagram showing OSR1 binding sites (purple box) upstream of Prnp transcription start site (TSS). **B)** pCAG-DsRed vector with full length Osr1 coding sequence inserted between Kpn1 and Not1 sites

Elevated levels of *Osr1* mRNA and proteins were confirmed by real-time and western blot analysis. Subsequently, endogenous Prnp transcripts and protein were also found to be increased in A7r5 cells (Fig 4.12A, B and C).

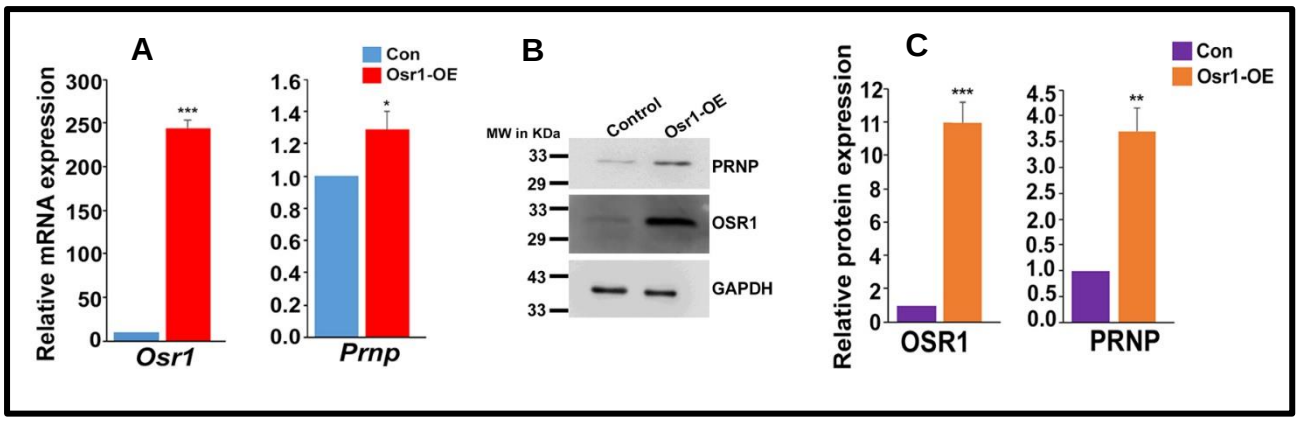

Figure 4.12. Osr1 overexpression leads to increased levels of endogenous Prnp. A) Relative transcripts levels of Osr1 and Prnp**. B)** Relative protein levels of OSR1 and PRNP. **C)** Quantification of the protein bands by NIH ImageJ software, after normalizing with the loading control GAPDH. Error bars represent SEM *p<0.05, **p<0.005, ***p<0.0005

To further authenticate our overexpression data, we knocked down endogenous *Osr1* mRNA and protein in A7r5 cells using short-hairpin RNA containing lentiviral particles (Fig 4.13).

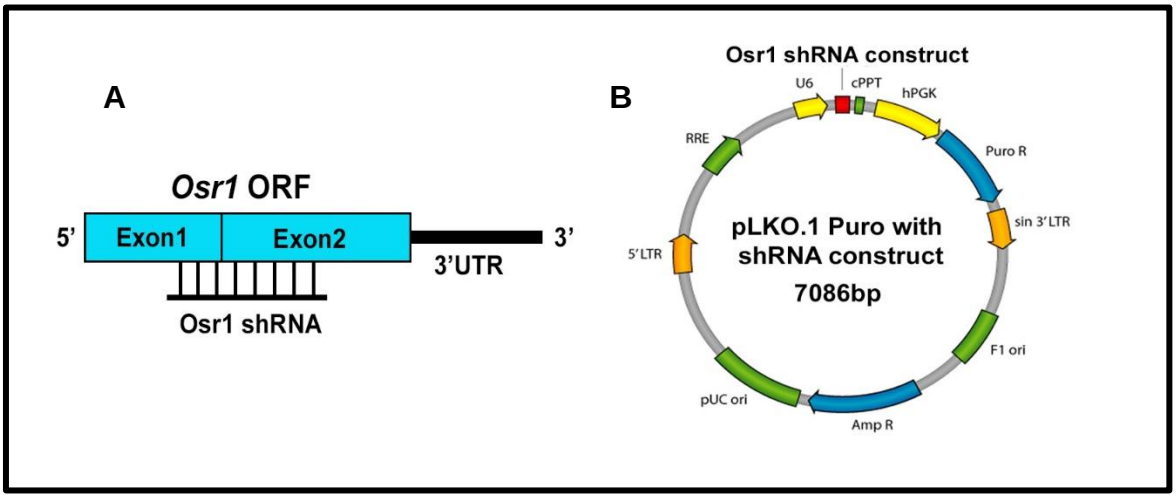

Figure 4.13. Designing and cloning of short hairpin RNAs targeting Osr1 ORF. A) Representative diagram showing short hairpin RNA targeting region within *Osr1* ORF**. B)** pLKO.1 vector with shRNA oligo targeting rat *Osr1*

resulting in concomitant decrease in both *Prnp* transcripts and protein levels (Fig 4.14 A, B and C).

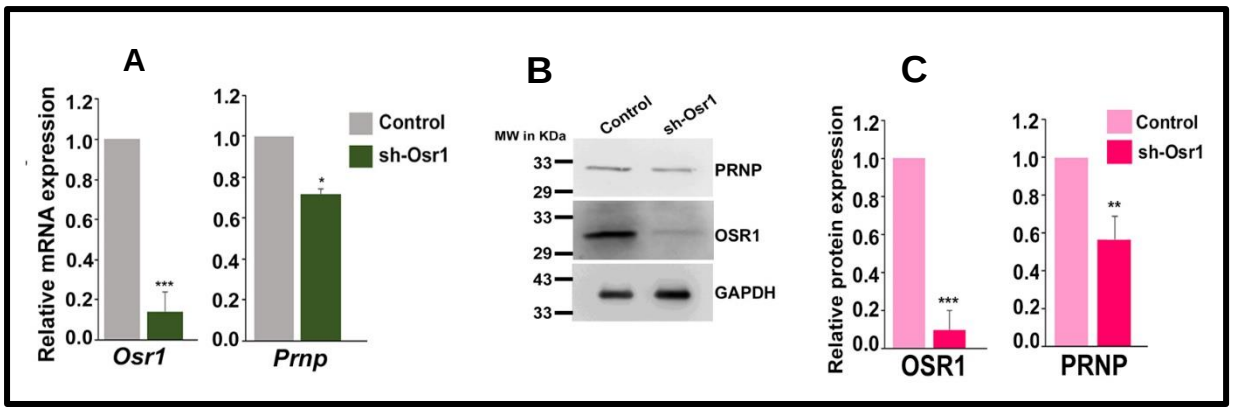

Figure 4.14. Osr1 downregulation leads to decreased levels of endogenous Prnp. A) Relative transcripts levels of Osr1 and Prnp**. B)** Relative protein levels of OSR1 and PRNP. **C)** Quantification of the protein bands by NIH ImageJ software, after normalizing with the loading control GAPDH. Error bars represent SEM *p<0.05, **p<0.005, ***p<0.0005

4.2.7 Trophoblast cells impede endogenous *Prnp* levels via OSR1 in A7r5 cells

In course of rat gestation, day 16.5 corresponds to the time point for maximum trophoblast invasion and day 19.5 corresponds to the time point when invasion is almost complete(De Rijk et al., 2002). Our tissue expression profile in rat metrial gland demonstrates that in vivo Prion levels peaks at E16.5 followed by sharp decline at E19.5. Therefore, to delineate the fate of Prnp in rat VSMC in presence of trophoblasts, we co-cultured A7r5 cells (in companion plates) with freshly isolated trophoblast cells (plated on inserts) from junctional zones of E16.5 rat placenta for 48 hours (Fig 4.15). This experimental model closely mimicked the in-vivo scenario the invasive trophoblast cells are in close proximity with the VSMCs as, although the two cells are physically separated but any factor(s) secreted by the trophoblasts can act upon the underlying A7r5 cells.

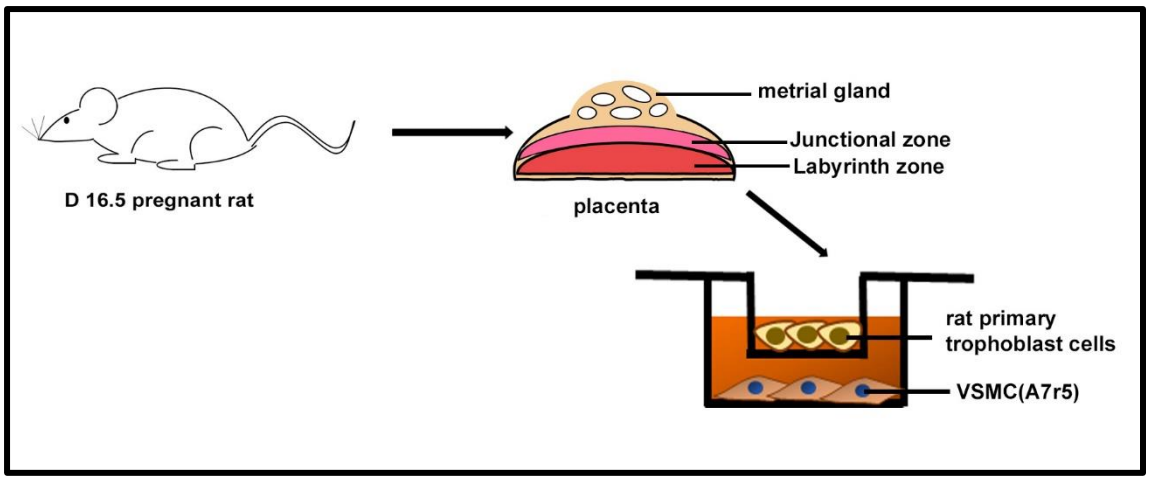

Figure 4.15 Schematic representation of a co-culture model with primary rat trophoblast cells and VSMCs.

In line with our in vivo data of Prnp expression, co-culture of A7r5 with E16.5 rat trophoblast cells led to significant downregulation of *Prnp* transcripts as well as PRNP protein (Fig 4.16A, B and C) following 48 hours of culture. Interestingly, the upstream regulator of prion, OSR1 also showed a similar decreasing pattern as analysed by real-time PCR and western-blotting (Fig 4.16A, B and C). Considering that, the primary trophoblasts do not express PRNP protein (Fig 4.16D and E), the observed altered levels of Prnp transcripts and protein can be ascribed to the VSMC pool only.

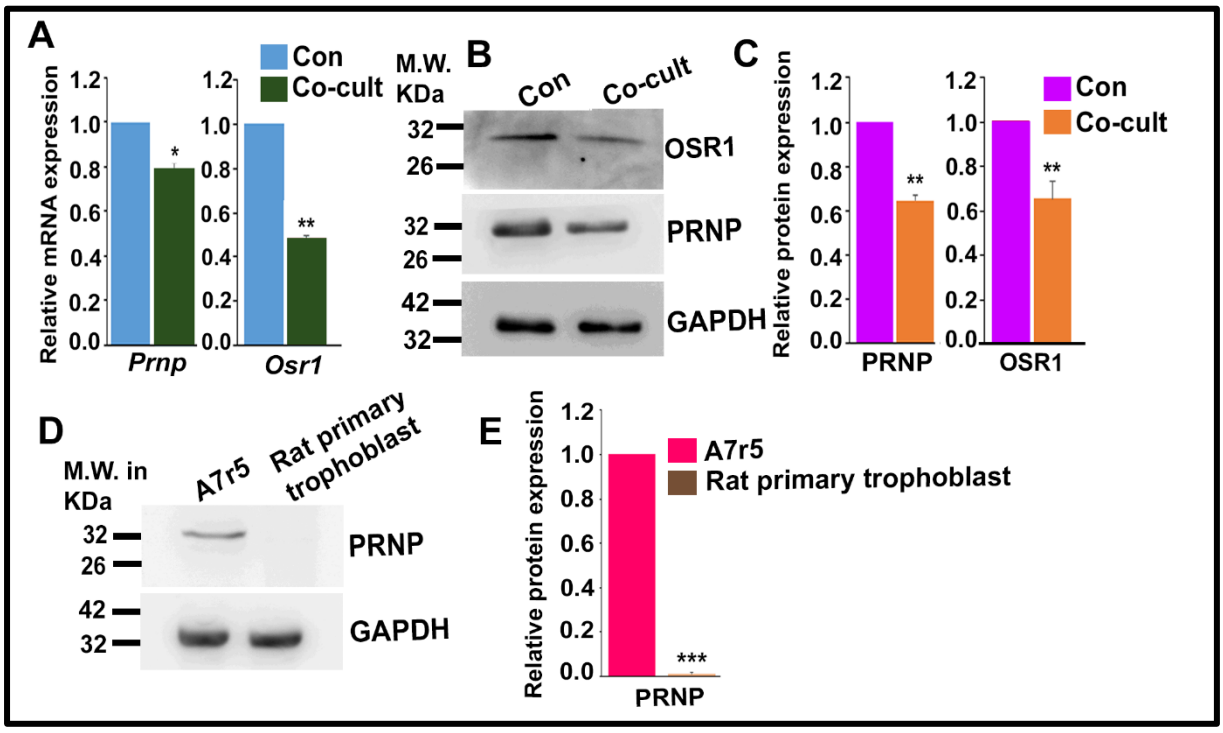

Figure 4.16. OSR1 leads to reduced expression of endogenous Prnp in VSMC in presence of trophoblasts. A) Relative transcripts levels of Prnp and Osr1**. B)** Relative protein levels of OSR1 and PRNP. **C)** Quantification of the protein bands by NIH ImageJ software, after normalizing with the loading control GAPDH. Error bars represent SEM *p<0.05, **p<0.005, ***p<0.0005

This data led us to speculate that, invasive trophoblasts might secrete factors which indirectly impede *Prnp* expression in VSMCs by inhibiting the expression of OSR1.

4.3 Discussion

Mechanism of VSMC migration under physiological and patho-physiological conditions has been well studied and extensively reviewed (Gerthoffer, 2007). Formation and degradation of focal contacts in continuous cycles, drives the cell forward while its trailing end remains still attached to the substratum. Activated FAK forms complex with the activated PDGFRβ and positively contributes to PDGFBB induced VSMC migration (Hauck et al., 2000). Prion protein is known to positively

influence metastatic activity of colorectal cancer cells both in vivo and in vitro (Wang et al., 2012). In gastric cancer cell line SCG7901 deletion of Prnp N-terminal domain decreased MMP11 promoter activity and consequently its metastatic ability in vivo (Y Pan et al., 2006). In the current study, by manipulating endogenous Prnp levels in A7r5 cells, we demonstrated that Prnp, not only promotes migration and invasion in VSMCs, but also forms an integral part of the PDGFRβ-FAK complex, exhilarating the growth-factor dependent migration. While the previous studies mainly focused on indirect effects of prion on cellular invasion and motility, we tried to establish a more straight-forward role of cellular prion, in directly coalescing “outside-in” migratory signals during normal mammalian embryogenesis.

Trophoblast cells isolated from first trimester human placenta expressed membrane-associated TRAIL and induced apoptosis of human aortic VSMC (R. J., Keogh et al., 2007). Expression of TRAIL in trans-differentiated trophendothelial cells was demonstrated by our laboratory (Paul et al., 2022). Our observation that RNA interference of PRNP in VSMCs caused apoptotic death led to our hypothesis that PRNP protects VSMCs from apoptotic cell death. Furthermore, our data on formation of immune-complex with PRNP and TRAIL receptor, DR4, in wild type A7r5 cells led us test whether PRNP can protect VSMCs from TRAIL-induced apoptosis. Signs of early apoptosis in Prnp knock down cells in presence of low doses of TRAIL poses it to be a tenable antagonist of TRAIL-DR4 apoptotic pathway. Anti-apoptotic property of prion in neurons have been previously documented (Bragason & Palsdottir, 2005; Roucou et al., 2003); where the authors have expressed a cytosolic isoform of the protein and shown its effect on Bax, or its interaction with a pro-apoptotic protein NRAGE, respectively. Compared to these observations, the novelty of our study lies in the fact that under physiological condition, cellular prion protein is typically located

in the outer leaflet of the plasma membrane with almost no cytosolic face. Therefore, our observations propose a more preferable mechanism by which prion protein confers its anti-apoptotic activity.

Role of Osr1 in vascular smooth muscle cells is still an ambiguous concept, therefore our study is one the earliest interpretation of its relevant function in rat aortic smooth muscle cells. Transactivation of *Prnp* promoter by Osr1 might have broader implications in developmental biology as precise timing for Prion expression in the VSMCs is crucial for their phenotypic modulation. Our data on expression of OSR-1 in VSMCs indicates that it might have other functions in regulating VSMCs. It is evident that OSR1 indirectly regulates VSMC migration via PRNP and thus play important role in uSAR.

As trophoblast invasion and its associated factors are an integral part of spiral artery remodeling, it was very important to trace the dynamics of Prnp expression in rat VSMCs with respect to trophoblasts. During rat gestation, E16.5 is the time point wherein maximum trophoblast invasion occurs and by E19.5 it nears completion. Our data from Chapter 3 revealed that PRNP expression in the VSMCs is highest at E16.5 and declines at E19.5. This apparent association of trophoblast invasion into metrial gland and PRNP expression in the VSMCs was recapitulated in the *in vitro* co-culture experiments. Primary rat trophoblast cells, isolated from E16.5 placentae, cultured with rat VSMC (A7r5 cells) for 48 hours led to significant downregulation PRNP as well as OSR1. The duration of this experiment was set to mimic the in vivo time points of trophoblast invasion and their effect on VSMCs in the metrial gland. The reciprocal relationship of Prnp and trophoblasts ex vivo can be co-related with decrease in Prnp in E19.5 metrial gland. Our observation suggests, when trophoblast invasion is minimal in the metrial gland Prion begins to be expressed by the VSMCs, thus

facilitating their survival and migration away from the arterial wall. As more numbers of trophoblasts infiltrate the region, their secretory factors suppress Prion in the VSMCs via Osr1 in an unknown mechanism, thereby retarding their motility and allowing them to undergo either de-differentiation (Nandy et al., 2020) or apoptosis.

CHAPTER 5

GLOBAL TRANSCRIPTOME ANALYSIS OF RAT VASCULAR SMOOTH MUSCLE CELLS TO DECIPHER THE ALTERATIONS OF BIOLOGICAL PROCESSES BY ALTERING ENDOGENOUS PRION EXPRESSION

5.1 Background

RNA-Sequencing is a high throughput strategy that uses Next-generation sequencing technique to examine and quantify the presence of RNA in a biological sample. It enables us to investigate the whole transcriptome single nucleotide polymorphism and differential gene expression among different treatment groups ((Han et al., 2015).

The RNA-Seq work flow has several steps, which can be summarized as follows: -

- Firstly, the RNA extracted from the respective samples need to be purified, followed by reverse transcribing them to complementary DNAs (cDNAs)
- For library preparation, cDNAs are fragmented and adapters are added in each end for permitting sequencing.
- Once the library is prepared, cDNA fragments are amplified, selected by size and then sequenced through NGS, producing short sequences throughout the entire length of its corresponding fragment.
- The short sequences are then aligned to a reference genome to obtain 'count' values. These counts are then statistically analyzed to identify differentially expressed genes.

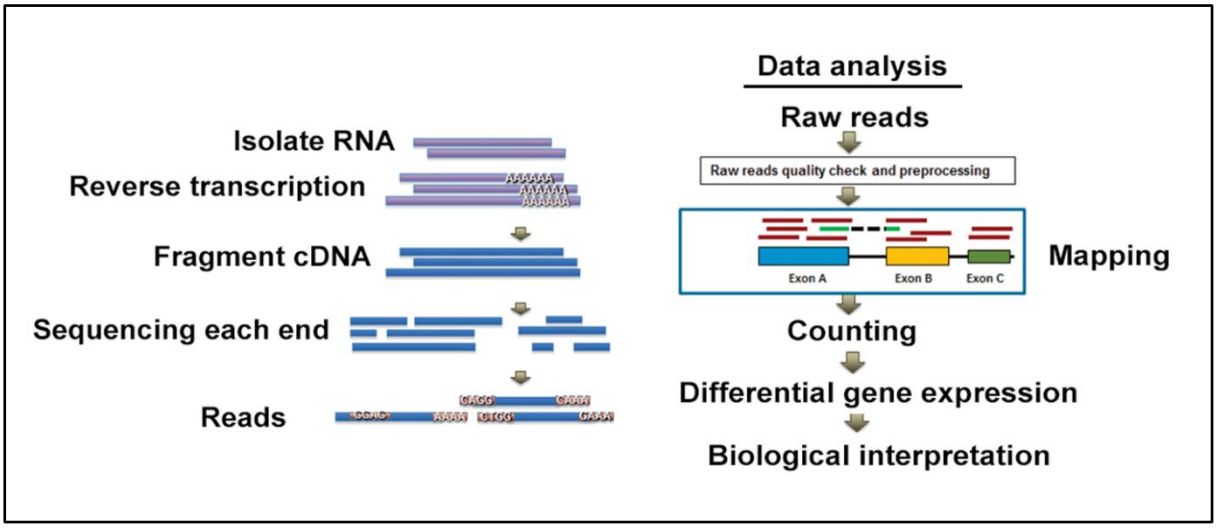

Figure 5.1. Illustrative representation of the workflow of RNA Sequencing

Unlike arrays RNA-Seq technology does not require species or transcript-specific probes. Moreover, due to hybridization principle, gene expression measurement in array, is limited by background signal (for low copy genes) or signal saturation (for high copy genes). On the other hand, RNA-Seq provides a wider range of data varying from novel transcripts, single nucleotide polymorphism, transcript variants, to small insertions or deletions (Wang Z et al., 2009; Wilhelm BT & Landry JR, 2009).

Compared to micro-array, RNA-Seq has emerged as a technology that can detect higher percentage of differentially expressed genes, especially rare transcripts, and weakly expressed genes (Li J et al., 2016).

5.2 Results

5.2.1 Fifty-one genes were found to be differentially regulated by Prnp in rat VSMCs

The multifaceted functions of PRNP in various organs, have prompted us to analyze its effect on other biological processes within VSMCs, by silencing its expression with shRNAs. To search for differentially expressed genes (DEGs), we employed high-throughput RNA sequencing workflow based on BAM files and count values. The generated count values were thoroughly scrutinized, and genes with count >= 500 with greater than 0.5 or less than -0.5 log2foldchnage and Pvalue <0.05 were considered for further validation. Thus, fifty-one DEGs were identified which is represented by the Volcano Plot (Fig 5.2A).

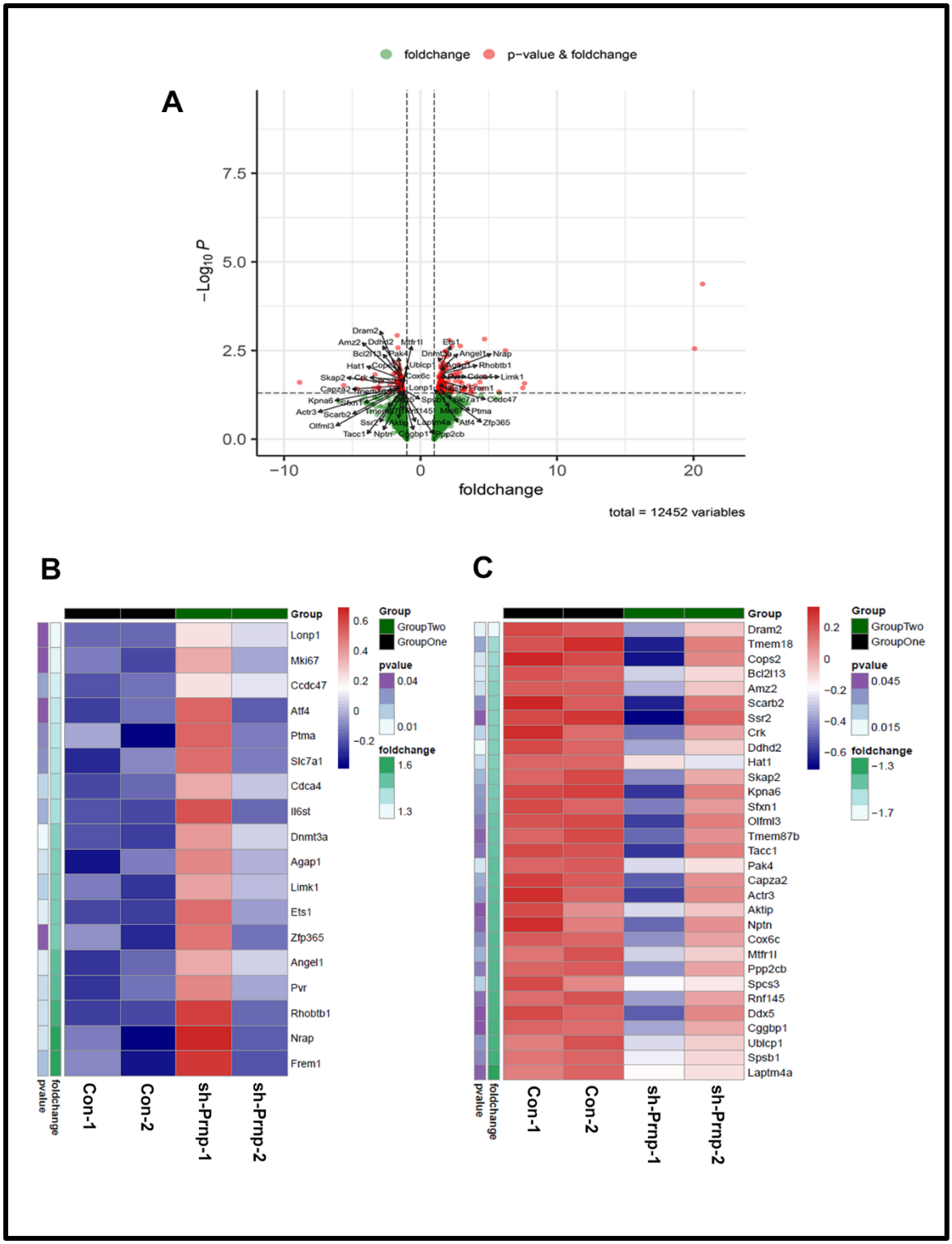

Figure 5.2. RNA Sequencing analysis of VSMCs by shRNA mediated silencing of endogenous prion expression. A) Volcano plot representing 51 differentially expressed genes. Dots towards the right of 0 point represent genes which show positive change in fold change, whereas dots towards the left of 0 point represent genes which show negative change in fold change, as compared to control. **B and C)** Heat maps representing fold change and p value of differentially expressed genes across Con and *Prnp* KD groups.

The extent of fold change in expression of individual genes across the Con and *Prnp* KD groups of different biological replicates is represented by two heat maps (Fig 5.2 B and C). These 51 DEGs were grouped into different biological pathways based on their individual functions and/or the biological processes they are involved in. As anticipated, we unveiled a wide range of biological pathways that are affected upon *Prnp* knockdown (Fig. 5.2). List of all the upregulated and downregulated genes are provided in table 4.1 and 4.2 respectively.

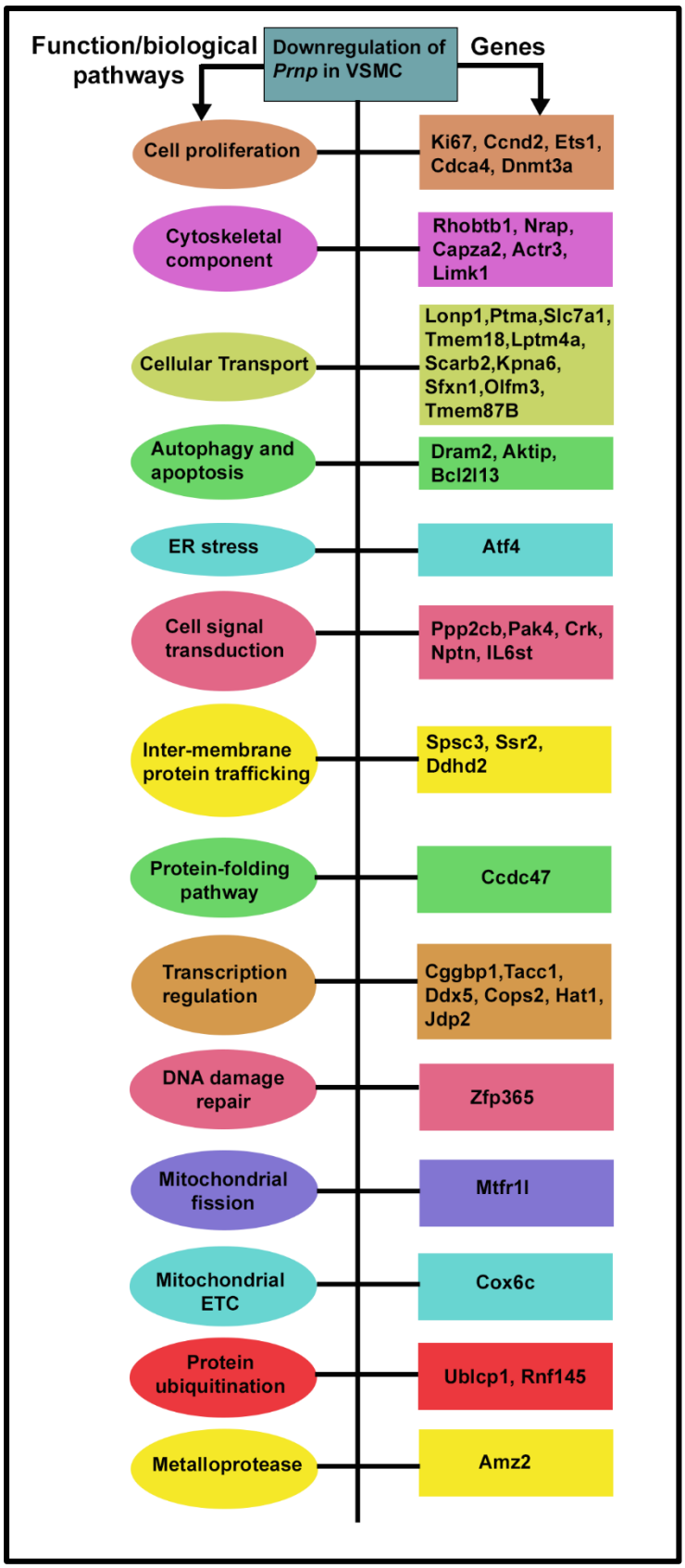

Figure 5.3. Function-based annotation of the 51 differentially expressed genes

The differential expression of individual gene of each functional group was further validated in different biological replicates by qRT-PCR using rpL7 as endogenous control. Out of 20 upregulated genes, 16 genes met the recommended cut off for Ct values, i.e., Ct<30, and their expression pattern matched with that of in-silico analysis data (Fig 5.4).

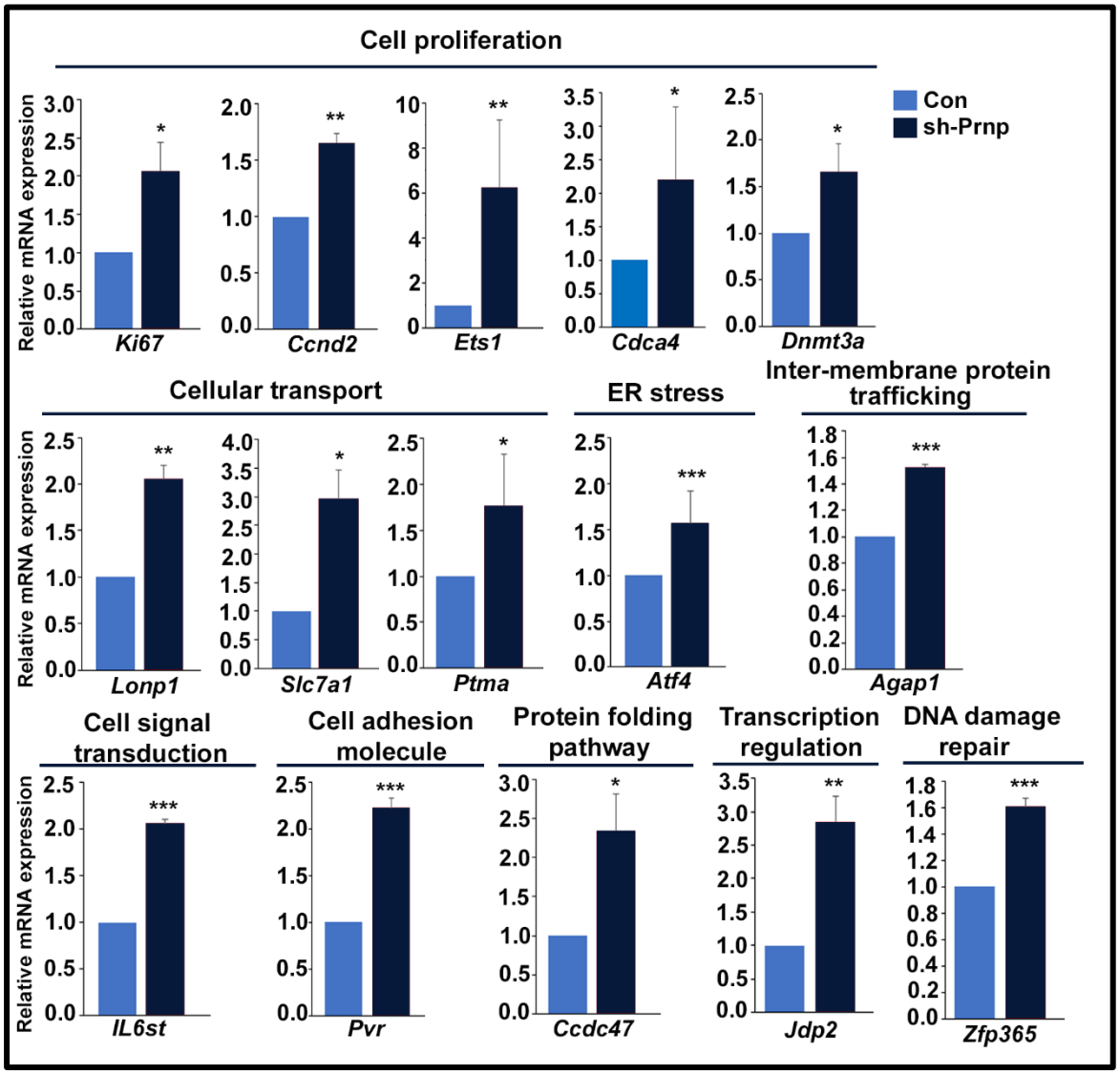

Figure 5.4. Bar graphs showing relative transcript levels of sixteen upregulated genes with Ct value <30. Error bars represent SEM. *p<0.05, **p<0.005, ***p<0.0005

Similarly, for downregulated genes, 24 out of 31 genes, met the recommended cut off for Ct values, i.e., Ct<30, and showed consistent decreased expression across replicates (Fig 5.5), as observed in bioinformatic analysis.

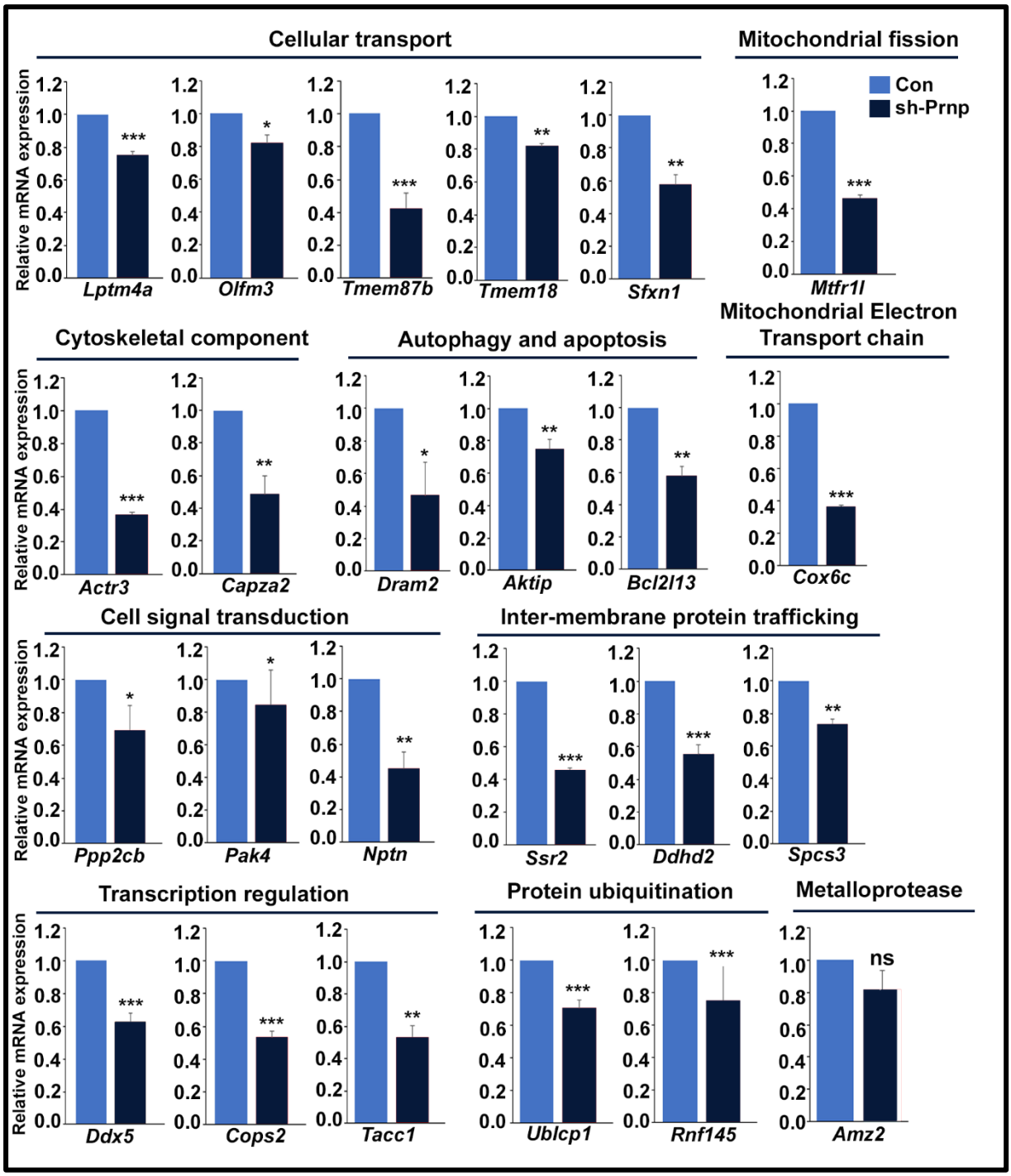

Figure 5.5. Bar graphs showing relative transcript levels of twenty-four downregulated genes with Ct value <30. Error bars represent SEM. *p<0.05, **p<0.005, ***p<0.0005, ns=non-significant

Table 4.1: List of upregulated genes

Serial No.	**Gene symbol**	**Gene name**	**Fold change**
1.	Lonp1	Lon peptidase1, mitochondrial	1.252963
2.	Mki67	Marker of proliferation, ki-67	1.275359
3.	Ccdc47	Coiled-coil domain containing 47	1.30692
4.	Atf4	Activating transcription factor 4	1.353007
5.	Ptma	Prothymosin alpha	1.363043
6.	Ccnd2	Cyclin D2	1.366797
7.	Jdp2	Jun dimerization protein 2	1.374523
8.	Slc7a1	Solute carrier family 7-member 1	1.382314
9.	Cdca4	Cell division cycle associated 4	1.398746
10.	IL6st	Interleukin 6 signal transducer	1.40445
11.	Dnmt3a	DNA methyltransferase 3 alpha	1.462486
12.	Agap1	ArfGAP with GTPase domain, ankyrin repeat and pH domain	1.476973
13.	Limk1	LIM domain kinase 1	1.480179

14.	Ets1	ETS proto-oncogene 1, transcription factor	1.485925
15.	Zfp365	Zinc finger protein 365	1.486166
16.	Angel 1	Angel homolog 1	1.539546
17.	Pvr	PVR cell adhesion molecule	1.54964
18.	Rhobtb1	Rho-related BTB domain containing 1	1.596004
19.	Nrap	Nebulin-related anchoring protein	1.651719
20.	Frem1	Fras1 related extracellular matrix 1	1.655388

Table 4.2: List of downregulated genes

Serial No.	**Gene symbol**	**Gene name**	**Fold change**
1.	Dram2	DNA-damage regulated autophagy modulator 2	-1.707657
2.	Tmem18	Transmembrane protein 18	-1.51378
3.	Cops2	COP9 signalosome subunit 2	-1.501311
4.	Bcl2l13	Bcl2 like 13	-1.481783
5.	Amz2	archaelysin family metallopeptidase 2	-1.460355
6.	Scarb2	scavenger receptor class B, member 2	-1.457937
7.	Ssr2	signal sequence receptor subunit 2	-1.457919
8.	Crk	CRK proto-oncogene, adaptor protein	-1.452163
9.	Ddhd2	DDHD domain containing 2	-1.451941

10.	Hat1	histone acetyltransferase 1	-1.450459
11.	Skap2	src kinase associated phosphoprotein 2	-1.433526
12.	Kpna6	karyopherin subunit alpha 6	-1.432212
13.	Sfxn1	sideroflexin 1	-1.423652
14.	Olfml3	olfactomedin-like 3	-1.404411
15.	Tmem87b	transmembrane protein 87B	-1.401391
16.	Tacc1	transforming, acidic coiled-coil containing protein 1	-1.392205
17.	Pak4	p21 (RAC1) activated kinase 4	-1.380079
18.	Capza2	capping actin protein of muscle Z-line subunit alpha 2	-1.380065
19.	Actr3	actin related protein 3	-1.374614
20.	Aktip	AKT interacting protein	-1.367184
21.	Nptn	neuroplastin	-1.3642
22.	Cox6c	cytochrome c oxidase subunit 6C	-1.35197
23.	Mtfr1l	mitochondrial fission regulator 1-like	-1.350715
24.	Ppp2cb	protein phosphatase 2 catalytic subunit beta	-1.342267
25.	Spcs3	signal peptidase complex subunit 3	-1.342161
26.	Rnf145	ring finger protein 145	-1.330836
27.	Ddx5	DEAD-box helicase 5	-1.324703
28.	Cggbp1	CGG triplet repeat binding protein 1	-1.317401
29.	Ublcp1	ubiquitin-like domain containing CTD phosphatase 1	-1.315474
30.	Spsb1	splA/ryanodine receptor domain and SOCS box containing 1	-1.302508

31.	Laptm4a	lysosomal protein transmembrane 4 alpha	-1.234861

5.2.2 Prnp constrains VSMC proliferation

Leading on from our validation result, downregulation of Prnp led to increase in proliferation markers in A7r5 cells. To test this hypothesis, we performed BrdU incorporation assay in cells transduced with either scramble virus (control) or cocktail of viruses containing three sh-oligos (sh-Prnp), as shown in Fig 5.6.

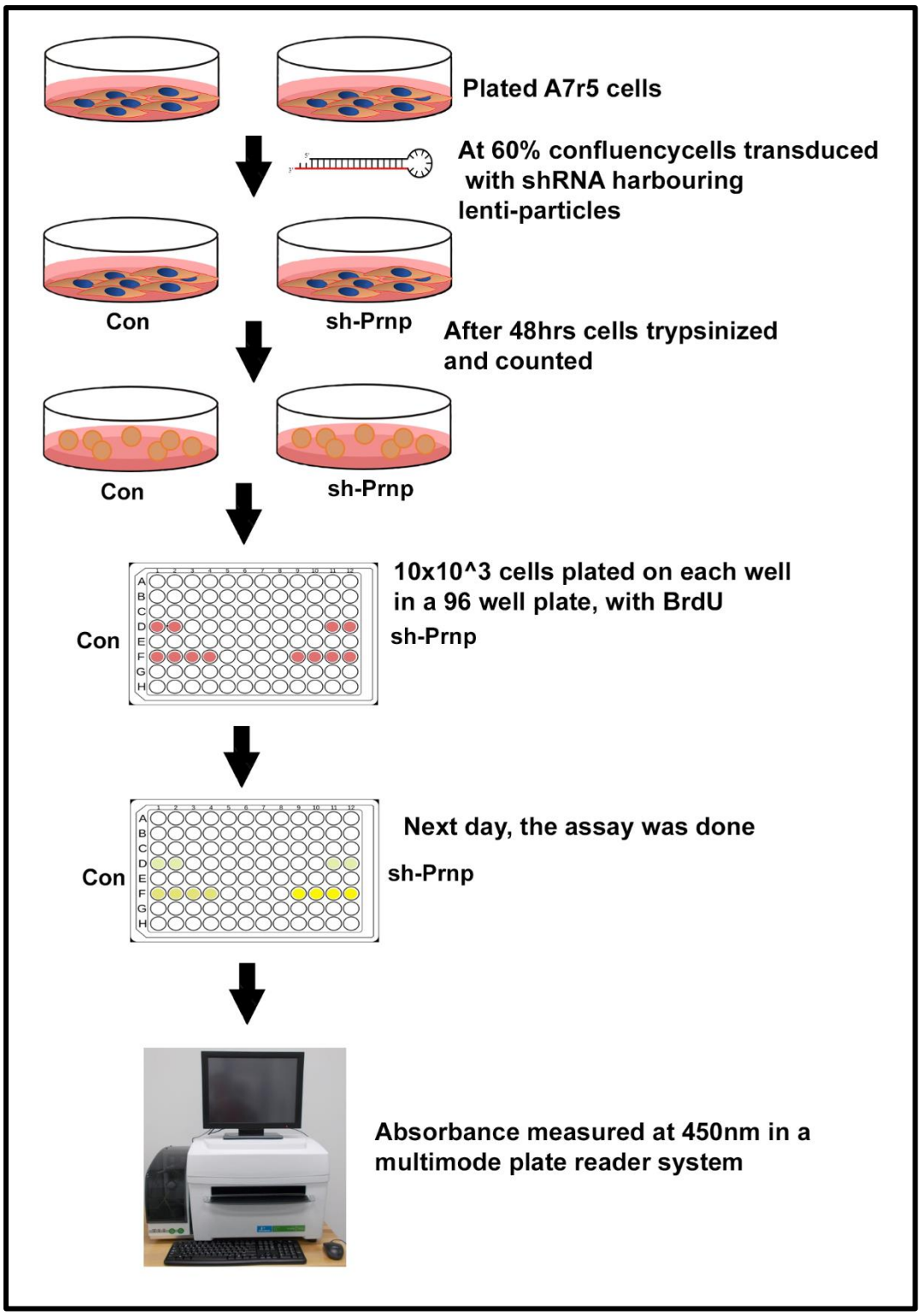

Figure 5.6. Flow chart depicting the step-by-step process of BrdU incorporation assay in control and Prnp downregulated cells

Depletion of PRNP led to almost 50% increase in BrdU incorporation by A7r5 cells, indicated by increased absorbance at 450nm (Fig. 5.7A). To corroborate this observation further, Ki-67 immuno-fluorescence staining was done in control and sh-Prnp cells, which showed a greater number of Ki-67 positive cells in the latter group as compared to control group (Fig. 5.7B and C).

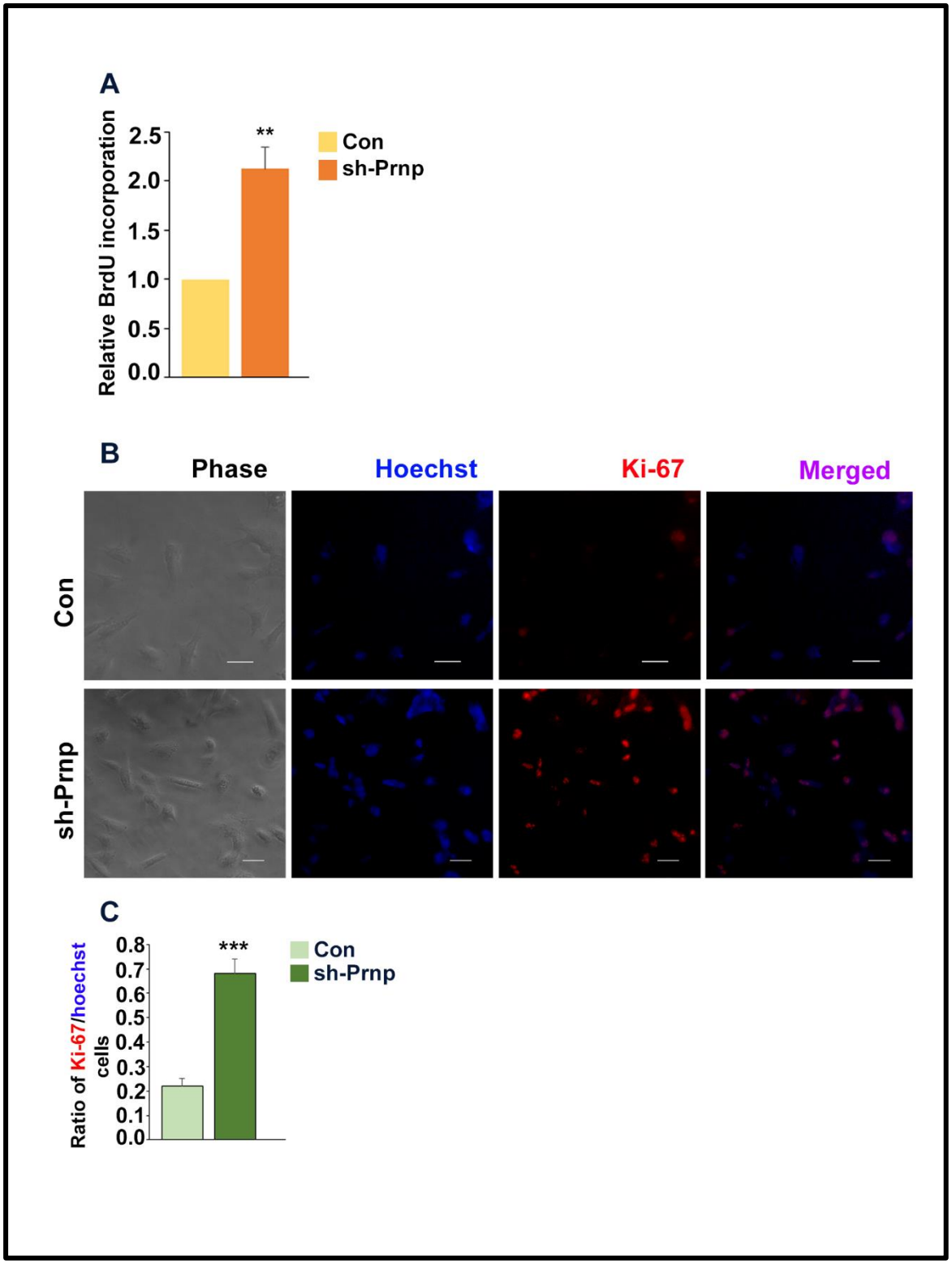
A
Relative BrdU incorporation
2.5
2.0
1.5
1.0
0.5
0.0
**
Con
sh-Prnp
B
Phase
Hoechst
Ki-67
Merged
Con
sh-Prnp
C
Ratio of Ki-67/hoechst cells
0.8
0.7
0.6
0.5
0.4
0.3
0.2
0.1
0.0
***
Con
sh-Prnp

Figure 5.7. Downregulation of PRNP promote VSMC proliferation. A) Bar graphs representing relative BrdU incorporation in Control versus Prnp KD cells, after measuring absorbance at 450nm. **B)** Ki-67 immuno-fluorescence staining (red) of Control (top panel) and Prnp KD cells (bottom panel). Nuclei are counterstained with Hoechst (blue). Scale bars shown here are 100µm. **C)** The ratio of Ki-67 positive nuclei and Hoechst nuclei were assessed by counting at least 6 different microscopic fields in 3 biological replicates. Error bars represent SEM. *p<0.05, **p<0.005, ***p<0.0005

5.3 Discussion

The ubiquitous presence of the prion protein makes it very challenging to decipher its exact biological role. To make an in-depth study about its nature, we therefore employed global transcriptome sequencing method by depleting its endogenous expression in rat VSMCs. Prion was indeed found to be involved in pathways, previously unheard of. For example, downregulation of an autophagic candidate Dram2, implies that prion might also assist in VSMC survival mechanism, other than inhibition of apoptosis. Similarly, candidates of DNA repair machinery, inter-membrane protein trafficking, protein ubiquitination, ER stress and mitochondrial electron transport chain, reveal some of the unexplored biological activities of cellular prion protein. We, have currently focused our study on its effect on VSMC proliferation and found that Prnp negatively regulates the same.

FINAL OVERVIEW

FINAL OVERVIEW

Establishment of the hemochorial placenta is a hallmark of eutherian mammals including humans and rodents; and spiral artery remodeling (SAR) is one of the many complex physiological phenomena that is indispensable for a successful pregnancy. This requires calibration of high resistance blood vessels to low resistance vessels to meet the increasing nutritive demands of the growing fetus. Various cellular and molecular components within the utero-placental component come into play during this elaborate process at various time-point of gestation.

Cellular Prion protein (PRNP), has emerged as a salient determinant for successful embryogenesis, in the last decade; yet a clear understanding of the biological role played by it remained elusive. In this study, we have attempted to shed light on the various molecular events, which Prnp might be involved in, to confer a healthy full-term pregnancy. On analysis of the implantation sites of rats an interesting observation was made regarding the cellular localization of the prion protein in the metrial gland. The vascular smooth muscle cells which drift away from the spiral arteries were identified as the major site of prion expression. That, Prnp indeed modulates VSMC migration and invasion was confirmed by scratch wound and cell invasion assays, using control and *Prnp* knock down VSMC cell line A7r5. It was quite intriguing that PRNP formed a ter-molecular complex with PDGFRβ-FAK. PDGFRβ-FAK complex has been well documented to enhance VSMC chemotaxis. This data clearly indicates that migration promoting function of PRNP is executed through the well-established PDGFRβ-FAK complex. Knockdown studies have also proved potential role of Prnp in smooth muscle cell survival. Formation of immune-complex with PRNP and TRAIL receptor, DR4, and subsequent increased apoptosis of $Prnp^{KD}$ cells fed with different doses of TRAIL, led us to speculate that PRNP can protect VSMCs from TRAIL-

induced apoptosis. Our data on transactivation of Prnp promoter by OSR-1 in VSMCs is rather intriguing.

VSMCs surrounding the spiral arteries typically remain in a contractile state. Trophoblast cell-induced de-differentiation leads to phenotypic switching in VSMCs that involve suppression of contractile markers expression and elevation of synthetic state markers. In-vitro co-culture of rat primary trophoblast cells with A7r5 was done to closely recapitulate the in vivo association of trophoblast and VSMC in the placental microenvironment. Interestingly, both OSR1 and PRNP were down regulated of. It is therefore evident that trophoblast cells surveil PRNP expression via OSR1. Furthermore, activation of PDGFRβ in VSMCs after co-culture with trophoblast cells has been previously demonstrated from our laboratory. Therefore, it may be inferred that a) heightened PRNP expression and PDGFRβ activation on E16.5 potentiate de-differentiated VSMC migration through the surrounding matrix away from the arterial wall thereby lowering the vessel resistance and creates more space for the trophoblast cells to maximally invade (E16.5), b) trophoblast surveilled dampening of PRNP expression, through Osr1, lead to retardation of VSMC movement away from the uterine spiral arteries making them more susceptible to TRAIL-mediated apoptosis.

Finally, our RNA-Seq data has unravelled novel genes from various biochemical processes that are directly or indirectly regulated by prion. Proliferation assays such as BrdU incorporation and immune-fluorescence staining with Ki67 reveal that Prnp impedes VSMC proliferation. As de-differentiated VSMCs often exhibit increased proliferation, our data brings forth an unconventional finding which might have broader implications in understanding the physiological role of prion during SAR.

In conclusion, this work has aimed in deciphering the molecular function moonlighting effect of cellular prion with respect to utero-placental development in rat models. We

have elucidated how prion moonlights various aspects of spiral artery remodelling in VSMCs, thus providing insights into one of the complicated physiological processes occurring during pregnancy.

REFERENCES

REFERENCES

1. Ain, R., Canham, L. N., & Soares, M. J. (2003). Gestation stage-dependent intrauterine trophoblast cell invasion in the rat and mouse: novel endocrine phenotype and regulation. *Developmental Biology*, *260*(1), 176–190. https://doi.org/10.1016/S0012-1606(03)00210-0
2. Ain, R., Konno, T., Canham, L. N., & Soares, M. J. (n.d.). Phenotypic Analysis of the Rat Placenta. In *Placenta and Trophoblast* (pp. 293–312). Humana Press. https://doi.org/10.1385/1-59259-983-4:293
3. Ain, R., & Soares, M. J. (2004). Is the metrial gland really a gland? *Journal of Reproductive Immunology*, *61*(2), 129–131. https://doi.org/10.1016/j.jri.2004.01.002
4. Alfaidy, N., Chauvet, S., Donadio-Andrei, S., Salomon, A., Saoudi, Y., Richaud, P., Aude-Garcia, C., Hoffmann, P., Andrieux, A., Moulis, J.-M., Feige, J.-J., & Benharouga, M. (2013). Prion Protein Expression and Functional Importance in Developmental Angiogenesis: Role in Oxidative Stress and Copper Homeostasis. *Antioxidants & Redox Signaling*, *18*(4), 400–411. https://doi.org/10.1089/ars.2012.4637
5. Ashkar, A. A., di Santo, J. P., & Croy, B. A. (2000). Interferon γ Contributes to Initiation of Uterine Vascular Modification, Decidual Integrity, and Uterine Natural Killer Cell Maturation during Normal Murine Pregnancy. *Journal of Experimental Medicine*, *192*(2), 259–270. https://doi.org/10.1084/jem.192.2.259
6. Aucouturier, P., Geissmann, F., Damotte, D., Saborio, G. P., Meeker, H. C., Kascsak, R., Kascsak, R., Carp, R. I., & Wisniewski, T. (2001). Infected splenic dendritic cells are sufficient for prion transmission to the CNS in mouse scrapie. *Journal of Clinical Investigation*, *108*(5), 703–708. https://doi.org/10.1172/JCI13155
7. Baldauf, E., McBride, P. A., & Beekes, M. (1998). Cerebral targeting indicates vagal spread of infection in hamsters fed with scrapie. *Journal of General Virology*, *79*(3), 601–607. https://doi.org/10.1099/0022-1317-79-3-601
8. Bate, C., Tayebi, M., Diomede, L., Salmona, M., & Williams, A. (2009). Glimepiride Reduces the Expression of PrPC, Prevents PrPSc Formation and Protects against Prion Mediated Neurotoxicity. *PLoS ONE*, *4*(12), e8221. https://doi.org/10.1371/journal.pone.0008221
9. Beekes, M., & McBride, P. A. (2000). Early accumulation of pathological PrP in the enteric nervous system and gut-associated lymphoid tissue of hamsters orally

infected with scrapie. *Neuroscience Letters*, *278*(3), 181–184. https://doi.org/10.1016/S0304-3940(99)00934-9

10. Bencsik, A., Lezmi, S., Hunsmann, G., & Baron, T. (2001). Close Vicinity of PrP Expressing Cells (FDC) with Noradrenergic Fibers in Healthy Sheep Spleen. *Developmental Immunology*, *8*(3–4), 235–241. https://doi.org/10.1155/2001/40871
11. Bendheim, P. E., Brown, H. R., Rudelli, R. D., Scala, L. J., Goller, N. L., Wen, G. Y., Kascsak, R. J., Cashman, N. R., & Bolton, D. C. (1992). Nearly ubiquitous tissue distribution of the scrapie agent precursor protein. *Neurology*, *42*(1), 149–149. https://doi.org/10.1212/WNL.42.1.149
12. Bessen, R. A., & Marsh, R. F. (1994). Distinct PrP properties suggest the molecular basis of strain variation in transmissible mink encephalopathy. *Journal of Virology*, *68*(12), 7859–7868. https://doi.org/10.1128/jvi.68.12.7859-7868.1994
13. BORNFELDT, K. E., RAINES, E. W., GRAVES, L. M., SKINNER, M. P., KREBS, E. G., & ROSS, R. (1995). Platelet-derived Growth Factor. *Annals of the New York Academy of Sciences*, *766*(1 Receptor Acti), 416–430. https://doi.org/10.1111/j.1749-6632.1995.tb26691.x
14. Bose, R., & Ain, R. (2020). Dynamics of Cellular PRION expression during utero-placental development. *International Conference of Women's Reproductive Health Held at ICMR-NIRRH*, 13–13.
15. Bragason, B. T., & Palsdottir, A. (2005). Interaction of PrP with NRAGE, a protein involved in neuronal apoptosis. *Molecular and Cellular Neuroscience*, *29*(2), 232–244. https://doi.org/10.1016/j.mcn.2005.02.013
16. Brosens, I., Robertson, W. B., & Dixon, H. G. (1967). The physiological response of the vessels of the placental bed to normal pregnancy. *The Journal of Pathology and Bacteriology*, *93*(2), 569–579. https://doi.org/10.1002/path.1700930218
17. Brown, D. R., Clive, C., & Haswell, S. J. (2001). Antioxidant activity related to copper binding of native prion protein. *Journal of Neurochemistry*, *76*(1), 69–76. https://doi.org/10.1046/j.1471-4159.2001.00009.x
18. Bulmer, J. N., Innes, B. A., Levey, J., Robson, S. C., & Lash, G. E. (2012). The role of vascular smooth muscle cell apoptosis and migration during uterine spiral artery remodeling in normal human pregnancy. *The FASEB Journal*, *26*(7), 2975–2985. https://doi.org/10.1096/fj.12-203679
19. Burton, G. J., Jauniaux, E., & Watson, A. L. (1999). Maternal arterial connections to the placental intervillous space during the first trimester of human pregnancy: The

Boyd Collection revisited. *American Journal of Obstetrics and Gynecology*, *181*(3), 718–724. https://doi.org/10.1016/S0002-9378(99)70518-1

20. Burton, G. J., Watson, A. L., Hempstock, J., Skepper, J. N., & Jauniaux, E. (2002). Uterine Glands Provide Histiotrophic Nutrition for the Human Fetus during the First Trimester of Pregnancy. *The Journal of Clinical Endocrinology & Metabolism*, *87*(6), 2954–2959. https://doi.org/10.1210/jcem.87.6.8563
21. Campbell, J. J., Qin, S., Unutmaz, D., Soler, D., Murphy, K. E., Hodge, M. R., Wu, L., & Butcher, E. C. (2001). Unique Subpopulations of CD56+ NK and NK-T Peripheral Blood Lymphocytes Identified by Chemokine Receptor Expression Repertoire. *The Journal of Immunology*, *166*(11), 6477–6482. https://doi.org/10.4049/jimmunol.166.11.6477
22. Caughey, B., & Raymond, G. J. (1991). The scrapie-associated form of PrP is made from a cell surface precursor that is both protease- and phospholipase-sensitive. *JBC*, *266*(27), 18217–182123.
23. Cetin, I., & Antonazzo, P. (2009). The Role of the Placenta in Intrauterine Growth Restriction (IUGR). *Zeitschrift Für Geburtshilfe Und Neonatologie*, *213*(03), 84–88. https://doi.org/10.1055/s-0029-1224143
24. Chakraborty, D., Rumi, M. A. K., Konno, T., & Soares, M. J. (2011). Natural killer cells direct hemochorial placentation by regulating hypoxia-inducible factor dependent trophoblast lineage decisions. *Proceedings of the National Academy of Sciences*, *108*(39), 16295–16300. https://doi.org/10.1073/pnas.1109478108
25. Chen, Z., Zhang, J., Hatta, K., Lima, P. D. A., Yadi, H., Colucci, F., Yamada, A. T., & Croy, B. A. (2012). DBA-Lectin Reactivity Defines Mouse Uterine Natural Killer Cell Subsets with Biased Gene Expression1. *Biology of Reproduction*, *87*(4). https://doi.org/10.1095/biolreprod.112.102293
26. Collinge, J., Sidle, K. C. L., Meads, J., Ironside, J., & Hill, A. F. (1996). Molecular analysis of prion strain variation and the aetiology of “new variant” CJD. *Nature*, *383*(6602), 685–690. https://doi.org/10.1038/383685a0
27. Coulter, D. E., & Wieschaus, E. (1988). Gene activities and segmental patterning in Drosophila: analysis of odd-skipped and pair-rule double mutants. *Genes & Development*, *2*(12b), 1812–1823. https://doi.org/10.1101/gad.2.12b.1812
28. Cross, J., Werb, Z., & Fisher, S. (1994). Implantation and the placenta: key pieces of the development puzzle. *Science*, *266*(5190), 1508–1518. https://doi.org/10.1126/science.7985020

29. Croy, B. A., & Kiso, Y. (1993). Granulated metrial gland cells: A natural killer cell subset of the pregnant murine uterus. *Microscopy Research and Technique*, *25*(3), 189–200. https://doi.org/10.1002/jemt.1070250302
30. Croy, B., He, H., Esadeg, S., Wei, Q., McCartney, D., Zhang, J., Borzychowski, A., Ashkar, A., Black, G., Evans, S., Chantakru, S., van den Heuvel, M., & Yamada, A. (2003). Uterine natural killer cells: insights into their cellular and molecular biology from mouse modelling. *Reproduction*, 149–160. https://doi.org/10.1530/rep.0.1260149
31. Cuille, J. (1939). Experimental transmission of trembling to the goat. *C.R. Seances Acad. Sci.*, 1058–1160.
32. Das, A. S., & Zou, W.-Q. (2016). Prions: Beyond a Single Protein. *Clinical Microbiology Reviews*, *29*(3), 633–658. https://doi.org/10.1128/CMR.00046-15
33. Daude, N., Wohlgemuth, S., Brown, R., Pitstick, R., Gapeshina, H., Yang, J., Carlson, G. A., & Westaway, D. (2012). Knockout of the prion protein (PrP)-like *Sprn* gene does not produce embryonic lethality in combination with PrP^{C}-deficiency. *Proceedings of the National Academy of Sciences*, *109*(23), 9035–9040. https://doi.org/10.1073/pnas.1202130109
34. De Rijk, E. P. C. T., Van Esch, E., & Flik, G. (2002). Pregnancy Dating in the Rat: Placental Morphology and Maternal Blood Parameters. *Toxicologic Pathology*, *30*(2), 271–282. https://doi.org/10.1080/019262302753559614
35. De Wolf, F., Robertson, W. B., & Brosens, I. (1975). The ultrastructure of acute atherosis in hypertensive pregnancy. *American Journal of Obstetrics and Gynecology*, *123*(2), 164–174. https://doi.org/10.1016/0002-9378(75)90522-0
36. D'Errico, J. N., & Stapleton, P. A. (2019). Developmental onset of cardiovascular disease—Could the proof be in the placenta? *Microcirculation*, *26*(8). https://doi.org/10.1111/micc.12526
37. Duprez, D. (2002). Signals regulating muscle formation in the limb during embryonic development. *The International Journal of Developmental Biology*, *46*(7), 915–925.
38. Ehsani, S., Tao, R., Pocanschi, C. L., Ren, H., Harrison, P. M., & Schmitt-Ulms, G. (2011). Evidence for Retrogene Origins of the Prion Gene Family. *PLoS ONE*, *6*(10), e26800. https://doi.org/10.1371/journal.pone.0026800
39. Enari, M., Flechsig, E., & Weissmann, C. (2001). Scrapie prion protein accumulation by scrapie-infected neuroblastoma cells abrogated by exposure to a prion protein

antibody. *Proceedings of the National Academy of Sciences*, *98*(16), 9295–9299. https://doi.org/10.1073/pnas.151242598

40. Faas, M. M., & de Vos, P. (2017). Uterine NK cells and macrophages in pregnancy. *Placenta*, *56*, 44–52. https://doi.org/10.1016/j.placenta.2017.03.001
41. Faris, R., Moore, R. A., Ward, A., Race, B., Dorward, D. W., Hollister, J. R., Fischer, E. R., & Priola, S. A. (2017). Cellular prion protein is present in mitochondria of healthy mice. *Scientific Reports*, *7*(1), 41556. https://doi.org/10.1038/srep41556
42. Ferenczy, A., Bertrand, G., & Gelfand, M. M. (1979). Proliferation kinetics of human endometrium during the normal menstrual cycle. *American Journal of Obstetrics and Gynecology*, *133*(8), 859–867. https://doi.org/10.1016/0002-9378(79)90302-8
43. Gerthoffer, W. T. (2007). Mechanisms of vascular smooth muscle cell migration. *Circ Res*, *100*(5), 607–621.
44. Guimond, M.-J., Luross, J. A., Wang, B., Terhorst, C., Danial, S., & Anne Croy, B. (1997). Absence of Natural Killer Cells during Murine Pregnancy is Associated with Reproductive Compromise in TgE26 Mice1. *Biology of Reproduction*, *56*(1), 169–179. https://doi.org/10.1095/biolreprod56.1.169
45. Hammer, A., Blaschitz, A., Daxböck, C., Walcher, W., & Dohr, G. (1999). Fas and Fas-Ligand Are Expressed in the Uteroplacental Unit of First-Trimester Pregnancy. *American Journal of Reproductive Immunology*, *41*(1), 41–51. https://doi.org/10.1111/j.1600-0897.1999.tb00074.x
46. Han, Y., Gao, S., Muegge, K., Zhang, W., & Zhou, B. (2015). Advanced Applications of RNA Sequencing and Challenges. *Bioinformatics and Biology Insights*, *9s1*, BBI.S28991. https://doi.org/10.4137/BBI.S28991
47. Haraguchi, T., Fisher, S., Olofsson, S., Endo, T., Groth, D., Tarentino, A., Borchelt, D. R., Teplow, D., Hood, L., Burlingame, A., Lycke, E., Kobata, A., & Prusiner, S. B. (1989). Asparagine-linked glycosylation of the scrapie and cellular prion proteins. *Archives of Biochemistry and Biophysics*, *274*(1), 1–13. https://doi.org/10.1016/0003-9861(89)90409-8
48. Harland W., & Mossman. (1987). *Vertebrate fetal membranes [print] : comparative ontogeny and morphology, evolution, phylogenetic significance, basic functions, research opportunities*.
49. Harris, D. A. (2003). Trafficking, turnover and membrane topology of PrP. *British Medical Bulletin*, *66*(1), 71–85. https://doi.org/10.1093/bmb/66.1.71

50. Harris, L. K., Keogh, R. J., Wareing, M., Baker, P. N., Cartwright, J. E., Aplin, J. D., & Whitley, G. S. J. (2006). Invasive Trophoblasts Stimulate Vascular Smooth Muscle Cell Apoptosis by a Fas Ligand-Dependent Mechanism. *The American Journal of Pathology*, *169*(5), 1863–1874. https://doi.org/10.2353/ajpath.2006.060265
51. Hauck, C. R., Hsia, D. A., & Schlaepfer, D. D. (2000). Focal Adhesion Kinase Facilitates Platelet-derived Growth Factor-BB-stimulated ERK2 Activation Required for Chemotaxis Migration of Vascular Smooth Muscle Cells. *Journal of Biological Chemistry*, *275*(52), 41092–41099. https://doi.org/10.1074/jbc.M005450200
52. Hemberger, M., Hanna, C. W., & Dean, W. (2020). Mechanisms of early placental development in mouse and humans. *Nature Reviews Genetics*, *21*(1), 27–43. https://doi.org/10.1038/s41576-019-0169-4
53. Hu, D., Yin, C., Luo, S., Habenicht, A. J. R., & Mohanta, S. K. (2019). Vascular Smooth Muscle Cells Contribute to Atherosclerosis Immunity. *Frontiers in Immunology*, *10*. https://doi.org/10.3389/fimmu.2019.01101
54. Huang, P., Lian, F., Wen, Y., Guo, C., & Lin, D. (2013). Prion protein oligomer and its neurotoxicity. *Acta Biochimica et Biophysica Sinica*, *45*(6), 442–451. https://doi.org/10.1093/abbs/gmt037
55. James, R. G., Kamei, C. N., Wang, Q., Jiang, R., & Schultheiss, T. M. (2006). Odd-skipped related 1 is required for development of the metanephric kidney and regulates formation and differentiation of kidney precursor cells. *Development*, *133*(15), 2995–3004. https://doi.org/10.1242/dev.02442
56. Joe, A. W. B., Yi, L., Natarajan, A., Le Grand, F., So, L., Wang, J., Rudnicki, M. A., & Rossi, F. M. V. (2010). Muscle injury activates resident fibro/adipogenic progenitors that facilitate myogenesis. *Nature Cell Biology*, *12*(2), 153–163. https://doi.org/10.1038/ncb2015
57. Kadler, K. E., Hill, A., & Canty-Laird, E. G. (2008). Collagen fibrillogenesis: fibronectin, integrins, and minor collagens as organizers and nucleators. *Current Opinion in Cell Biology*, *20*(5), 495–501. https://doi.org/10.1016/j.ceb.2008.06.008
58. Keogh, R. J. , Harris, L. K. , Freeman, A. , Baker, P. N., Aplin, J. D., Whitely, G. S. , & Cartwright, J. E. (2007). Fetal-derived trophoblast use the apoptotic cytokine tumor necrosis factor-alpha-related apoptosis-inducing ligand to induce smooth muscle cell death. *Circ Res*, *100*(6), 834–841.
59. Keogh, R. J., Harris, L. K., Freeman, A., Baker, P. N., Aplin, J. D., Whitley, G. StJ., & Cartwright, J. E. (2007). Fetal-Derived Trophoblast Use the Apoptotic Cytokine

Tumor Necrosis Factor-α–Related Apoptosis-Inducing Ligand to Induce Smooth Muscle Cell Death. *Circulation Research*, *100*(6), 834–841. https://doi.org/10.1161/01.RES.0000261352.81736.37

60. KIMBERLIN, R. H., & WILESMITH, J. W. (1994). Bovine Spongiform Encephalopathy. *Annals of the New York Academy of Sciences*, *724*(1 Slow Infectio), 210–220. https://doi.org/10.1111/j.1749-6632.1994.tb38911.x
61. King, A., Jokhi, P. P., Smith, S. K., Sharkey, A. M., & Loke, Y. W. (1995). Screening for cytokine mRNA in human villous and extravillous trophoblasts using the reverse-transcriptase polymerase chain reaction (RT-PCR). *Cytokine*, *7*(4), 364–371. https://doi.org/10.1006/cyto.1995.0046
62. Kliman, H. J. (2000). Uteroplacental Blood Flow. *The American Journal of Pathology*, *157*(6), 1759–1768. https://doi.org/10.1016/S0002-9440(10)64813-4
63. Korshunov, V. A., & Berk, B. C. (2008). Smooth muscle apoptosis and vascular remodeling. *Current Opinion in Hematology*, *15*(3), 250–254. https://doi.org/10.1097/MOH.0b013e3282f97d71
64. Lash, G. E., Pitman, H., Morgan, H. L., Innes, B. A., Agwu, C. N., & Bulmer, J. N. (2016). Decidual macrophages: key regulators of vascular remodeling in human pregnancy. *Journal of Leukocyte Biology*, *100*(2), 315–325. https://doi.org/10.1189/jlb.1A0815-351R
65. Li J, Hou R, & Niu X. (2016). Comparison of microarray and RNA-Seq analysis of mRNA expression in dermal mesenchymal stem cells. . *Biotechnol Lett.* , *38*, 33–41.
66. Ma, J., & Lindquist, S. (2001). Wild-type PrP and a mutant associated with prion disease are subject to retrograde transport and proteasome degradation. *Proceedings of the National Academy of Sciences*, *98*(26), 14955–14960. https://doi.org/10.1073/pnas.011578098
67. Ma, J., & Lindquist, S. (2002). Conversion of PrP to a Self-Perpetuating PrP ^{Sc} -like Conformation in the Cytosol. *Science*, *298*(5599), 1785–1788. https://doi.org/10.1126/science.1073619
68. Mabbott, N. A., Mackay, F., Minns, F., & Bruce, M. E. (2000). Temporary inactivation of follicular dendritic cells delays neuroinvasion of scrapie. *Nature Medicine*, *6*(7), 719–720. https://doi.org/10.1038/77401
69. Maignien, T., Lasmé zas, C. I., Beringue, V., Dormont, D., & Deslys, J.-P. (1999). Pathogenesis of the oral route of infection of mice with scrapie and bovine

spongiform encephalopathy agents. *Journal of General Virology*, *80*(11), 3035–3042. https://doi.org/10.1099/0022-1317-80-11-3035

70. Makzhami, S., Passet, B., Halliez, S., Castille, J., Moazami-Goudarzi, K., Duchesne, A., Vilotte, M., Laude, H., Mouillet-Richard, S., BÃ©ringue, V., Vaiman, D., & Vilotte, J.-L. (2014). The prion protein family: a view from the placenta. *Frontiers in Cell and Developmental Biology*, *2*. https://doi.org/10.3389/fcell.2014.00035
71. Mariani, S. M., & Krammer, P. H. (1998). Differential regulation of TRAIL and CD95 ligand in transformed cells of the T and B lymphocyte lineage. *European Journal of Immunology*, *28*(3), 973–982. https://doi.org/10.1002/(SICI)1521-4141(199803)28:03<973::AID-IMMU973>3.0.CO;2-T
72. McKinley, M. P., Bolton, D. C., & Prusiner, S. B. (1983). A protease-resistant protein is a structural component of the Scrapie prion. *Cell*, *35*(1), 57–62. https://doi.org/10.1016/0092-8674(83)90207-6
73. McNally, K. L., Ward, A. E., & Priola, S. A. (2009). Cells Expressing Anchorless Prion Protein Are Resistant to Scrapie Infection. *Journal of Virology*, *83*(9), 4469–4475. https://doi.org/10.1128/JVI.02412-08
74. MIELE, G., BLANCO, A. R. A., BAYBUTT, H., HORVAT, S., MANSON, J., & CLINTON, M. (2003). Embryonic Activation and Developmental Expression of the Murine Prion Protein Gene. *Gene Expression*, *11*(1), 1–12. https://doi.org/10.3727/000000003783992324
75. Miranda, A., Pericuesta, E., Ramírez, M. Á., & Gutierrez-Adan, A. (2011). Prion Protein Expression Regulates Embryonic Stem Cell Pluripotency and Differentiation. *PLoS ONE*, *6*(4), e18422. https://doi.org/10.1371/journal.pone.0018422
76. Montrasio, F., Frigg, R., Glatzel, M., Klein, M. A., Mackay, F., Aguzzi, A., & Weissmann, C. (2000). Impaired Prion Replication in Spleens of Mice Lacking Functional Follicular Dendritic Cells. *Science*, *288*(5469), 1257–1259. https://doi.org/10.1126/science.288.5469.1257
77. Moore, M. W., Klein, R. D., Fariñas, I., Sauer, H., Armanini, M., Phillips, H., Reichardt, L. F., Ryan, A. M., Carver-Moore, K., & Rosenthal, A. (1996). Renal and neuronal abnormalities in mice lacking GDNF. *Nature*, *382*(6586), 76–79. https://doi.org/10.1038/382076a0

78. Nandy, D., Das, S., Islam, S., & Ain, R. (2020). Molecular regulation of vascular smooth muscle cell phenotype switching by trophoblast cells at the maternal-fetal interface. *Placenta*, *93*, 64–73. https://doi.org/10.1016/j.placenta.2020.02.017
79. Nishizawa, H., Pryor-Koishi, K., Kato, T., Kowa, H., Kurahashi, H., & Udagawa, Y. (2007). Microarray Analysis of Differentially Expressed Fetal Genes in Placental Tissue Derived from Early and Late Onset Severe Pre-eclampsia. *Placenta*, *28*(5–6), 487–497. https://doi.org/10.1016/j.placenta.2006.05.010
80. Nüsslein-Volhard, C., & Wieschaus, E. (1980). Mutations affecting segment number and polarity in Drosophila. *Nature*, *287*(5785), 795–801. https://doi.org/10.1038/287795a0
81. O'Brien, L. L., Guo, Q., Bahrami-Samani, E., Park, J.-S., Hasso, S. M., Lee, Y.-J., Fang, A., Kim, A. D., Guo, J., Hong, T. M., Peterson, K. A., Lozanoff, S., Raviram, R., Ren, B., Fogelgren, B., Smith, A. D., Valouev, A., & McMahon, A. P. (2018). Transcriptional regulatory control of mammalian nephron progenitors revealed by multi-factor cistromic analysis and genetic studies. *PLOS Genetics*, *14*(1), e1007181. https://doi.org/10.1371/journal.pgen.1007181
82. Pan, K. M., Baldwin, M., Nguyen, J., Gasset, M., Serban, A., Groth, D., Mehlhorn, I., Huang, Z., Fletterick, R. J., & Cohen, F. E. (1993). Conversion of alpha-helices into beta-sheets features in the formation of the scrapie prion proteins. *Proceedings of the National Academy of Sciences*, *90*(23), 10962–10966. https://doi.org/10.1073/pnas.90.23.10962
83. Pan, Y. , Zhao, L., Liang, J., Liu, J., Shi, Y., & Liu, N. (2006). Cellular prion protein promotes invasion and metastasis of gastric cancer. *FASEB J* , *20*(11), 1886–1888.
84. Passet, B., Young, R., Makhzami, S., Vilotte, M., Jaffrezic, F., Halliez, S., Bouet, S., Marthey, S., Khalifé, M., Kanellopoulos-Langevin, C., Béringue, V., Le Provost, F., Laude, H., & Vilotte, J.-L. (2012). Prion Protein and Shadoo Are Involved in Overlapping Embryonic Pathways and Trophoblastic Development. *PLoS ONE*, *7*(7), e41959. https://doi.org/10.1371/journal.pone.0041959
85. Paul, M. , Chakraborty, S. , Islam, S. , & Ain, R. (2022). Trans-differentiation of trophoblast stem cells: implications in placental biology. *Life Sc Alliance* , *6*(3).
86. Picut, C. A., Swanson, C. L., Parker, R. F., Scully, K. L., & Parker, G. A. (2009). The Metrial Gland in the Rat and Its Similarities to Granular Cell Tumors. *Toxicologic Pathology*, *37*(4), 474–480. https://doi.org/10.1177/0192623309335632

87. Pijnenborg, R., Bland, J. M., Robertson, W. B., & Brosens, I. (1983). Uteroplacental arterial changes related to interstitial trophoblast migration in early human pregnancy. *Placenta*, *4*(4), 397–413. https://doi.org/10.1016/S0143-4004(83)80043-5
88. Pijnenborg, R., Dixon, G., Robertson, W. B., & Brosens, I. (1980). Trophoblastic invasion of human decidua from 8 to 18 weeks of pregnancy. *Placenta*, *1*(1), 3–19. https://doi.org/10.1016/S0143-4004(80)80012-9
89. Pijnenborg, R., McLaughlin, P. J., Vercruysse, L., Hanssens, M., Johnson, P. M., Keith, J. C., & Van Assche, F. A. (1998). Immunolocalization of tumour necrosis factor-α (TNF-α) in the placental bed of normotensive and hypertensive human pregnancies. *Placenta*, *19*(4), 231–239. https://doi.org/10.1016/S0143-4004(98)90054-6
90. Pijnenborg, R., Vercruysse, L., & Hanssens, M. (2006). The Uterine Spiral Arteries In Human Pregnancy: Facts and Controversies. *Placenta*, *27*(9–10), 939–958. https://doi.org/10.1016/j.placenta.2005.12.006
91. Prusiner, S. B. (1982). Novel Proteinaceous Infectious Particles Cause Scrapie. *Science*, *216*(4542), 136–144. https://doi.org/10.1126/science.6801762
92. Prusiner, S. B. (1998). Prions. *Proceedings of the National Academy of Sciences*, *95*(23), 13363–13383. https://doi.org/10.1073/pnas.95.23.13363
93. Prusiner, S., & Hadlow, W. (1979). Slow transmissible diseases of the nervous system. *Academic, New York*.
94. Qi, X.-F., Kim, D.-H., Yoon, Y.-S., Jin, D., Huang, X.-Z., Li, J.-H., Deung, Y.-K., & Lee, K.-J. (2009). Essential involvement of cross-talk between IFN-γ and TNF-α in CXCL10 production in human THP-1 monocytes. *Journal of Cellular Physiology*, *220*(3), 690–697. https://doi.org/10.1002/jcp.21815
95. Race, R., Jenny, A., & Sutton, D. (1998). Scrapie Infectivity and Proteinase K-Resistant Prion Protein in Sheep Placenta, Brain, Spleen, and Lymph Node: Implications for Transmission and Antemortem Diagnosis. *The Journal of Infectious Diseases*, *178*(4), 949–953. https://doi.org/10.1086/515669
96. Rensen, S. S. M., Doevendans, P. A. F. M., & van Eys, G. J. J. M. (2007). Regulation and characteristics of vascular smooth muscle cell phenotypic diversity. *Netherlands Heart Journal*, *15*(3), 100–108. https://doi.org/10.1007/BF03085963
97. Robson, A., Harris, L. K., Innes, B. A., Lash, G. E., Aljunaidy, M. M., Aplin, J. D., Baker, P. N., Robson, S. C., & Bulmer, J. N. (2012). Uterine natural killer cells initiate

spiral artery remodeling in human pregnancy. *The FASEB Journal*, *26*(12), 4876–4885. https://doi.org/10.1096/fj.12-210310

98. Rogers, M., Yehiely, F., Scott, M., & Prusiner, S. B. (1993). Conversion of truncated and elongated prion proteins into the scrapie isoform in cultured cells. *Proceedings of the National Academy of Sciences*, *90*(8), 3182–3186. https://doi.org/10.1073/pnas.90.8.3182
99. Rosario, G. X., Konno, T., & Soares, M. J. (2008). Maternal hypoxia activates endovascular trophoblast cell invasion. *Developmental Biology*, *314*(2), 362–375. https://doi.org/10.1016/j.ydbio.2007.12.007
100. Rossant, J., & Cross, J. C. (2001). Placental development: Lessons from mouse mutants. *Nature Reviews Genetics*, *2*(7), 538–548. https://doi.org/10.1038/35080570
101. Roucou, X., Guo, Q., Zhang, Y., Goodyer, C. G., & LeBlanc, A. C. (2003). Cytosolic Prion Protein Is Not Toxic and Protects against Bax-mediated Cell Death in Human Primary Neurons. *Journal of Biological Chemistry*, *278*(42), 40877–40881. https://doi.org/10.1074/jbc.M306177200
102. Rudd, P. M., Wormald, M. R., Wing, D. R., Prusiner, S. B., & Dwek, R. A. (2001). Prion Glycoprotein: Structure, Dynamics, and Roles for the Sugars. *Biochemistry*, *40*(13), 3759–3766. https://doi.org/10.1021/bi002625f
103. Runic, R., Lockwood, C. J., Ma, Y., Dipasquale, B., & Guller, S. (1996). Expression of Fas ligand by human cytotrophoblasts: implications in placentation and fetal survival. *The Journal of Clinical Endocrinology & Metabolism*, *81*(8), 3119–3122. https://doi.org/10.1210/jcem.81.8.8768884
104. Safar, J., Wille, H., Itri, V., Groth, D., Serban, H., Torchia, M., Cohen, F. E., & Prusiner, S. B. (1998). Eight prion strains have PrPSc molecules with different conformations. *Nature Medicine*, *4*(10), 1157–1165. https://doi.org/10.1038/2654
105. Schmitt-Ulms, G., Ehsani, S., Watts, J. C., Westaway, D., & Wille, H. (2009). Evolutionary Descent of Prion Genes from the ZIP Family of Metal Ion Transporters. *PLoS ONE*, *4*(9), e7208. https://doi.org/10.1371/journal.pone.0007208
106. Searle, R. F., Jones, R. K., & Bulmer, J. N. (1999). Phenotypic Analysis and Proliferative Responses of Human Endometrial Granulated Lymphocytes during the Menstrual Cycle1. *Biology of Reproduction*, *60*(4), 871–878. https://doi.org/10.1095/biolreprod60.4.871

107. Sibai, B., Dekker, G., & Kupferminc, M. (2005). Pre-eclampsia. *The Lancet*, *365*(9461), 785–799. https://doi.org/10.1016/S0140-6736(05)17987-2

108. Smith, S. D., Dunk, C. E., Aplin, J. D., Harris, L. K., & Jones, R. L. (2009). Evidence for Immune Cell Involvement in Decidual Spiral Arteriole Remodeling in Early Human Pregnancy. *The American Journal of Pathology*, *174*(5), 1959–1971. https://doi.org/10.2353/ajpath.2009.080995

109. So, P. L., & Danielian, P. S. (1999). Cloning and expression analysis of a mouse gene related to Drosophila odd-skipped. *Mechanisms of Development*, *84*(1–2), 157–160. https://doi.org/10.1016/S0925-4773(99)00058-1

110. Soares, M. J., Chakraborty, D., Karim Rumi, M. A., Konno, T., & Renaud, S. J. (2012). Rat placentation: An experimental model for investigating the hemochorial maternal-fetal interface. *Placenta*, *33*(4), 233–243. https://doi.org/10.1016/j.placenta.2011.11.026

111. Socha, M. W., Malinowski, B., Puk, O., Wartęga, M., Stankiewicz, M., Kazdepka-Ziemińska, A., & Wiciński, M. (2021). The Role of NF-κB in Uterine Spiral Arteries Remodeling, Insight into the Cornerstone of Preeclampsia. *International Journal of Molecular Sciences*, *22*(2), 704. https://doi.org/10.3390/ijms22020704

112. Sparkes, R. S., Simon, M., Cohn, V. H., Fournier, R. E., Lem, J., Klisak, I., Heinzmann, C., Blatt, C., Lucero, M., & Mohandas, T. (1986). Assignment of the human and mouse prion protein genes to homologous chromosomes. *Proceedings of the National Academy of Sciences*, *83*(19), 7358–7362. https://doi.org/10.1073/pnas.83.19.7358

113. STAHL, N. (1987). Scrapie prion protein contains a phosphatidylinositol glycolipid. *Cell*, *51*(2), 229–240. https://doi.org/10.1016/0092-8674(87)90150-4

114. Steele, A. D., Lindquist, S., & Aguzzi, A. (2007). The Prion Protein Knockout Mouse. *Prion*, *1*(2), 83–93. https://doi.org/10.4161/pri.1.2.4346

115. Taraboulos, A., Rogers, M., Borchelt, D. R., McKinley, M. P., Scott, M., Serban, D., & Prusiner, S. B. (1990). Acquisition of protease resistance by prion proteins in scrapie-infected cells does not require asparagine-linked glycosylation. *Proceedings of the National Academy of Sciences*, *87*(21), 8262–8266. https://doi.org/10.1073/pnas.87.21.8262

116. Thaler, I., Manor, D., Itskovitz, J., Rottem, S., Levit, N., Timor-Tritsch, I., & Brandes, J. M. (1990). Changes in uterine blood flow during human pregnancy.

American Journal of Obstetrics and Gynecology, *162*(1), 121–125. https://doi.org/10.1016/0002-9378(90)90834-T

117. Torres, M., Gomez-Pardo, E., Dressler, G. R., & Gruss, P. (1995). Pax-2 controls multiple steps of urogenital development. *Development*, *121*(12), 4057–4065. https://doi.org/10.1242/dev.121.12.4057

118. Turco, M. Y., & Moffett, A. (2019). Development of the human placenta. *Development*, *146*(22). https://doi.org/10.1242/dev.163428

119. TURK, E., TEPLOW, David. B., HOOD, L. E., & PRUSINER, S. B. (1988). Purification and properties of the cellular and scrapie hamster prion proteins. *European Journal of Biochemistry*, *176*(1), 21–30. https://doi.org/10.1111/j.1432-1033.1988.tb14246.x

120. Vallecillo-García, P., Orgeur, M., vom Hofe-Schneider, S., Stumm, J., Kappert, V., Ibrahim, D. M., Börno, S. T., Hayashi, S., Relaix, F., Hildebrandt, K., Sengle, G., Koch, M., Timmermann, B., Marazzi, G., Sassoon, D. A., Duprez, D., & Stricker, S. (2017). Odd skipped-related 1 identifies a population of embryonic fibro-adipogenic progenitors regulating myogenesis during limb development. *Nature Communications*, *8*(1), 1218. https://doi.org/10.1038/s41467-017-01120-3

121. Wang, Q., Lan, Y., Cho, E.-S., Maltby, K. M., & Jiang, R. (2005). Odd-skipped related 1 (Odd1) is an essential regulator of heart and urogenital development. *Developmental Biology*, *288*(2), 582–594. https://doi.org/10.1016/j.ydbio.2005.09.024

122. Wang, Q., Qian, J., Wang F., & Ma, Z. (2012). Cellular prion protein accelerates colorectal cancer metastasis via the Fyn-SP1-SATB1 axis. . *Oncol Rep* , *28*(6), 2029–2034.

123. Wang Z, Gerstein M, & Snyder M. (2009). RNA-Seq: a revolutionary tool for transcriptomics. *Nat Rev Genet.*, *10*, 57–63.

124. Wei XW, Z. Y. W. F. T. F. and L. Y. (2022). The role of extravillous trophoblasts and uterine NK cells in vascular remodeling during pregnancy. *Front. Immunol*, *13*.

125. Whitley, G. St. J., & Cartwright, J. E. (2010). Cellular and Molecular Regulation of Spiral Artery Remodelling: Lessons from the Cardiovascular Field. *Placenta*, *31*(6), 465–474. https://doi.org/10.1016/j.placenta.2010.03.002

126. Wilhelm BT, ., & Landry JR. (2009). RNA-Seq—quantitative measurement of expression through massively parallel RNA sequencing. *Methods.*, *48*, 249–257.

127. Xu, P.-X., Adams, J., Peters, H., Brown, M. C., Heaney, S., & Maas, R. (1999). Eya1-deficient mice lack ears and kidneys and show abnormal apoptosis of organ primordia. *Nature Genetics*, *23*(1), 113–117. https://doi.org/10.1038/12722

128. Young, R., Bouet, S., Polyte, J., Le Guillou, S., Passet, B., Vilotte, M., Castille, J., Beringue, V., Le Provost, F., Laude, H., & Vilotte, J.-L. (2011). Expression of the prion-like protein Shadoo in the developing mouse embryo. *Biochemical and Biophysical Research Communications*, *416*(1–2), 184–187. https://doi.org/10.1016/j.bbrc.2011.11.021

129. Zhou, Y., Damsky, C. H., & Fisher, S. J. (1997). Preeclampsia is associated with failure of human cytotrophoblasts to mimic a vascular adhesion phenotype. One cause of defective endovascular invasion in this syndrome? *Journal of Clinical Investigation*, *99*(9), 2152–2164. https://doi.org/10.1172/JCI119388

PUBLICATIONS AND CONFERENCES

Publications in SCI journals: -

1. **Bose R**, Jana S. S, and Ain R (2023) Cellular Prion protein moonlights vascular smooth muscle cell fate: surveilled by trophoblast cells. ***Journal of Cellular Physiology*****.** doi: 10.1002/jcp.31130 **Impact Factor 5.6**
2. Saha S, **Bose R***, Chakraborty S and Ain R (2022) Tipping the balance toward stemness in trophoblast: Metabolic programming by Cox6B2. ***FASEB Journal***. 36 (11), e22600. **Impact Factor 5.83 (* equal contribution)**
3. Chakraborty S, **Bose R**, Islam S, Das S, Ain R. (2020) Harnessing Autophagic Network is Essential for Trophoblast Stem Cell Differentiation. ***Stem Cells and Development*** Apr 15. doi: 10.1089/scd.2019.0296. **Impact Factor 4.3**
4. **Bose R**, Ain R. (2018) Regulation of Transcription by Circular RNAs. ***Advances in Experimental Medicine and Biology*****;** 1087:81-94. doi:10.1007/978-981-13-1426-1_7. Springer,Singapore. **Impact Factor 3.65**

Publications in Proceedings: -

1. **Rumela Bose** and Rupasri Ain: Dynamics of Cellular PRION expression during utero-placental development. In the proceedings of International Conference of Women's Reproductive Health at NIRRH. PP-13
2. **Rumela Bose,** Sarmita Sanjay Jana, and Rupasri Ain: Cellular Prion protein regulates vascular smooth muscle cell migration at the maternal fetal interface. In the proceedings of 90th Annual meeting of the Society of the Biological Chemists, India. PP-340

Conference and Awards: -

1. Awarded with the prestigious "**Shyama Prasad Mukherjee Fellowship**" for securing 9Th rank in CSIR-UGC NET (Life Sciences).

2. Attended and presented poster entitled "Dynamics of Cellular PRION expression during utero-placental development" at the International Conference of Women's Reproductive Health held on 20-23 February 2020 at NIRRH, Mumbai, Maharashtra.

3. **Best poster award** at the International Conference of Women's Reproductive Health held on 20-23 February 2020 at NIRRH, Mumbai, Maharashtra.

4. Attended and presented poster entitled "Cellular Prion protein regulates vascular smooth muscle cell migration at the maternal fetal interface" at the 90th Annual Meeting of the Society of Biological Chemists, India through online mode 16-19th December 2021.